UNIVERSITY OF SOUTHERN CALIFORNIA

DEPARTMENT OF CIVIL ENGINEERING

SOIL-STRUCTURE INTERACTION EFFECTS ON FORCED VIBRATION TESTS

by

J. E. Luco

Department of Applied Mechanics and Engineering Sciences
University of California, San Diego

H. L. Wong and M. D. Trifunac

Department of Civil Engineering
University of Southern California

Report 86-05

Los Angeles, California

September 1986

TABLE OF CONTENTS

	Page
ABSTRACT	v
1. INTRODUCTION	1
2. DESCRIPTION OF THE MILLIKAN LIBRARY BUILDING	4
3. SUMMARY OF PREVIOUS EXPERIMENTAL STUDIES	7
4. EXPERIMENTAL DETERMINATION OF THE FREQUENCY RESPONSE	17
5. A MODEL FOR THE RESPONSE OF THE SUPERSTRUCTURE	29
6. FIXED-BASE NATURAL FREQUENCIES AND MODAL DAMPING VALUES	33
7. CONTRIBUTION OF THE BASE MOTION TO THE TOTAL RESPONSE	41
8. A MODEL FOR THE COMPLETE SOIL-STRUCTURE SYSTEM	46
9. IMPEDANCE FUNCTIONS FOR THE FOUNDATION	50
10. COMPARISON OF EXPERIMENTAL AND THEORETICAL RESULTS	56
11. EXPERIMENTAL EVALUATION OF IMPEDANCE FUNCTIONS	66
12. APPROXIMATE SOLUTION OF THE INTERACTION EQUATIONS	74
13. EFFECTS OF THE SAN FERNANDO EARTHQUAKE ON THE MILLIKAN LIBRARY SYSTEM	82
14. CONCLUSIONS	93
ACKNOWLEDGEMENT	95
REFERENCES	96
APPENDIX A. DESCRIPTION OF APPARATUS AND EXPERIMENTAL PROCEDURES	98
APPENDIX B. EFFECTS OF SOIL-STRUCTURE INTERACTIONS ON THE TORSIONAL RESPONSE	106

ABSTRACT

Experimental and analytical studies of the effects of soil-structure interaction on the response of a structure during forced vibration tests are presented. Forced vibrations tests designed to isolate the effects of soil-structure interaction are described and the results obtained for the nine-story reinforced concrete Millikan Library building are analyzed. It is shown that it is possible to determine experimentally the fixed-base natural frequencies and modal damping ratios of the superstructure. These values may be significantly different from the resonant frequencies and damping ratios of the complete structure-foundation-soil system.

In the case of the Millikan Library it is found that the rigid-body motion associated with translation and rocking of the base accounts for more than 30 percent of the total response on the roof and that the deformation of the superstructure at the fundamental frequencies of the system is almost entirely due to the inertial forces generated by translation and rocking of the base.

Comparisons of the experimental and calculated response reveal that it is possible to predict accurately the effects of soil-structure interaction during forced vibration tests. Finally, the apparent changes in behavior of the Millikan Library as a result of the San Fernando earthquake are discussed.

1. INTRODUCTION

Full-scale forced vibration tests are commonly used to determine the natural frequencies, modal damping values and mode shapes of structures. In some cases, the experimentally determined values are used to define some of the parameters appearing in a mathematical model of the structure; in other cases, the results of forced vibration tests are used to validate structural models employed in computational analyses. The frequent practice in interpreting the results of forced vibration tests is to neglect the effects of the interaction between the structure and the soil. Such simplifying assumption may lead to serious errors in that resonant frequencies, energy dissipation and other dynamic characteristics of the complete structure-foundation-soil system are ascribed to the superstructure. The typical result is that the fixed-base natural frequencies of the structure are underestimated while the energy dissipation in the structure is overestimated.

The principal objective of this study is to analyze in detail the effects of soil-structure interaction during forced vibration tests. In particular, an attempt is made at isolating structural characteristics, such as fixed-base natural frequencies and energy dissipation mechanism, as well as foundation-soil characteristics, such as foundation impedance functions, from forced vibration test results which involve the complete structure-foundation-soil system.

Although a large number of theoretical studies of the interaction between structures and the supporting soil have been made and a variety of highly sophisticated analytical models have been proposed, the experimental study of the interaction phenomenon has been very limited. The second objective of this study is associated with the need of illustrating the interaction effects under controlled experimental conditions. A final objective corresponds to the desire of testing one of the mathematical soil-structure interaction models by attempting to reproduce the experimental observations.

For the purpose of the study the nine-story reinforced concrete Millikan Library Building was selected as experimental site. The Millikan Library has been the subject of a large number of forced vibration tests (Kuroiwa, 1967; Jennings and Kuroiwa, 1968; Trifunac, 1972; Foutch *et al.*,

1975; Luco *et al.*, 1975) and ambient vibration tests (Blandford *et al.*, 1968; Trifunac, 1972; McLamore, 1972; Udwadia and Trifunac, 1973). Accelerograms for the 1968 Borrego Mountain, 1970 Lytle Creek and 1971 San Fernando earthquakes have been recorded in the Library and a number of studies on its seismic response have been conducted (Crouse, 1973; Udwadia and Trifunac, 1974; Iemura and Jennings, 1973). In addition, detailed soil mechanics information is available (Converse Foundation Engineers, 1959) and shear wave velocity profiles have been determined in the vicinity of the site (Eguchi *et al.*, 1976; Shannon and Wilson, Inc. and Agbabian Assoc., 1976).

Besides the wealth of information available, other reasons have guided the selection of Millikan Library as experimental site. An initial experimental study of the effects of soil-structure interaction during forced vibration tests conducted by Jennings and Kuroiwa (1968) led to the conclusion that the rigid body motion of the superstructure due to compliance of the soil contributed less than 3 percent to the total motion at the top of the structure for vibrations in the N-S direction. More detailed tests performed by Foutch, Luco, Trifunac and Udwadia (1975) indicated that the rigid-body motion contributes approximately 29 percent to the total motion at the top in disagreement with the previous tests. Although an error in the data reduction in the initial experiments cannot be ruled out, Foutch and Jennings (1978) argue that the change in soil-structure interaction effects is real and corresponds to degradation of the foundation system as a result of the San Fernando earthquake of 1971. Another aspect that needs to be analyzed corresponds to the observation that the resonant frequencies of the Millikan Library seem to have changed as a result of the San Fernando earthquake (Udwadia and Trifunac, 1974). The fundamental resonant frequencies in the N-S and E-W directions measured immediately after the earthquake were 5 and 14 percent lower than the corresponding values before the earthquake. It is important to establish whether these reductions are associated with degradation of the superstructure or changes in the foundation system.

After a brief description of the Millikan Library building and a summary of the results of previous experiments, a model of the superstructure and the tests required to isolate the charac-

teristics of the superstructure are described. A detailed study of the contribution of the motion of the base to the total motion at the top of the superstructure is followed by the development of a mathematical model of the complete structure-foundation-soil system. Comparisons of the theoretical and experimental results at the base and top of the structure are made and the possibility of determining experimentally the foundation impedance functions is explored. Finally, some approximate relations that permit the estimation of the interaction effects are presented and utilized to study the effects of the San Fernando earthquake on the Millikan Library system.

2. DESCRIPTION OF THE MILLIKAN LIBRARY BUILDING

The Robert A. Millikan Library is a nine-story reinforced concrete building located on the campus of the California Institute of Technology. The structure has a basement and an enclosed roof area. The typical floor plan covers an area of 21 × 23 m (69 × 75 ft) and the building stands 43.9 m (144 ft) above the first floor level and 48.2 m (158 ft) above the basement slab (see Fig. 1.). The majority of the lateral loads in the transverse (N-S) direction are resisted by 30 cm (12-in) reinforced concrete shear walls located on the east and west ends of the building. In the longitudinal (E-W) direction the 30 cm (12-in) reinforced concrete walls of the central core provide most of the lateral resistance. The north-side and south-side facades are precast window wall panels connected to the main structure with steel angle clips. The floor system consists of 23 cm (9-in) slabs of lightweight concrete reinforced in two directions and supported by reinforced concrete beams. The total weight of the superstructure is estimated at 1.05×10^8 Newtons (23.5×10^6 lbs).

The foundation system of the library consists of a central pad 9.75 m (32 ft) wide and 1.22 m (4 ft) deep which runs in the E-W direction and extends from the east curved shear wall to the west curved shear wall (Fig. 2). Also provided are beams 3 m (10 ft) wide by 0.61 m (2 ft) deep which run E-W beneath the rows of columns at the north and south ends of the building. These beams are connected to the central pad by stepped beams. The contact between the central pad and the underlying soil is approximately 7 m (23 ft) below the first-floor level. The plan dimensions of the foundation are approximately 23.3 × 25.1 m (76.5 × 82.5 ft) with additional areas of dimensions 9.9 × 1.7 m (32.5 × 5.5 ft) and 9.9 × 3.5 m (32.5 × 11.5 ft) at the east and west extremes, respectively. The total weight of the foundation is estimated at $0.14 \times 10^8 N$ (3.2×10^6 lbs). The foundation rests on alluvium composed of medium to dense sands mixed with gravel. The alluvium at the site extends about 275 m (900 ft) to bedrock.

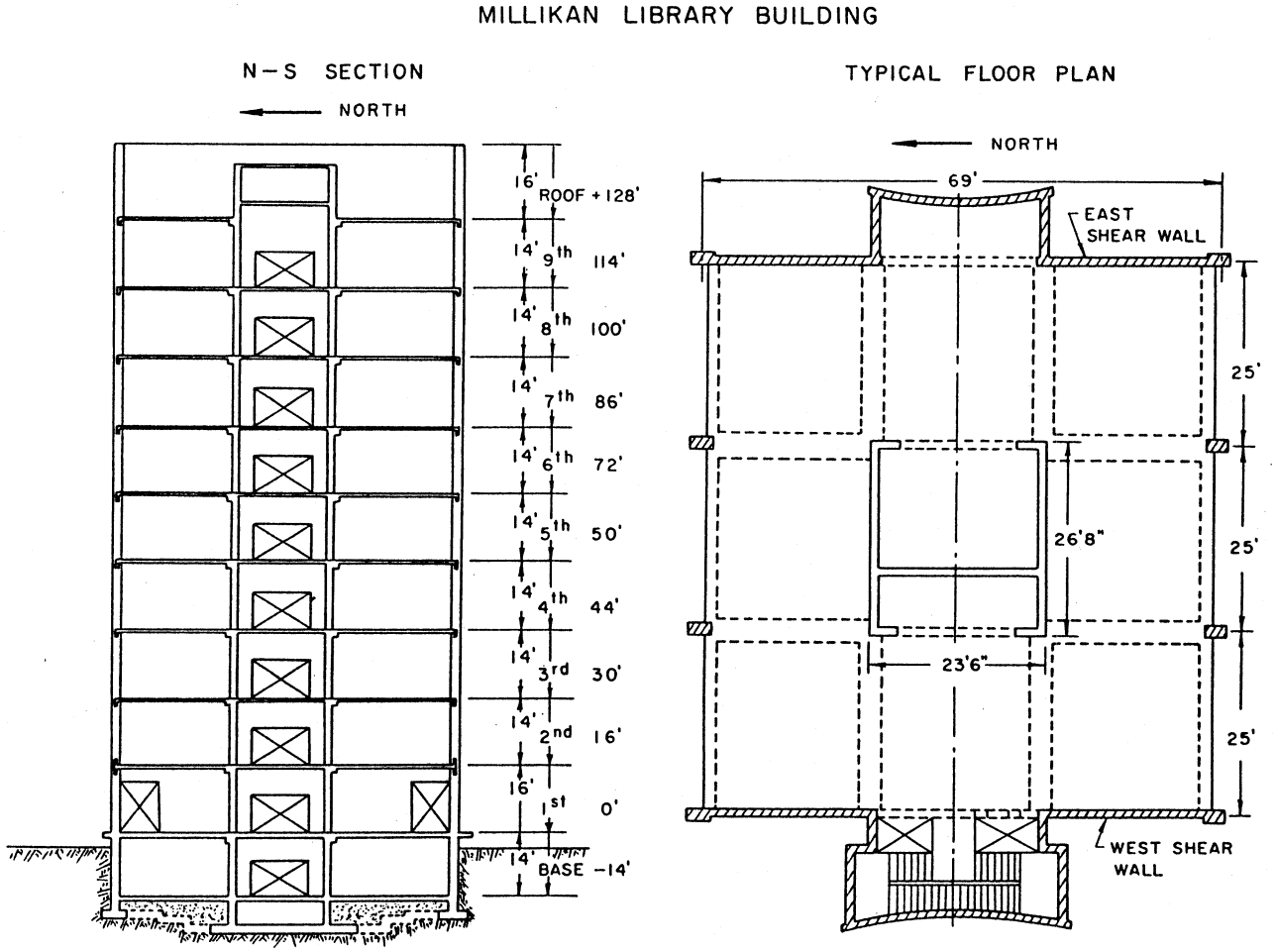

Figure 1. Millikan Library Building: N-S elevation and typical floor plan.

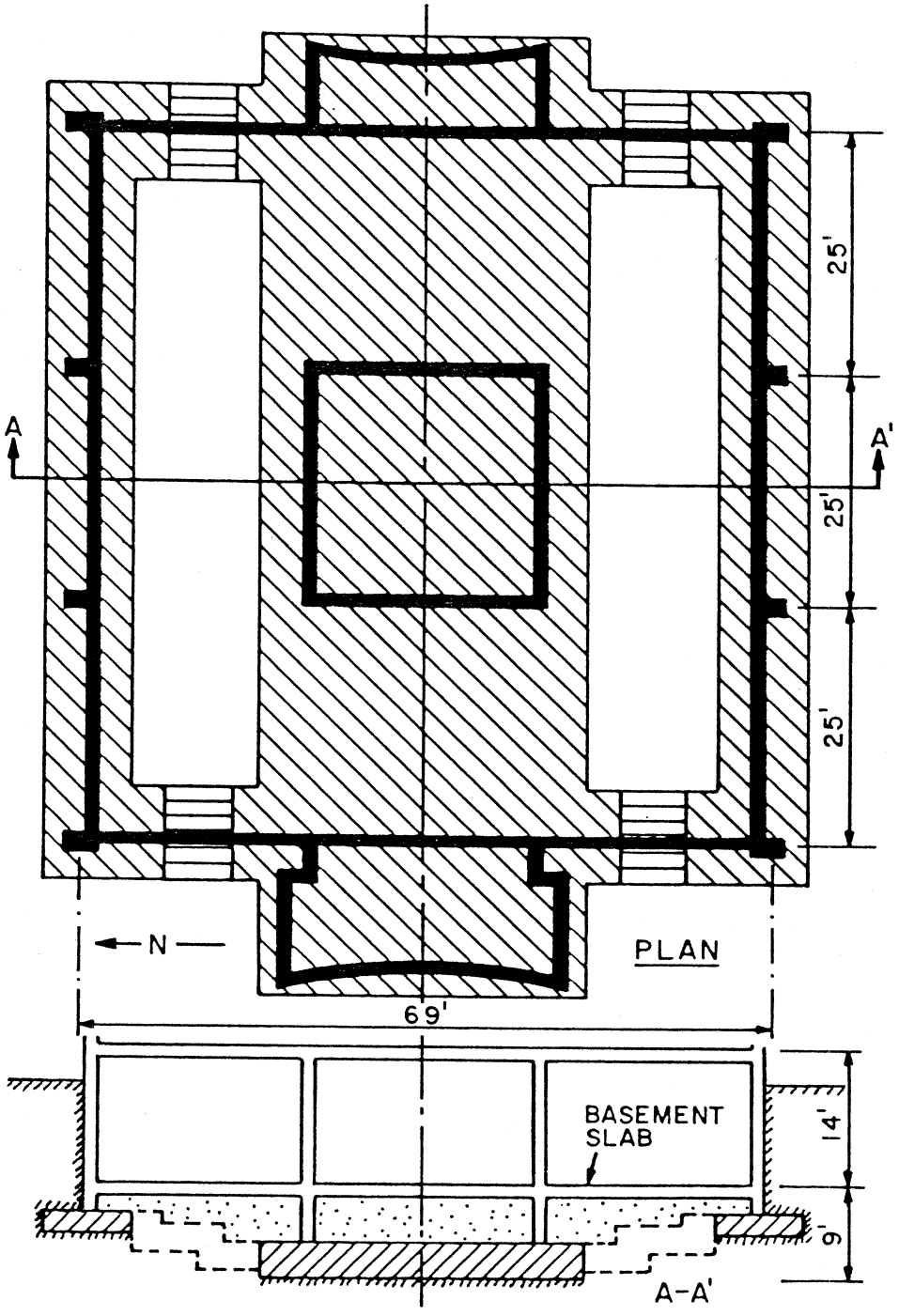

Figure 2. Millikan Library: foundation system.

3. SUMMARY OF PREVIOUS EXPERIMENTAL STUDIES

Since 1966 the Millikan Library Building has been subjected to a number of ambient, man-excited and shaker-excited vibration tests. A list of the experimentally determined apparent fundamental resonant frequencies in the N-S and E-W directions is presented in Table 1. The most recent forced vibration tests indicate fundamental resonant frequencies of 1.8 and 1.2 cps in the N-S and E-W directions, respectively. Inspection of the results presented in Table 1 reveals that the most recent values of the resonant frequencies are somewhat lower than those determined in the initial forced and ambient vibration tests. In particular, comparison of the results of ambient vibration tests before and after the 1971 San Fernando earthquake indicates reductions of 5 and 14 percent for the resonant frequencies in the N-S and E-W directions. Detailed moving window analyses of the response during the San Fernando earthquake show marked reductions in the apparent resonant frequencies within the duration of the strong shaking followed by partial recovery at the end of the excitation (Udwadia and Trifunac, 1974). Whether the observed reductions in resonant frequencies correspond mainly to changes in the soil, foundation or superstructure remains an open question.

Vibration tests of the Millikan Library Building have also provided estimates of apparent modal damping in the neighborhood of the first resonant frequency as listed in Table 2. These values are of the order of 1.5 percent for both the N-S and E-W directions. A study of the E-W response of the Library during the San Fernando earthquake indicates that the average apparent damping during the first 43 secs of the strong motion portion of the excitation may have been as high a 5.5 percent (Udwadia and Marmarelis, 1976).

In an experiment performed in 1974 the Millikan Library Building was forced into resonance by a vibration generator located at the roof and the three-dimensional motion at 51 locations on each of four floors, the basement slab and the roof were measured for shaking in both the N-S and E-W directions (Foutch *et al.*, 1975). The resulting floor deformation patterns are illustrated in Figs. 3 and 4 for vibrations in the N-S and E-W directions, respectively. The patterns of deformation of the west shear wall for N-S excitation and of a section through the central core for E-W

TABLE 1. APPARENT RESONANT FREQUENCIES : FIRST MODE MILLIKAN LIBRARY BUILDING

Test	FREQUENCY-CPS N-S	FREQUENCY-CPS E-W
Forced Vibration Test (1966-67) (Kuroiwa, 1967)	1.89-1.98	1.46-1.51
Ambient Vibration Test (March 1967) (Blandford *et al.*, 1968)	1.91	1.49
Ambient Vibration Test (April 1968) (Udwadia and Trifunac, 1973)	1.89	1.45
Ambient Vibration Test (July 1969) (Udwadia and Trifunac, 1973)	1.89	1.45
Lytle Creek Earthquake Transfer Function (Sept. 1970) (Udwadia and Trifunac, 1974)	1.90-2.00	1.30-1.50
San Fernando Earthquake Transfer Function (Feb. 1971) (Udwadia and Trifunac, 1974)	1.50-1.90	1.00-1.50
San Fernando Earthquake (Feb. 1971) (Iemura and Jennings, 1973)	-	0.82-1.43
San Fernando Earthquake (Feb. 1971) Linear Model (Udwadia and Marmarelis, 1976)	-	1.02-1.11
Ambient Vibration Test (Feb. 1971) (McLamore, 1972)	1.80	1.25
Ambient Vibration Test (March 1971) (Udwadia and Trifunac, 1973)	-	1.30
Man Excited Vibration Test (Dec. 1972) (Udwadia and Trifunac, 1973)	1.77	1.37
Ambient Vibration Test (April 1973) (Udwadia and Marmarelis, 1976)	-	1.28
Forced Vibration Test (1974) (Foutch *et al.*, 1975)	1.76	1.21
Forced Vibration Test (July 1975) (Present Study)	1.79	1.21

TABLE 2. APPARENT MODAL DAMPING, FIRST MODE MILLIKAN LIBRARY BUILDING

Test	APPARENT MODAL DAMPING-PERCENT	
	N-S	E-W
Forced Vibration Test (1966-67) (Kuroiwa, 1967)	1.2-1.8	0.7-1.7
Ambient Vibration Test (March 1967) (Blandford *et al.*, 1968)	1.6	1.5
San Fernando Earthquake Relative Motion (Feb. 1971) (Iemura and Jennings, 1973)	-	1.0-13.0
San Fernando Earthquake (Feb. 1971) Linear Model (Udwadia and Marmarelis, 1967)	-	3.5-5.5
Ambient Vibration Test (April 1973) (Udwadia and Marmarelis, 1976)	-	1.3
Forced Vibration Test (July 1975) (Present Study)	1.8	1.8

excitations are shown in Fig. 5. The observations indicate that for N-S excitations each floor remains essentially plane experiencing an almost uniform translation and an almost uniform rotation about an E-W axis. For excitation in the E-W direction, each floor experiences an almost uniform translation while the average rotation is almost zero. In this case the central core introduces a marked bending of the floor slabs.

Amplified views of the patterns of deformation of the basement slab for excitation in the N-S and E-W directions are shown in Figs. 6 and 7, respectively. For vibrations in the N-S direction, the stiff shear walls on the east and west ends of the building cause an almost rigid translation of the basement slab together with an almost uniform rotation about the E-W axis of symmetry of the base (Fig. 6). Some deviations from this average rigid-body motion may be observed at the location of the central core and at the north and south ends of the slab. In this case, the deformation of the basement slab resembles that of a flexible rectangular plate with two rigid edges (east and west ends) vibrating on top of an elastic medium. For vibrations in the E-W direction, the central core induces large localized deformation of the basement slab (Fig. 7).

The results of the experiment conducted by Foutch *et al.* (1975), indicate that the interaction of the structure and the soil has a marked effect on the response during forced vibration tests. In particular, for N-S vibrations, it was found that the translation of the basement slab was 4 percent of the motion at the roof and that the average rotation of the basement slab multiplied by the height of the structure amounted to 25 percent of the roof motion. Thus, the rigid body motion of the structure due to soil compliance contributed 29 percent of the roof response. These results are in sharp contrast with those of a previous study (Kuroiwa, 1967) which indicate that the rigid body motion contributes less than 3 percent to the N-S response at the roof and which led Jennings and Kuroiwa (1968) to the conclusion that the structure behaved essentially as if it were fixed at the foundation level. The present study is motivated in part by the need to explain this discrepancy.

In related experiments the three-dimensional motion of the soil surface generated by the forces that the foundation exerts on soil during forced vibration tests were recorded in the

immediate neighborhood of the Library and in one quadrant of the Pasadena area extending to a distance of six kilometers (four miles) from the building (Foutch *et al.*, 1975; Luco *et al.*, 1975). These studies reveal that the motion of the foundation distorts the soil surface in the vicinity of the building and generates Rayleigh and Love waves which can be easily measured at considerable distances from the structure.

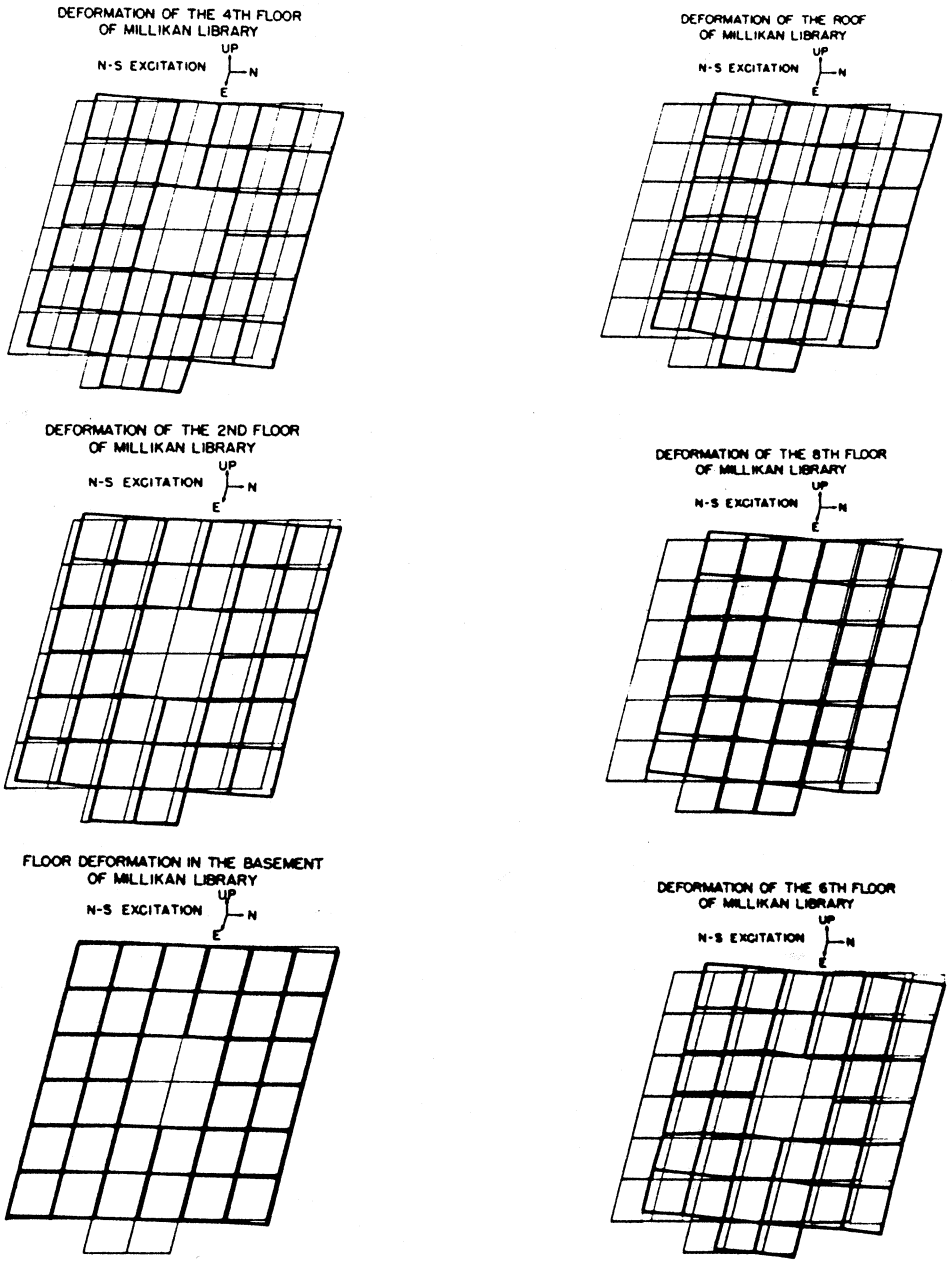

Figure 3. Floor deformation patterns for N-S vibrations.

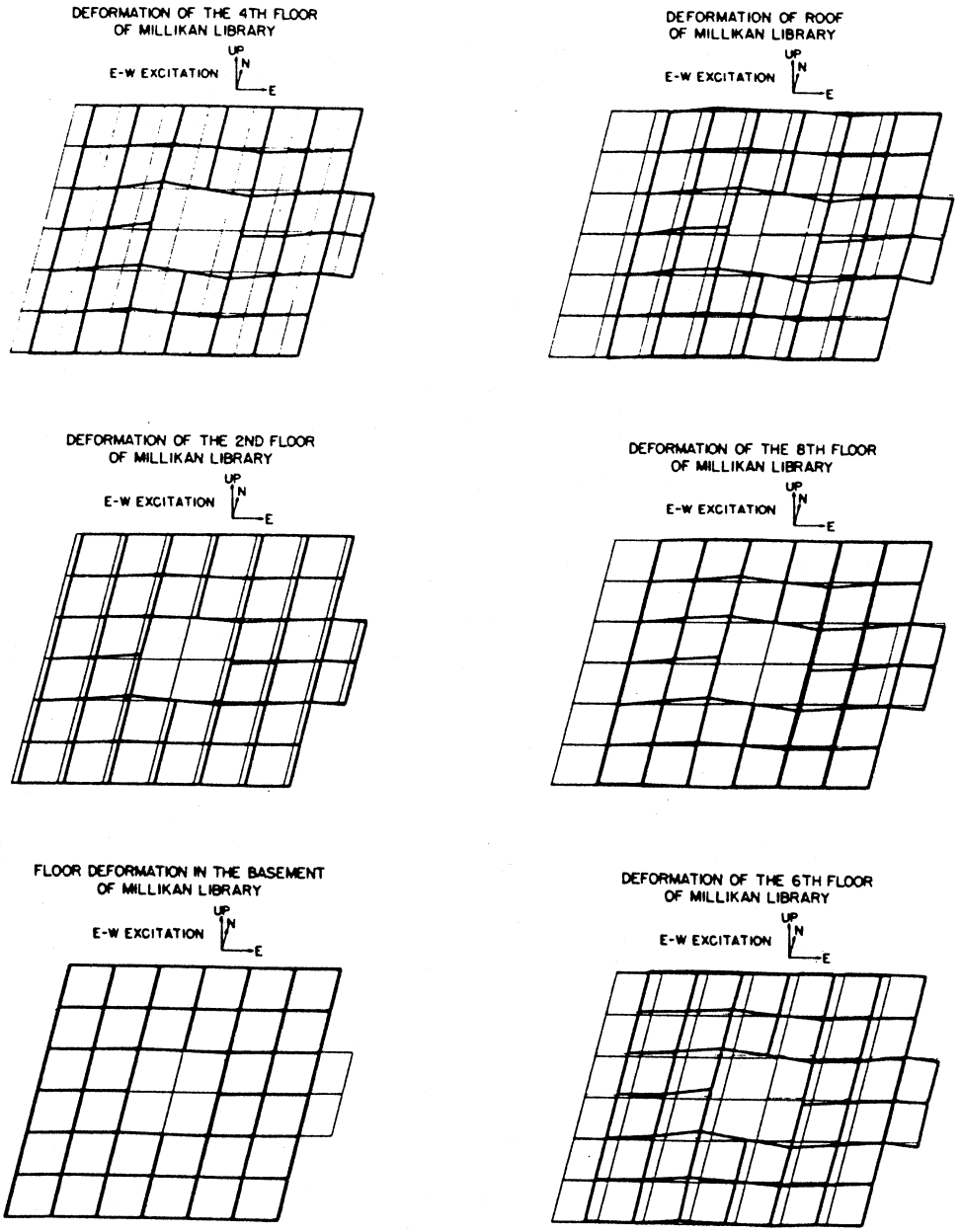

Figure 4. Floor deformation patterns for E-W vibrations.

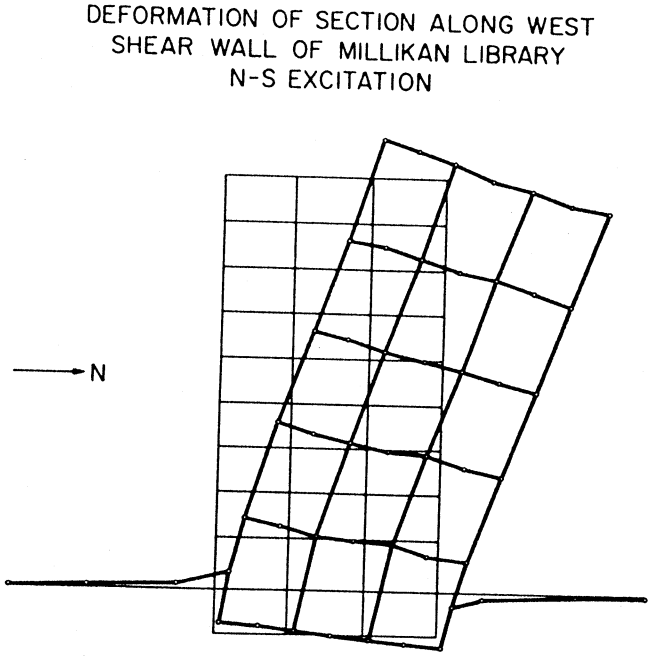

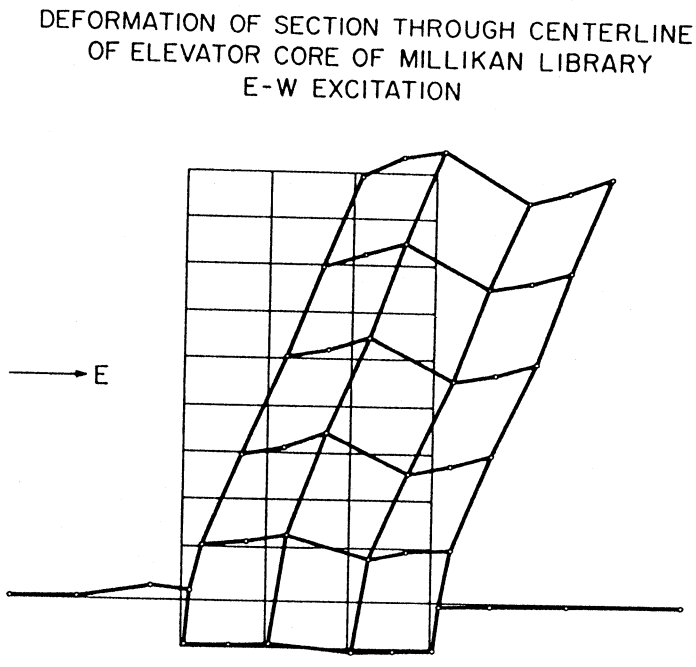

Figure 5. (a) Deformation of section along west shear wall: N-S excitation;

(b) Deformation of section through centerline of elevator core: E-W excitation.

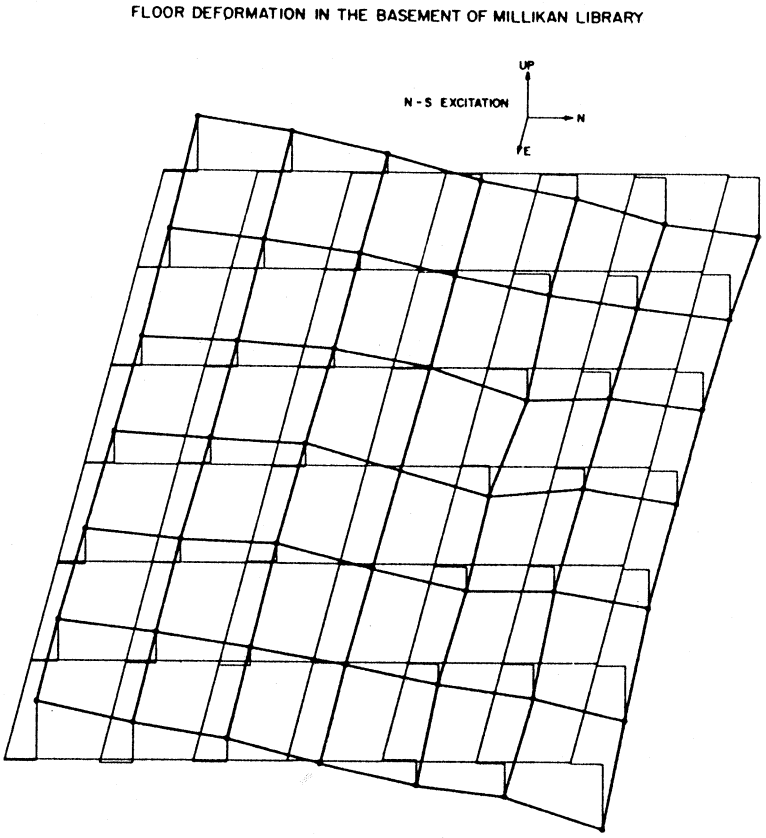

Figure 6. Deformation of the basement slab: N-S vibrations.

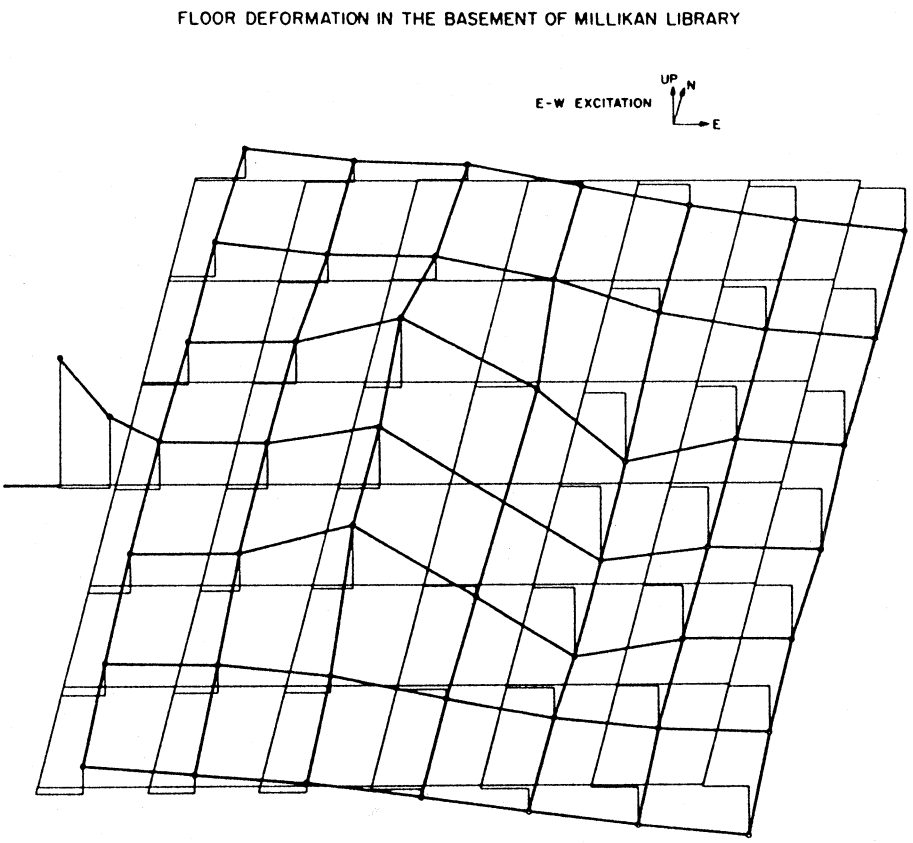

Figure 7. Deformation of the basement slab: E-W vibrations.

4. EXPERIMENTAL DETERMINATION OF THE FREQUENCY RESPONSE

A set of forced vibration tests designed with the purpose of isolating the effects of soil-structure interaction was conducted by the authors in 1975. In these tests the N-S and E-W steady-state response of the Millikan Library to a harmonic exciting force produced by an eccentric-mass vibration generator mounted on the roof was measured. The response of the building was recorded at four points, three of which were located on the basement slab (stations 1, 2 and 3) while the fourth point was located on the roof (station 4). The locations of the recording stations for vibrations in the N-S and E-W directions are shown in Fig. 8. The horizontal motion of the basement slab and of the roof were recorded at station 1 and 4, respectively, while the vertical motion of the basement slab was recorded at stations 2 and 3. For vibrations in the N-S direction, the response was determined at 116 distinct frequencies in the range 0.8 to 2.50 Hz. For vibrations in the E-W direction, the response was recorded at 67 frequencies in the range from 0.8 to 1.75 Hz.

The recording system consisted of four Model SS-1 Ranger-type seismometers (moving coil, velocity-type transducers with natural period in the vicinity of 1 sec), an Earth Sciences SC-201A signal conditioner, an Ampex SP-300 tape recorder and two Brush recorders. In addition, an instrument designed to determine the phase of the forcing function with respect to its peak value was also used. For each frequency of excitation, the output of the four seismometers amplified by the signal conditioner was recorded on a common time basis on the tape recorder and plotted on the Brush recorders. The phase of the forcing function was also recorded. The data was corrected to account for the effects introduced by the seismometers and the signal conditioner. Details of the corrections used are presented in Appendix A.

The resulting corrected data corresponding to the displacements at the four recording stations can be described by the functions

$$y_j(\omega) = Y_j(\omega) \exp\left\{ i \left[\omega t - \phi_j(\omega) \right] \right\} , \quad (j = 1, 4) \tag{1}$$

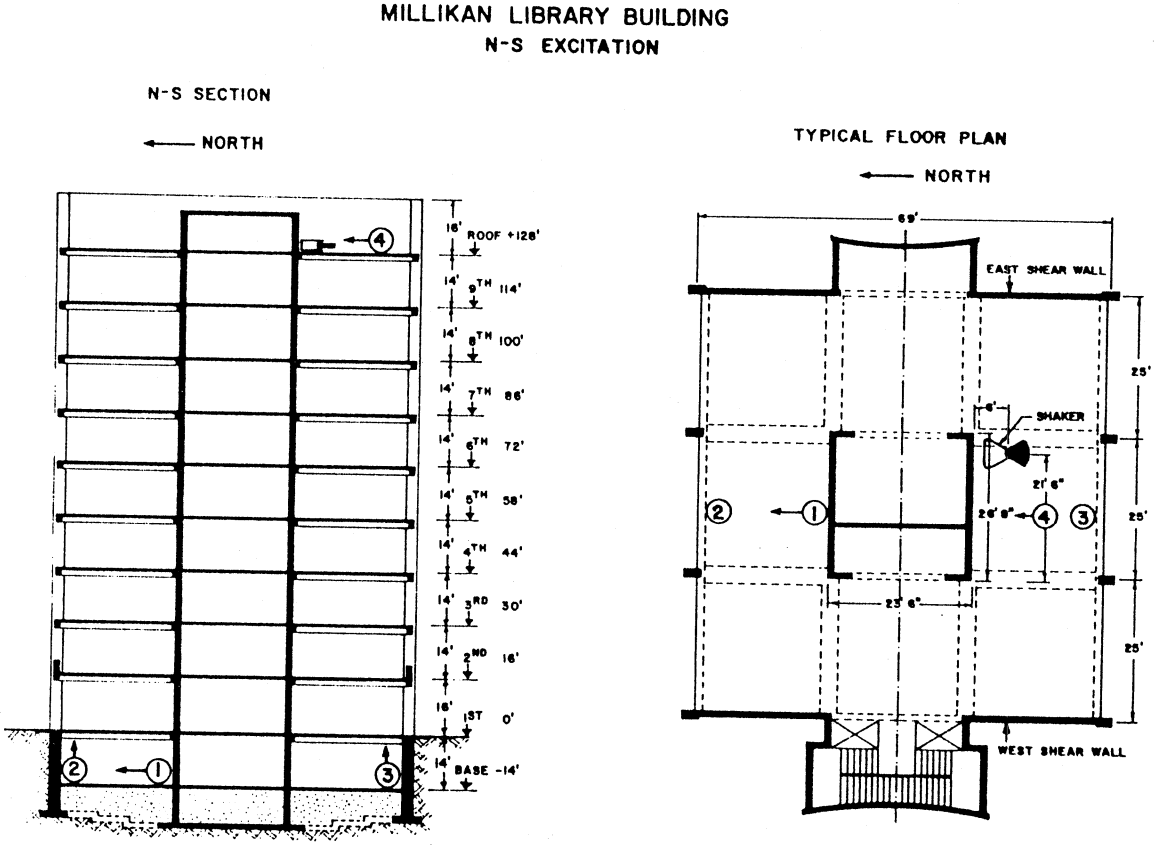

Figure 8a. Location of the four Ranger seismometers and of the shaker for N-S vibrations.

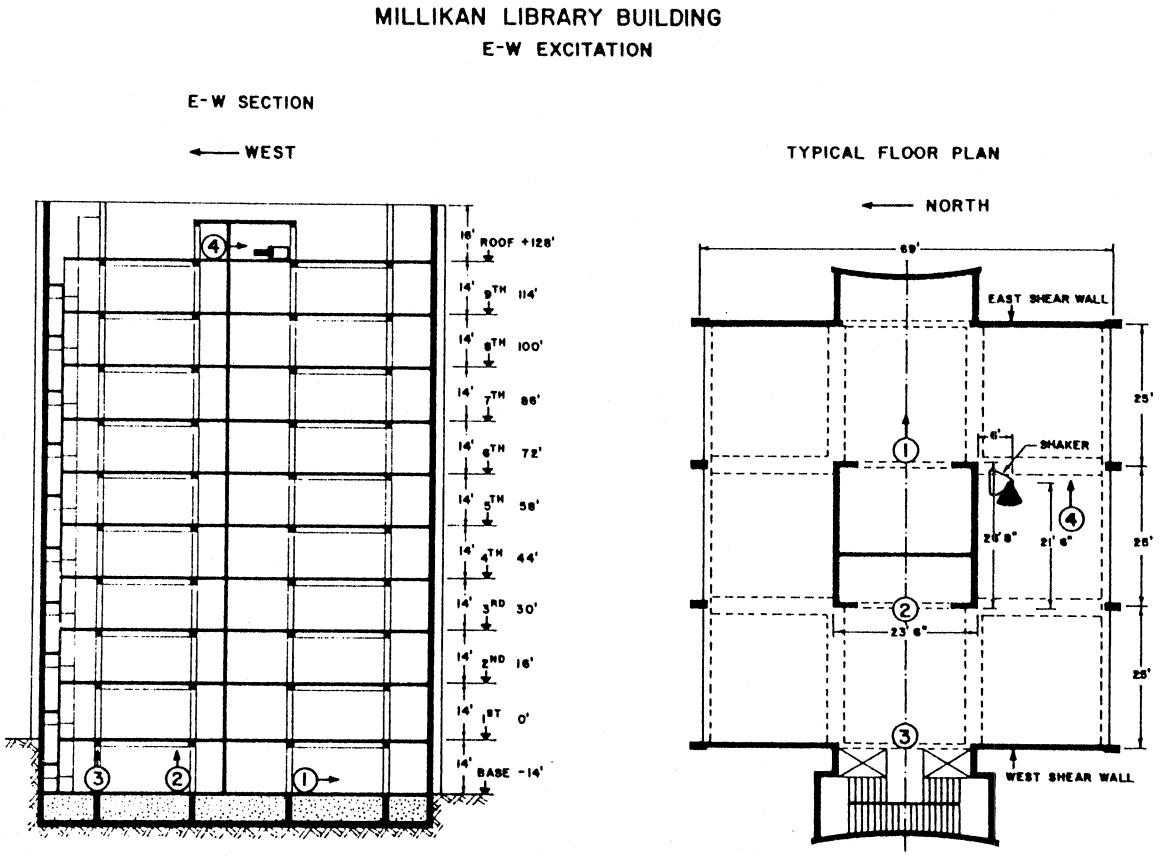

Figure 8b. Location of the four Ranger seismometers and of the shaker for E-W vibrations.

where, ω represents the frequency of the excitation, $Y_j(\omega)$ denotes the amplitude of the displacement at the *jth* station, and $\phi_j(\omega)$ represents the phase of the motion at the *jth* station with respect to the force that the vibration generator exerts on the roof. The harmonic force that the vibration generator applies on the roof is given by

$$f_T(\omega) = F_T(\omega) \exp(i\omega t) \tag{2}$$

where $F_T(\omega) = 103.6\ \omega^2$ Newtons ($23.3\ \omega^2$ lb) (Keightley, Housner and Hudson, 1961).

Assuming that the deformation patterns of the basement and roof slabs determined in previous experiments (Foutch *et al.*, 1975) remain unchanged for frequencies in the neighborhood of the first resonant frequency, it is possible to use the response at the four recording stations to estimate the translation and rotation of the basement slab and the translation of the roof. In particular, the average translation and rotation of the basement slab, $\overline{U}_b e^{i\omega t}$ and $\overline{\Phi}_b e^{i\omega t}$, and the average total translation of the roof, $\overline{U}_T e^{i\omega t}$, can be expressed in the form

$$\overline{U}_b = 1.10\, Y_1 e^{-i\phi_1},\quad H\overline{\Phi}_b = -3.07\, Y_2 e^{-i\phi_2} + 3.34\, Y_3 e^{-i\phi_3},\quad \overline{U}_T = Y_4 e^{-i\phi_4} \tag{3}$$

for N-S vibrations, and

$$\overline{U}_b = 1.14\, Y_1 e^{-i\phi_1},\quad H\overline{\Phi}_b = 1.70\, Y_2 e^{-i\phi_2} + 2.14\, Y_3 e^{-i\phi_3},\quad \overline{U}_T = Y_4 e^{-i\phi_4} \tag{4}$$

for E-W vibrations. In Eqs. (3) and (4), $H = 43.3$ m (142 ft) denotes the height of the roof slab with respect to the basement slab.

For vibrations in the N-S direction, the response of the superstructure is controlled by the motion of the shear walls along the east and west ends of the building. The translation at the base of the shear walls, $U_b e^{i\omega t}$, can be approximated by the average translation of the foundation $\overline{U}_b e^{i\omega t}$, i.e., $U_b = \overline{U}_b$. The rotation of the base of the shear walls about an E-W axis, $\Phi_b e^{i\omega t}$, can be expressed in terms of the average rotation of the foundation, $\overline{\Phi}_b e^{i\omega t}$, by

$$\Phi_b = \alpha\overline{\Phi}_b \tag{5}$$

where $\alpha = 1.3$.

For E-W vibrations, the response of the superstructure is highly affected by the motion of the central core. The translation at the base of the central core, $U_b e^{i\omega t}$, can be approximated by the average E-W translation of the foundation ($U_b = \overline{U}_b$). The rotation of the base of the central core about a N-S axis, $\Phi_b e^{i\omega t}$, can be expressed in terms of the average rotation of the complete foundation, $\overline{\Phi}_b e^{i\omega t}$, as in Eq. (5), where, in this case, $\alpha = 3.33$.

The coefficients appearing in Eqs. (3) and (4) connecting the average translation and rotation of the foundation with the response at the recording stations have been derived from the deformation patterns shown in Figs. 6 and 7. The values of the coefficient α appearing in Eq. (5) and connecting the rotation of the shear walls and of the core walls to the average rotation of the foundation have also resulted from the data in these figures.

The amplitudes and phases of $\overline{U}_b$, $H\overline{\Phi}_b$, $H\Phi_b$ and $\overline{U}_T$ for vibrations in the N-S direction are plotted versus frequency in Figs. 9 and 10, respectively. The corresponding quantities for E-W vibrations are presented in Figs. 11 and 12. In Fig. 9 the amplitudes of the motion at the basement slab level and at the roof for N-S excitation are plotted on a logarithmic scale versus the frequency of excitation. The average rotation of the base $\overline{\Phi}_b$ and the rotation of the base of the shear walls Φ_b have been multiplied by $H = 43.3$ m (142 ft), the height of the roof with respect to the basement slab. The results shown indicate that the response at both the roof and the basement slab reach peak amplitudes at the same frequency of 1.79 Hz which corresponds to the fundamental resonant frequency of the complete soil-structure system for vibrations in the N-S direction. By considering the width of the peaks, it is found that the complete system damping ratio has a value of 1.8 percent. At the resonant frequency the amplitude of the basement translation is 4.0 percent of the amplitude of the total roof translation. The contribution of the rigid-body rotation, $H\Phi_b$, associated with rotation of the base of the shear walls amounts to 33.1 percent of the total roof motion. If the average rotation of the basement slab is used as reference, the contribution of the rigid-body rotation, $H\overline{\Phi}_b$, amounts to 25.6 percent of the total roof motion. These percentages remain approximately constant in the frequency range from 1 to 2.5 Hz.

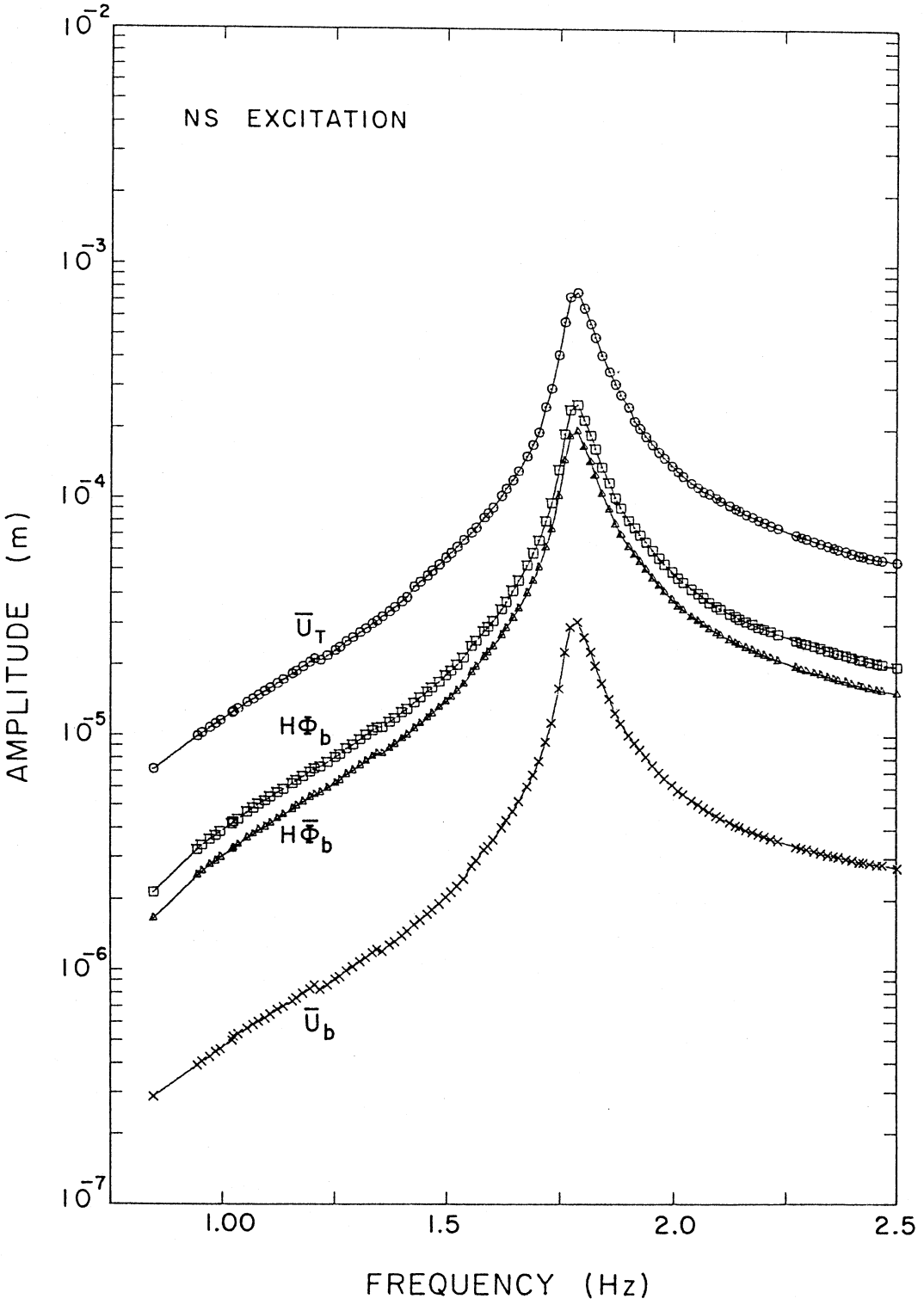

Figure 9. Amplitudes of the response for N-S excitation.

The phases of the N-S response at the roof and basement levels with respect to the forcing function (e.g. $\overline{U}_T = | \overline{U}_T | \exp\left[- iph\,(\overline{U}_T)\right]$) plotted versus the frequency of excitation are shown in Fig. 10. Inspection of Fig. 10 indicates that the different response components are essentially in phase with each other (except for the translation of the base which lags the other components). For low frequencies, the response of the system is in phase with the forcing function. At the resonant system frequency the response is 90 ° out of phase with the force at the roof while for higher frequencies the phase difference becomes 180 °.

The results shown in Figs. 11 and 12 indicate that for E-W vibrations the fundamental system frequency corresponds to 1.21 Hz and that the system damping is also 1.8 percent. For E-W vibration, the translation of the basement slab amounts to 1.2 percent of the roof response while the rigid-body rotation, $H\Phi_b$, associated with rotation of the central core amounts to 20.7 percent of the total roof response. If the average rotation of the basement slab is taken as reference, the rigid-body rotation $H\overline{\Phi}_b$ contributes 6.2 percent of the total roof motion.

These tests confirm the experimental results of Foutch *et al.* (1975) which reveal significant soil-structure interaction effects during forced vibration tests. For N-S vibrations, the rigid-body motion of the superstructure associated with compliance of the soil corresponds to 37 percent of the roof response if it is assumed that the superstructure is driven by the shear walls and to 30 percent if it is assumed that the structure reacts to the average basement rotation. The relative motion of the roof with respect to the displaced and rotated basement slab

$$U_T = \overline{U}_T - U_b - H\Phi_b \quad \text{or} \quad U'_T = \overline{U}_T - U_b - H\overline{\Phi}_b\,, \tag{6}$$

representing deformation of the superstructure, amounts to 63 or 71 percent of the roof response depending on whether the motion of the base of the shear walls or the average motion of the foundation is taken as reference. It will be shown later that a major portion of this deformation of the superstructure is associated with the inertial forces created by the translation and rotation of the base. Under these conditions it can be stated that the effects of soil-structure interaction dominate the response in the N-S direction.

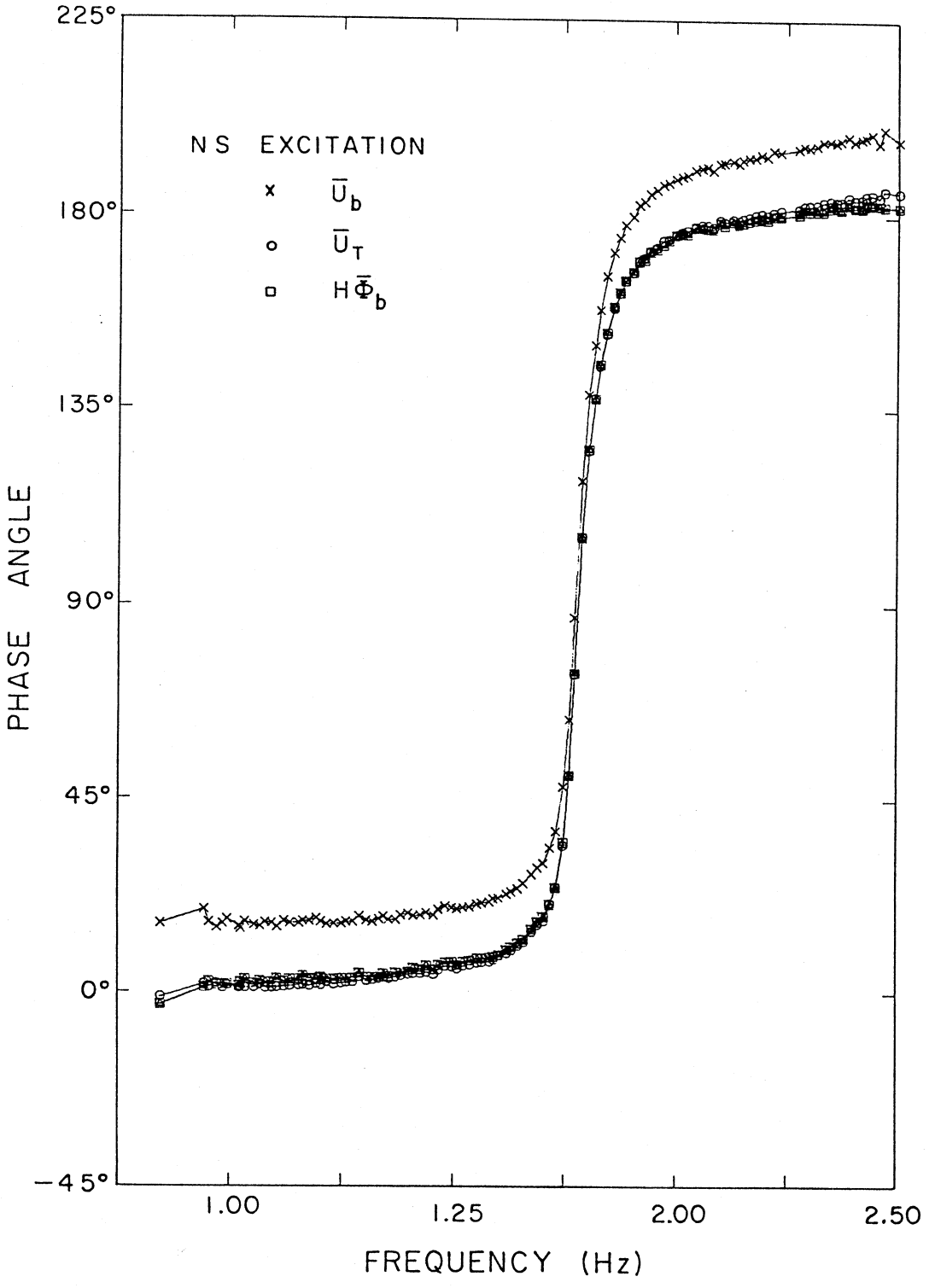

Figure 10. Phase of the response for N-S excitation.

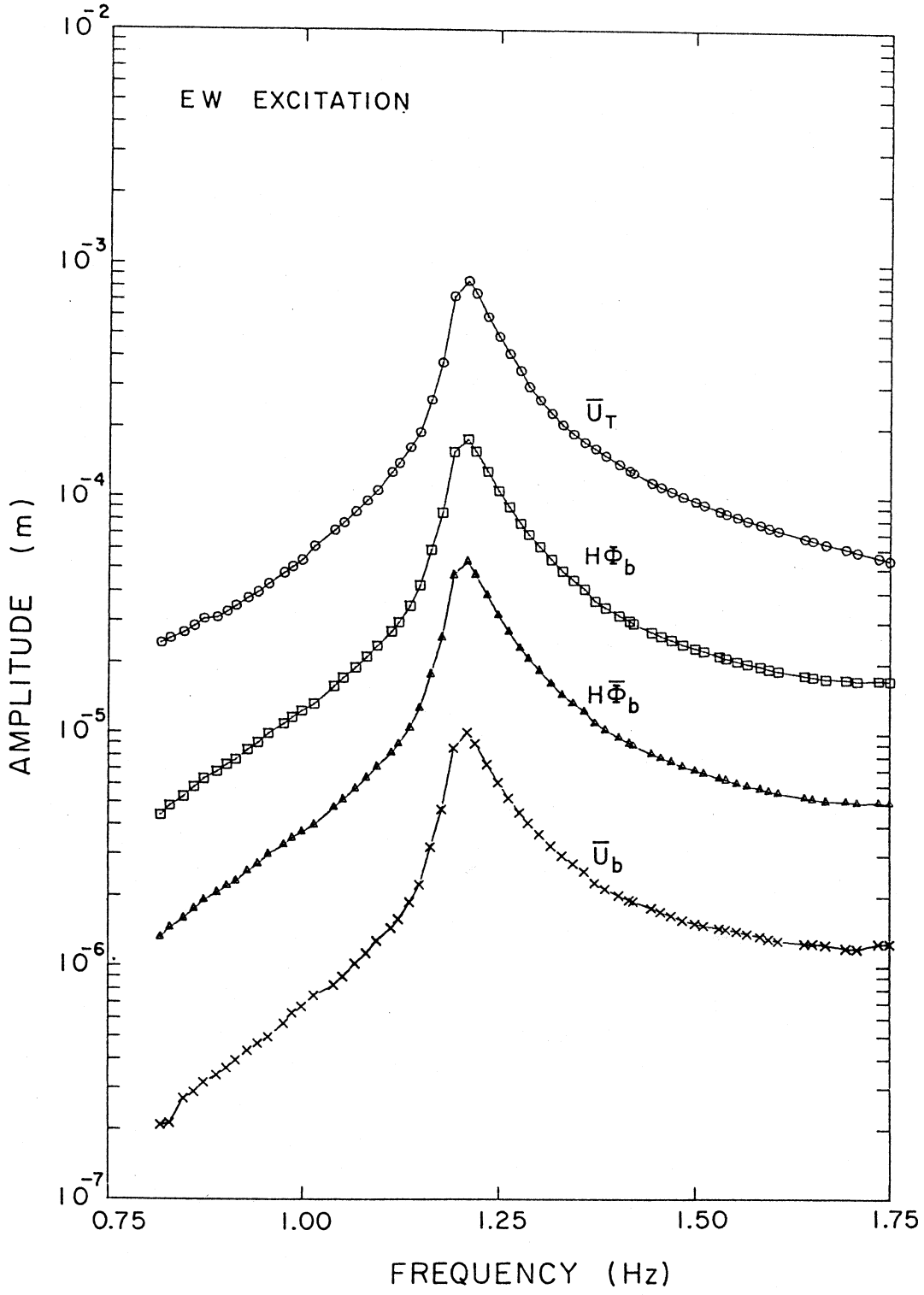

Figure 11. Amplitude of the response for E-W excitation.

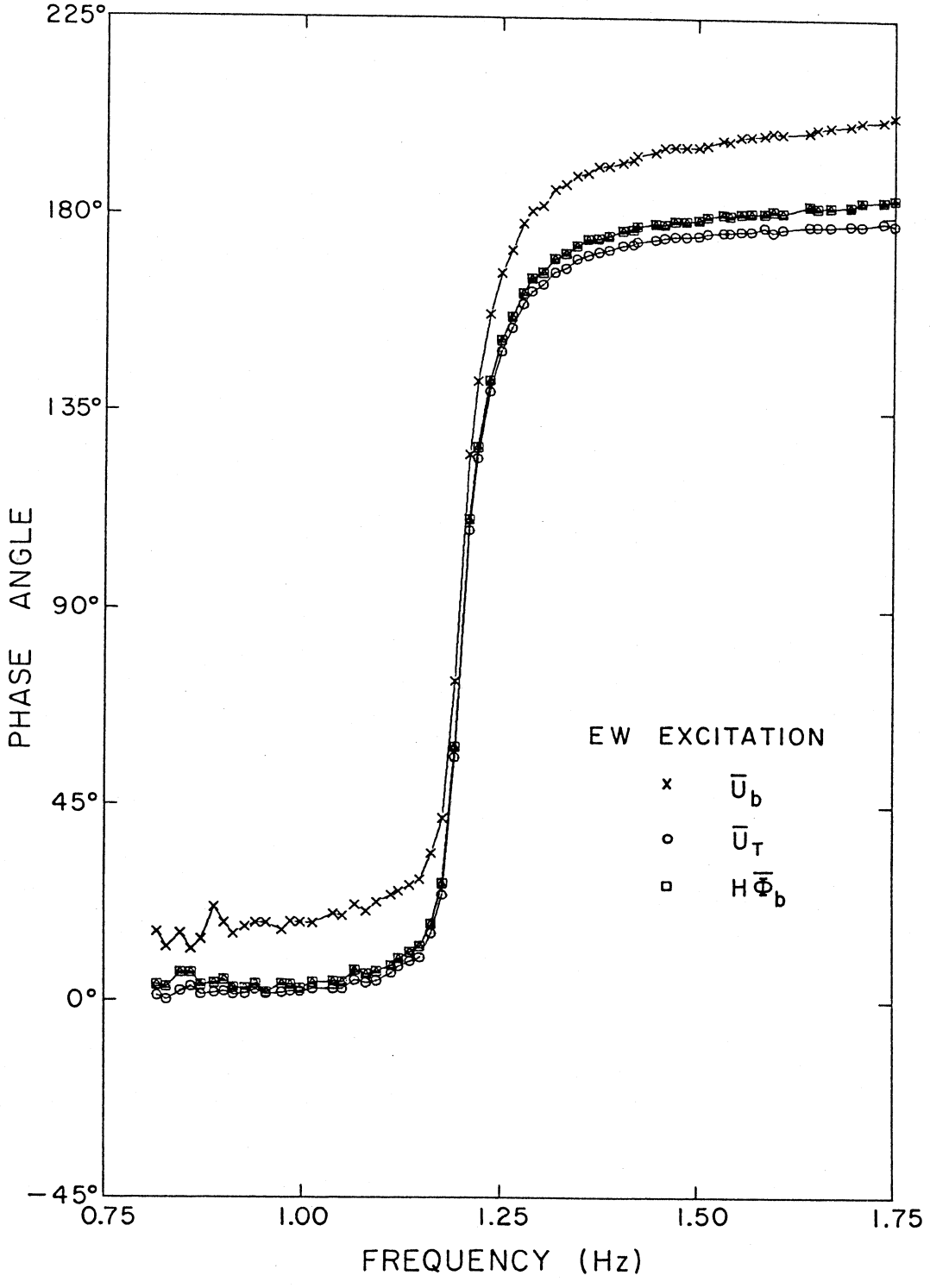

Figure 12. Phase of the response for E-W excitation.

For vibrations in the E-W directions, the rigid-body motion of the structure associated with foundation compliance amounts to 22 percent of the roof response if it is assumed that the response of the superstructure is controlled by the motion of the base of the central core, and to 7 percent if it is assumed that the superstructure is driven by the average motion of the basement slab. The lower interaction effects for E-W vibrations can be attributed to the higher flexibility of the superstructure in that direction. The response of the system at the fundamental resonant frequencies is summarized in Table 3.

TABLE 3. RESPONSE AT THE FUNDAMENTAL SYSTEM FREQUENCY

	N-S Vibrations	E-W Vibrations
Fundamental System Frequency: $\tilde{f}_1 = \tilde{\omega}_1/2\pi$ (Hz)	1.79	1.21
System damping $\tilde{\xi}_1$	0.018	0.018
$\lvert \overline{U}_T \rvert$ (m)	7.59×10^{-4}	8.49×10^{-4}
$\lvert U_T \rvert = \lvert \overline{U}_T - H\Phi_b - U_b \rvert$ (m)	4.79×10^{-4}	6.63×10^{-4}
$\lvert H\Phi_b \rvert$ (m)	2.51×10^{-4}	1.76×10^{-4}
$\lvert U'_T \rvert = \lvert \overline{U}_T - H\overline{\Phi}_b - U_b \rvert$ (m)	5.36×10^{-4}	7.86×10^{-4}
$\lvert H\overline{\Phi}_b \rvert$ (m)	1.94×10^{-4}	0.53×10^{-4}
$\lvert U_b \rvert$ (m)	0.306×10^{-4}	0.100×10^{-4}
$F_T/\omega^2 M_b$ (m)	0.0973×10^{-4}	0.0973×10^{-4}
$\lvert U_T/\overline{U}_T \rvert$	0.631	0.781
$\lvert H\Phi_b/\overline{U}_T \rvert$	0.331	0.207
$\lvert U_b/\overline{U}_T \rvert$	0.040	0.012
$\lvert U'_T/\overline{U}_T \rvert$	0.706	0.926
$\lvert H\overline{\Phi}_b/\overline{U}_T \rvert$	0.256	0.062
$\lvert U_b/\overline{U}_T \rvert$	0.040	0.012
$\lvert F_T/\omega^2 M_b \overline{U}_T \rvert$	0.013	0.011

5. A MODEL FOR THE RESPONSE OF THE SUPERSTRUCTURE

The tests described in the previous section indicate that the base of the Millikan Library Building undergoes significant translation and rotation when a harmonic force is applied at the roof level. Under these conditions it is not possible to analyze the test results by assuming a fixed base model. To study the effects that the base translations and rotations may have on the structural response it is convenient to consider the model of the superstructure shown in Fig. 13. The superstructure is represented by a lumped mass model excited at the top level by the force $F_T e^{i\omega t}$ that the harmonic vibration generator applies on the roof. The harmonic translation of the base is represented by $U_b e^{i\omega t}$ and the harmonic rotation of the base about a horizontal axis is represented by $\Phi_b e^{i\omega t}$.

The total harmonic displacement at the *jth* level $\overline{U}_j e^{i\omega t}$ $(j = 1, N)$ may be written in the form

$$\overline{U}_j e^{i\omega t} = (U_b + h_j \Phi_b + U_j) e^{i\omega t} \tag{7}$$

in which $U_j e^{i\omega t}$ represents the displacement at the *jth* level associated with deformation of the superstructure and h_j denotes the height of the *jth* level with respect to the basement slab.

The equation of motion for harmonic vibrations of the superstructure is

$$-\omega^2[M]\{\overline{U}\} + i\omega[C]\{U\} + [K]\{U\} = \{F\} \tag{8}$$

where $\{\overline{U}\}$ and $\{U\}$ represent the total and relative displacement vectors, respectively, and

$$\{F\} = (0, 0, 0..., F_T)^T \tag{9}$$

denotes the vector of external forces applied to the superstructure. The $N \times N$ matrices $[M]$, $[C]$, and $[K]$ correspond to the mass, damping and stiffness matrices for the superstructure on a rigid base.

Substitution from Eq. (7) into Eq. (8) leads to

$$\Big(-\omega^2[M] + i\omega[C] + [K]\Big)\{U\} = \{F\} + \omega^2[M]\Big(\{1\}\, U_b + \{h\}\, \Phi_b\Big) \tag{10}$$

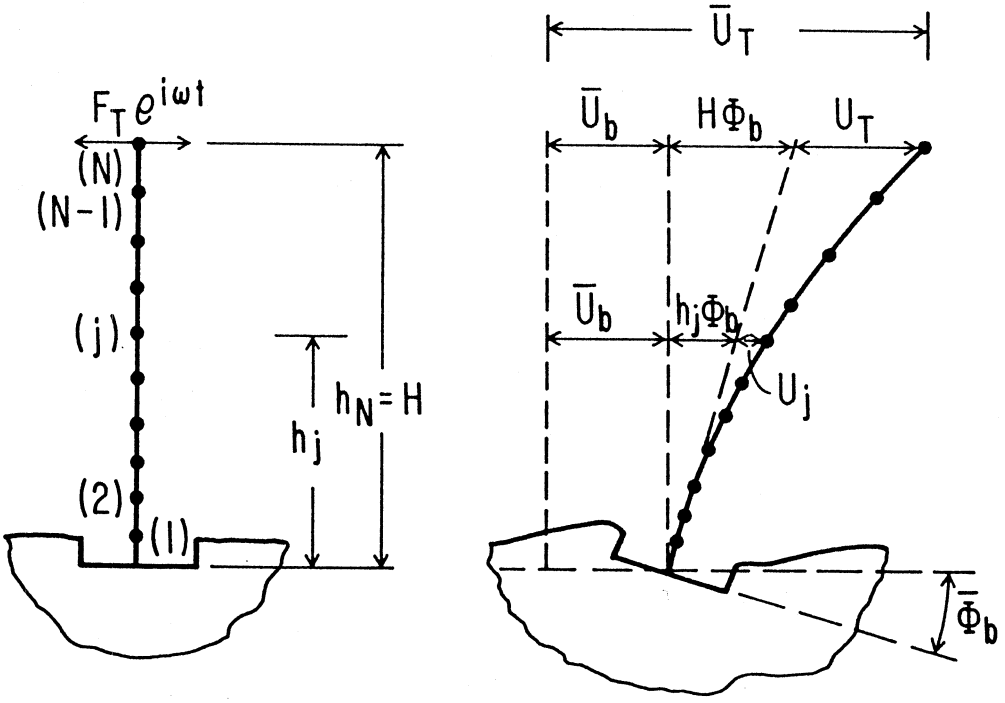

Figure 13. Model of the superstructure.

in which

$$\{1\} = (1, 1,..., 1)^T \quad ,$$
$$\{h\} = (h_1, h_2,..., h_N)^T \quad . \tag{11}$$

Assuming that the superstructure, when fixed at the base, has classical normal modes it is possible to introduce the change of variables

$$\{U\} = \sum_{r=1}^{N} \left\{\phi^{(r)}\right\} \eta_r \tag{12}$$

where $\left\{\phi^{(r)}\right\}$ is the *rth* fixed-base mode. After substitution from Eq. (12) into Eq. (10), it is found that

$$\eta_r = \frac{(\omega/\omega_r)^2}{1 - (\omega/\omega_r)^2 + 2i\xi_r(\omega/\omega_r)} \left(\frac{F_T}{\omega^2 M_r} + \beta_r U_b + \gamma_r H \Phi_b \right) \tag{13}$$

where

$$M_r = \left\{\phi^{(r)}\right\}^T [M] \left\{\phi^{(r)}\right\}, \quad \omega_r^2 = \frac{1}{M_r} \left\{\phi^{(r)}\right\}^T [K] \left\{\phi^{(r)}\right\}, \quad \xi_r = \frac{1}{2\omega_r M_r} \left\{\phi^{(r)}\right\}^T [C] \left\{\phi^{(r)}\right\} \tag{14}$$

and

$$\beta_r = \frac{1}{M_r} \left\{\phi^{(r)}\right\}^T [M] \{1\}, \quad \gamma_r = \frac{1}{HM_r} \left\{\phi^{(r)}\right\}^T [M] \{h\} \tag{15}$$

In the equations above, M_r denotes modal mass while ω_r and ξ_r correspond to the *rth* fixed-base natural frequency and modal damping, respectively. For convenience, it is assumed that the modes are normalized to unity at the top of the structure $\left(\phi_N^{(r)} = 1\right)$.

By use of Eqs. (7), (12) and (13), it can be shown that the total displacement at the *jth* level of the superstructure is given by

$$\overline{U}_j = U_b + h_j \Phi_b + \sum_{r=1}^{N} \frac{(\omega/\omega_r)^2}{1 - (\omega/\omega_r)^2 + 2i\xi_r(\omega/\omega_r)} \left(\frac{F_T}{\omega^2 M_r} + \beta_r U_b + \gamma_r H \Phi_b \right) \phi_j^{(r)} \quad (16)$$

where $\phi_j^{(r)}$ denotes the amplitude of the *rth* fixed-base mode at the *jth* level.

Equation (16) shows that the total displacement at the *jth* level may be thought as being formed by two parts: the first part $(U_b + h_j \Phi_b)$ corresponds to a rigid-body motion while the second part, given by the term with the summation sign, corresponds to the deformation of the superstructure. The form of this last term indicates that the deformation of the superstructure arises from the force applied at the top (terms proportional to F_T) and from the inertial forces associated with translation and rocking of the base (terms proportional to U_b and Φ_b).

6. FIXED-BASE NATURAL FREQUENCIES AND MODAL DAMPING VALUES

One of the desired applications of forced-vibration tests is the experimental isolation of the fixed-base natural frequencies and modal damping values of the superstructure. The model just described, and, in particular, Eq. (16) provide the basis for a procedure to accomplish this objective. Equation (16) involves the total motion at a given level of the structure $\overline{U}_j$, and the translation U_b and rocking angle Φ_b of the base. These quantities can be measured over a frequency range. In addition to the known amplitude F_T of the force that the vibration generator exerts on the roof, Eq. (16) also involves the modal quantities M_r, β_r and γ_r, and the modal amplitudes $\phi_j^{(r)}$. The modes of vibration can be obtained experimentally or they can be estimated from a fixed-base model of the structure. The quantities M_r, β_r and γ_r depend on the geometry and mass distribution of the superstructure and on the fixed-base modes of vibration as indicated in Eqs. (14) and (15). Fortunately, at least for the fundamental mode, these quantities are not very sensitive to the details of the structure and can be easily estimated. The values of M_r/M_b (where M_b is the total mass of the superstructure), β_r and γ_r for the first two modes of the Millikan Library are listed in Table 4. Since the values in the E-W and N-S directions are very similar, average values of $M_1/M_b = 0.35$, $\beta_1 = 1.42$ and $\gamma_1 = 1.07$ will be used in the subsequent analysis for both directions. The corresponding modal quantities for a uniform shear wall, a structure with a uniform mass distribution and a linear first mode, and a uniform beam are also listed in Table 4 for the purpose of comparison.

The above discussion indicates that all the quantities appearing in Eq. (16), except for the fixed-base frequencies ω_r and the damping ratios ξ_r, can be determined experimentally or estimated from the structural properties. Equation (16) can then be used to determine the modal constants ω_r and ξ_r. Consider the case in which the frequency of the excitation is in the neighborhood of the fundamental fixed-base natural frequency of the superstructure. In this case, the contribution of the higher modes to the total response can be neglected and Eq. (16) reduces at the top of the structure ($j = N$) to

TABLE 4. MODAL CHARACTERISTICS OF THE MILLIKAN LIBRARY

		First Mode			Second Mode		
		M_1/M_b^*	β_1	γ_1	M_2/M_b^*	β_2	γ_2
Millikan Library							
N-S	(1)	0.38	1.42	1.02	-	-	-
	(2)	0.35	1.42	1.12	-	-	-
E-W	(1)	0.33	1.44	1.08	0.40	-0.63	-0.08
	(2)	0.36	1.38	1.04	-	-	-
Uniform Shear Wall		0.50	1.27	0.81	0.50	-0.42	0.09
Uniform Mass Distribution and Linear First Mode		0.33	1.50	1.00	-	-	0.00
Uniform Beam		0.25	1.57	1.14	0.25	-0.87	-0.18
Values Used for N-S and E-W vibrations		0.35	1.42	1.07	0.40	-0.63	-0.08

* M_b total mass of the superstructure.

(1) Based on experimental mode shapes reported by Jennings and Kuroiwa (1968).

(2) Based on experimental mode shapes reported by Foutch *et al.* (1975).

$$\overline{U}_T = U_b + H\Phi_b + \frac{(F_T/\omega^2 M_1) + \beta_1 U_b + \gamma_1 H\Phi_b}{(\omega_1/\omega)^2 - 1 + 2i\,\xi_1(\omega_1/\omega)} \tag{17}$$

where $\overline{U}_T = \overline{U}_N$ corresponds to the total motion at the top of the structure. Defining the function

$$A(\omega) = \frac{(F_T/\omega^2 M_1) + \beta_1 U_b + \gamma_1 H\Phi_b}{\overline{U}_T - U_b - H\Phi_b} \tag{18}$$

which depends only on known quantities, it is possible to write Eq. (17) in the form

$$(\omega_1/\omega)^2 - 1 + 2i\,\xi_1(\omega_1/\omega) = A(\omega) \tag{19}$$

Taking real and imaginary parts of Eq. (19) and solving for ω_1 and ξ_1 leads to the following estimates for ω_1 and ξ_1:

$$\omega_1 = \omega\left[1 + \mathrm{Re}\,A(\omega)\right]^{1/2} \tag{20}$$

$$\xi_1 = \frac{\mathrm{Im}\,A(\omega)}{2\left[1 + \mathrm{Re}\,A(\omega)\right]^{1/2}} \quad . \tag{21}$$

The frequency response data presented in the previous section has been used to compute the estimates of the fixed-base natural frequency ω_1 and of the structural modal damping ratio ξ_1 as defined by Eqs. (20) and (21). The results obtained are shown in Figs. 14 through 17 plotted versus the frequency of the excitation. It must be pointed out that independent estimates of ω_1 and ξ_1 are obtained for each value of the excitation frequency.

Two sets of estimates have been obtained: the first set is based on the assumption that the superstructure responds to the average rotation of the foundation (i.e., $\alpha = 1$ in Eq. (5)); the second estimate is based on the assumption that the superstructure is driven by the rotation of the base of the shear walls for N-S vibrations ($\alpha = 1.3$) and by the rotation of the base of the central core for E-W vibrations ($\alpha = 3.33$). In Figs. 14 through 17, as well as in the rest of this report, the first estimate is labeled "rigid foundation" while the second estimate is labeled "flexible foundation."

The results presented in Fig. 14 for vibrations in the N-S direction indicate that the estimates of the fixed-base natural frequency under the "rigid foundation" assumption range from 2.16 to 2.29 Hz while the corresponding estimates under the "flexible foundation" assumption range from 2.30 to 2.44 Hz. At the fundamental system frequency, the estimates for the two conditions are 2.16 and 2.30 Hz, respectively. These estimates of the fixed-base natural frequencies are 21 and 28 percent higher than the current fundamental system frequency of 1.79 Hz and indicate that the interaction between the structure and the soil is significant for vibrations in the N-S direction. The results presented in Fig. 15 indicate that estimates of the E-W fixed-base natural frequency at the fundamental system frequency are 1.26 and 1.38 Hz corresponding to the rigid and flexible foundation assumption, respectively. These values are 4 and 14 percent higher than the current E-W fundamental system frequency of 1.21 Hz. Since earlier vibration tests indicate fundamental system frequencies in the E-W direction in excess of 1.45 Hz it seems that the assumption of a flexible foundation is more representative. The estimates of the fixed-base natural frequencies presented in Figs. 14 and 15 exhibit minima in the vicinity of the fundamental system frequencies where the response of the structure is maximum. These minima may be associated with nonlinear response of the superstructure. Given the limitations imposed by the accuracy of the experimental procedure it is not possible to arrive at a firm conclusion.

The estimates of the structural damping ratios for vibrations in the N-S and E-W directions are shown in Figs. 16 and 17, respectively. The estimates obtained range from 0 to 1.5 percent of critical damping. For N-S vibrations, a representative value in the vicinity of the fundamental system frequency is 1.2 percent. For vibrations in the E-W direction the estimates of the structural damping ratio depend on whether the foundation is assumed rigid or flexible. If the foundation is assumed rigid a representative value for ξ_1 in the vicinity of the fundamental system frequency is 1.2 percent. The corresponding value under the assumption of a flexible foundation is 0.8 percent. These estimates of the structural damping ratio are significantly lower than the damping ratio of the complete soil-structure system (1.8 percent). The results obtained indicate

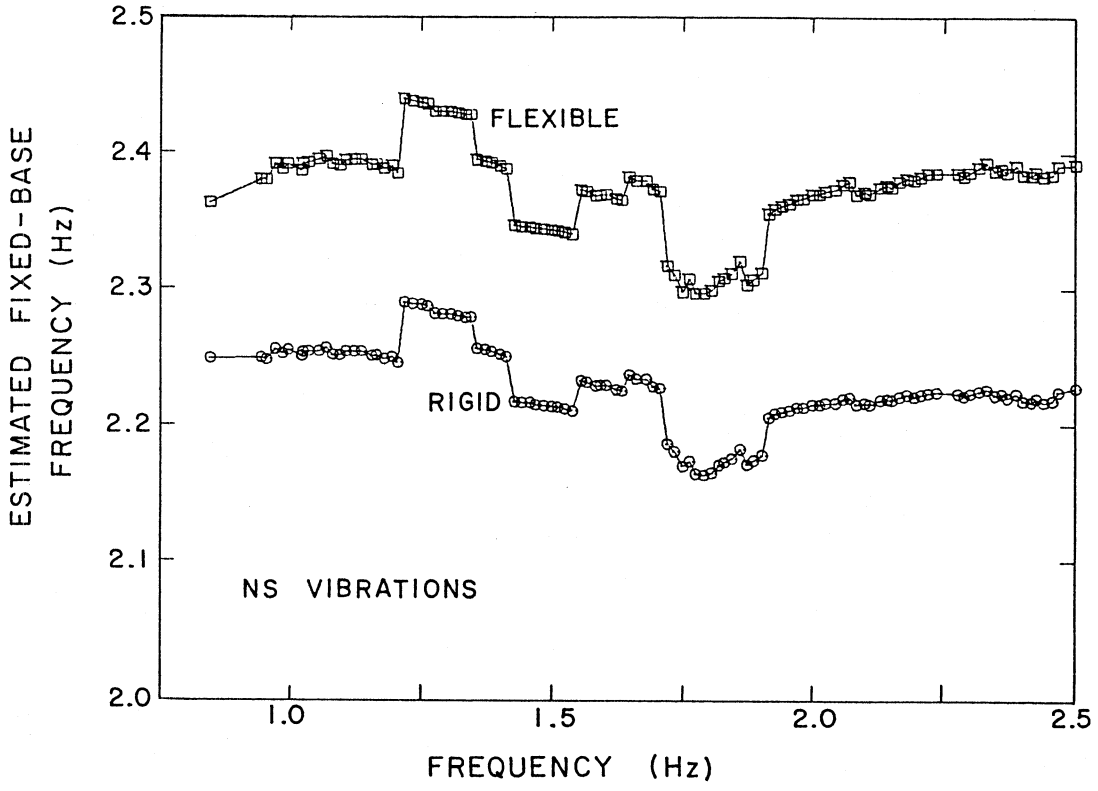

Figure 14. Estimates of the N-S fixed-base natural frequency.

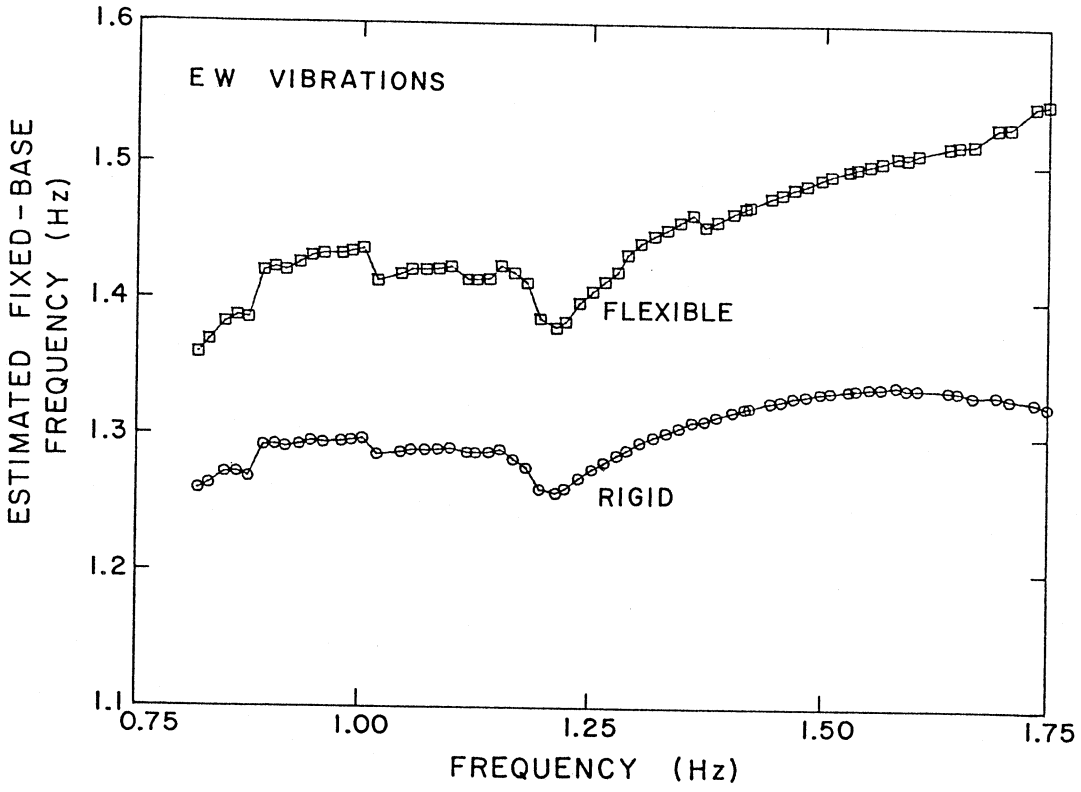

Figure 15. Estimates of the E-W fixed-base natural frequency.

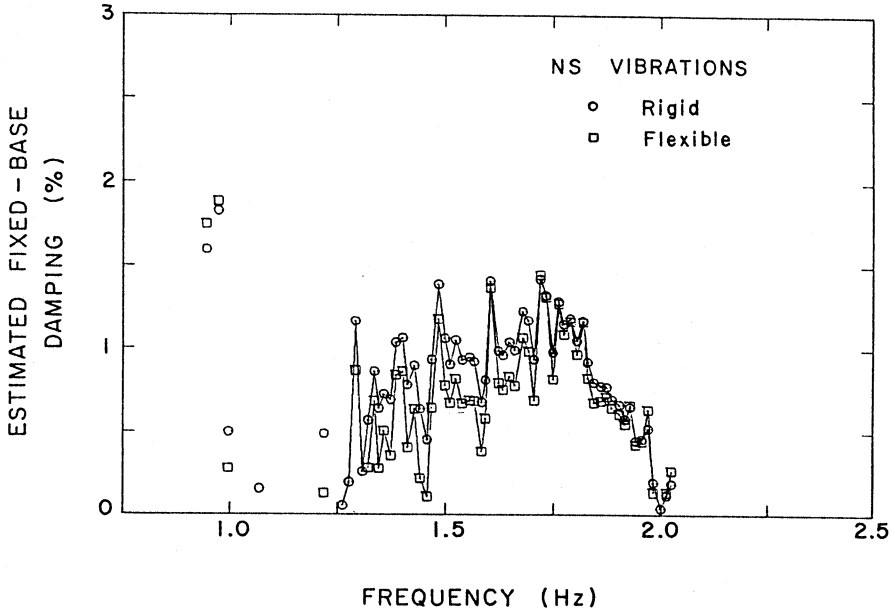

Figure 16. Estimates of the N-S modal damping ratio.

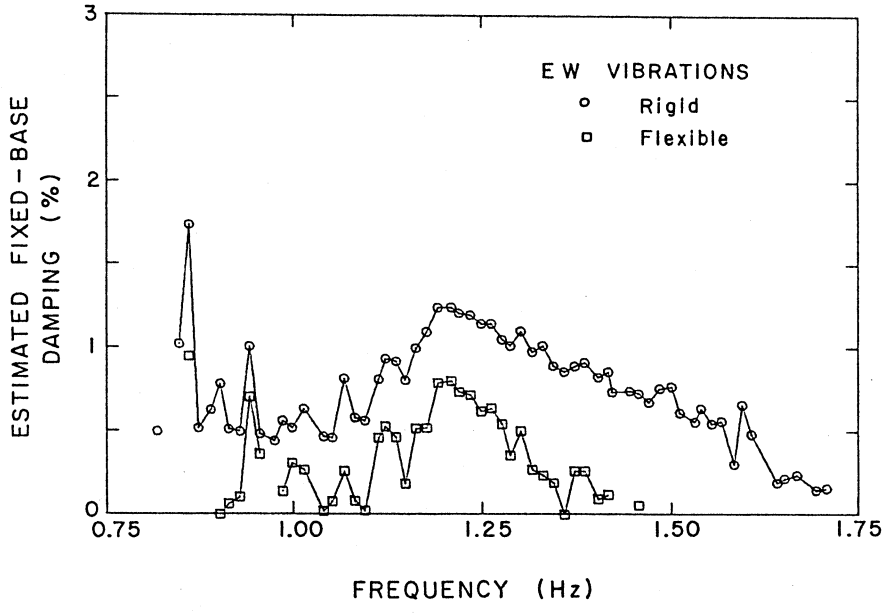

Figure 17. Estimates of the E-W modal damping ratio.

that damping values obtained from forced vibration tests without correction for the effects of soil-structure interaction may overestimate the energy dissipation in the superstructure.

The estimates of ξ_1 for frequencies close to the system frequencies (1.79 Hz and 1.21 Hz for N-S and E-W vibrations, respectively) are very sensitive to the phase differences between the response at the top and base of the structure. For frequencies away from the system frequencies, the estimates of ξ_1 are highly sensitive to the phase difference between the response at the top and the forcing function. Under these conditions small instrumental errors or errors in the parameters used to correct for instrument response may have a significant effect on the estimated damping values. The limitations in the accuracy of the phase measurements do not permit us to draw conclusions as to the nature of the energy dissipation mechanism in the structure. In particular, it is difficult to say whether attenuation should be modeled as viscous or hysteretic.

7. CONTRIBUTION OF THE BASE MOTION TO THE TOTAL RESPONSE

For frequencies in the neighborhood of the fundamental system frequency the total displacement at the top of the structure $\overline{U}_T$ can be approximated by

$$\overline{U}_T = U_b + H\Phi_b + \left[(F_T/\omega^2 M_1) + \beta_1 U_b + \gamma_1 H\Phi_b \right] Z_1(\omega) \tag{22}$$

where

$$Z_1(\omega) = \left[(\omega_1/\omega)^2 - 1 + 2i\,\xi_1(\omega_1/\omega) \right]^{-1} \tag{23}$$

The term $(U_b + H\Phi_b)$ represents the contribution of the rigid-body motion due to soil compliance to the total motion at the top. The last term in Eq. (22), i.e. $\left[(F_T/\omega^2 M_1) + \beta_1 U_b + \gamma_1 H\Phi_b \right] Z_1(\omega)$, reflects the contribution of the deformation of the superstructure to the total motion at the top. Equation (22) reveals that the deformation of the superstructure results from the effects of the force applied at the top $\left[(F_T/\omega^2 M_1)\, Z_1(\omega) \right]$ and from the effects of the inertial forces associated with translation and rocking of the base $\left((\beta_1 U_b + \gamma_1 H\Phi_b)\, Z_1(\omega) \right)$.

It must be pointed out that the interpretation of forced vibration tests is often made on the basis of the assumption that the base motion is negligible. In this case, the total motion at the top of the superstructure in the neighborhood of the fundamental frequency is approximately given by

$$\overline{U}_T = (F_T/\omega^2 M_1)\, Z_1(\omega) \quad . \tag{24}$$

Comparison of Eqs. (22) and (24) indicates that the effects of the base motion can be neglected only if (i) $| U_b + H\Phi_b | \ll | \overline{U}_T |$ and (ii) $| \beta_1 U_b + \gamma_1 H\Phi_b | \ll | F_T/\omega^2 M_1 |$. The first condition is satisfied in many cases, i.e., the rigid-body motion associated with ground compliance may be a small percentage of the total response. The second condition, however, is generally not satisfied. The term $F_T/\omega^2 M_1$ is proportional to the ratio of the eccentric mass of the vibration

generator to the total mass of the superstructure. In most cases this ratio is extremely small and, consequently, a small amount of translation or rocking of the foundation is sufficient to invalidate the second condition.

In the case of the Millikan Library, and for vibrations in the N-S direction, the rigid-body motion amounts to 37 percent of the total motion at the top already indicating significant interaction effects. The most important result, however, corresponds to the fact that at the fundamental system frequency (1.79 Hz) the quantity $| \beta_1 U_b + \gamma_1 H\Phi_b |$ is 11.2 times larger than the term $| F_T/\omega^2 M_1 |$ indicating that the deformation of the superstructure at that frequency is almost entirely caused by the inertial forces associated with motion of the foundation ($F_T/\omega^2 M_1 = 0.278 \times 10^{-4}$ m). The experimental results presented in Figs. 9 and 11 show that $| H\Phi_b | > | F_T/\omega^2 M_1 |$ over a range of frequencies, and, consequently, the inertial forces due to motion of the foundation will be more or equally important than those associated with the force applied at the top over a wide frequency range.

A vector representation of the complex quantities appearing in Eq. (22) is shown in Figs. 18a and 18b. Figure 18a represents the roof response at the fundamental system frequency ($\omega = \tilde{\omega}_1$), while Fig. 18b represents the response at the fundamental fixed-base natural frequency of the superstructure ($\omega = \omega_1$), both for vibrations in the N-S direction. For $\omega = \tilde{\omega}_1$, the total motion at the top of the structure, $\overline{U}_T$, as well as the translation and rotation of the base are essentially 90 ° out of phase with respect to the force at the top F_T. According to Eq. (22), the total motion at the top $\overline{U}_T$ corresponds to the vector sum of the terms U_b, $H\Phi_b$, $\beta_1 U_b Z_1(\omega)$, $\gamma_1 H\Phi_b Z_1(\omega)$ and $(F_T/\omega^2 M_1)\, Z_1(\omega)$. These terms are represented in Fig. 18a by the vectors OA, AB, BC, CD and DE, respectively. The total motion at the top, $\overline{U}_T$, is represented then by the vector OE, while the relative motion at the top, U_T, is represented by the vector BE. If the structure were supported on a rigid base, the total response at the top of the structure at a frequency of 1.79 Hz would correspond to the vector DE. Figure 18a illustrates that the motion of the base is responsible for almost the entire response at the fundamental system frequency. In

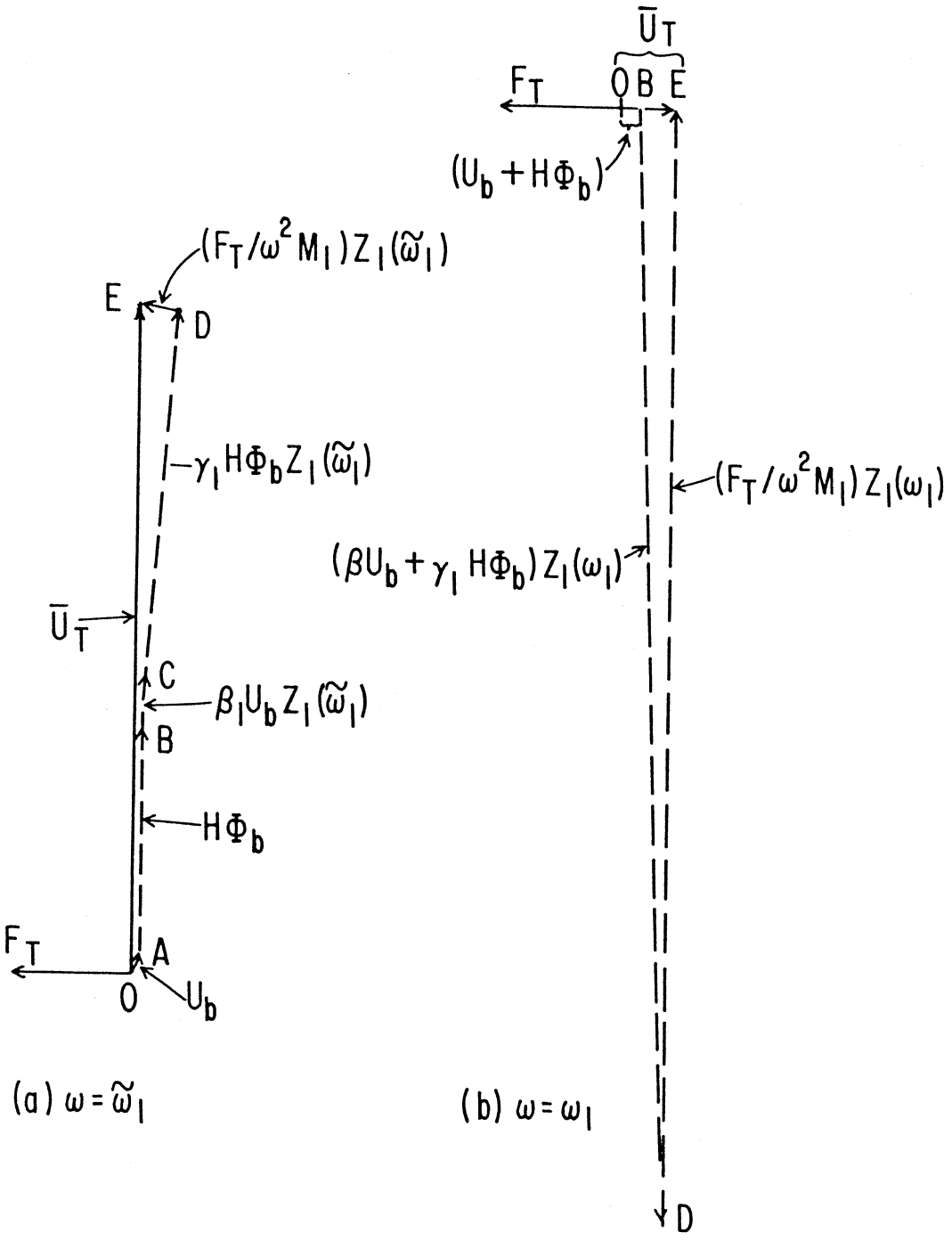

Figure 18. Vector representation of the contributions of the base translation and rotation to the total response at the top for N-S vibrations: (a) for $\omega = \tilde{\omega}_1$ and (b) for $\omega = \omega_1$.

particular, the total contribution of the motion of the base is represented by the vector OD which has an amplitude only slightly lower than the amplitude of the total response OE.

At the N-S fixed-base natural frequency of the superstructure (2.30 Hz) the total response at the top of the superstructure, represented by the vector OE in Fig. 18b, is essentially 180 ° out of phase with respect to the force F_T applied at the top. The contribution of the rigid-body motion and the relative displacement or deformation are represented by the vectors OB and BE, respectively. Figure 18b shows that in this case the deformation caused by the inertial forces due to motion of the base (vector BD) combine with the deformation due to the force applied at the top (vector DE) to yield the deformation at the top represented by the vector BE. If the structure were supported on a rigid base, the total response at the top at the fixed-base natural frequency (2.30 Hz) would be represented by the vector DE. It may be appreciated that the motion of the base has significantly modified the response of the structure at this frequency. Comparison of the vector DE in Fig. 18b with the total response represented by vector OE in Fig. 18a indicates that the soil-structure interaction effects have not only introduced a frequency shift, but have also modified the amplitude of the response that would have been obtained on the assumption of a fixed base.

Finally, if as customary, the system is modelled as a structure on a rigid base with a fixed-base natural frequency equal to the fundamental system frequency ($\omega_1 = \tilde{\omega}_1$) and a modal damping equal to the system modal damping ($\xi_1 = \tilde{\xi}_1 = 0.018$) the total response at the resonant frequency (1.79 Hz) would coincide with the experimentally determined total response represented by the vector OE in Fig. 18a. The nature of the response obtained by use of this model, however, is completely different from that obtained by considering the motion of the base. The equivalent fixed-base model would indicate that the total roof response is due to deformation of the superstructure while the experiments indicate that 37 percent of the response is associated with rigid-body motion due to soil compliance. In addition, the equivalent fixed-base model would predict that at the resonant frequency (1.79 Hz) the deformation of the superstructure would be due to the force applied at the top, while consideration of the base motion reveals that

the deformation of the superstructure, at that frequency, is mainly due to the inertial forces induced by motion of the base.

The above discussion is based on the experimental results obtained for N-S vibrations of the Millikan Library. For vibrations in the E-W direction the situation is similar, although in this case, in addition to the effects of soil compliance, the deformability of the foundation in the neighborhood of the central core also plays an important role. In the E-W direction the rigid-body motion associated with translation and rotation of the base of the central core contributes 22 percent of the total response at the roof. The deformation of the superstructure at the E-W system frequency (1.21 Hz) is again essentially controlled by the inertial forces due to motion of the base; the term $| \beta_1 U_b + \gamma_1 H \Phi_b |$ is, in this case, 7.3 times larger than $| F_T/\omega^2 M_1 |$.

8. A MODEL FOR THE COMPLETE SOIL-STRUCTURE SYSTEM

The experimental observations just described indicate that the interaction between the Millikan Library Building and the soil has a marked effect on the response of the structure during forced vibration tests. It is of interest then to attempt to reproduce the experimental observations by use of a simple mathematical model of the soil-structure system.

Previous studies of the response of the foundation of the Millikan Library (Wong, Luco and Trifunac, 1977) indicate that although the foundation experiences some deformation, the relation between the base forces and moments and the average translation and rotation of the base can be obtained by use of a rigid foundation model. Thus, if $H_S e^{i\omega t}$ and $M_S e^{i\omega t}$ represent the force and moment that the foundation exerts on the soil and $\overline{U}_b e^{i\omega t}$ and $\overline{\Phi}_b e^{i\omega t}$ represent the average translation and rotation of the base, it is possible to write

$$H_S = GL(K_{HH}\overline{U}_b + K_{HM}L\overline{\Phi}_b) \tag{25}$$

$$M_S = GL^2(K_{MH}\overline{U}_B + K_{MM}L\overline{\Phi}_b) \tag{26}$$

where K_{HH}, $K_{HM} = K_{MH}$, K_{MM} represent the complex frequency-dependent impedance functions for the foundation assumed rigid. The impedance functions are normalized by a shear modulus of reference G and a characteristic length L. Details of the foundation and soil models used to determine the impedance functions are presented in the following section.

For later use it is convenient to write Eqs. (25) and (26) in terms of the displacement $U_b = \overline{U}_b$ and rotation $\Phi_b = \alpha\overline{\Phi}_b$ of the active elements of the foundation (shear walls and central core for N-S and E-W vibrations, respectively). In this case Eqs. (26) and (27) transform into

$$\begin{Bmatrix} H_S \\ M_S/H \end{Bmatrix} = GL[\overline{K}] \begin{Bmatrix} U_b \\ H\Phi_b \end{Bmatrix} \tag{27}$$

where

$$[\overline{K}] = \begin{bmatrix} K_{HH} & \alpha^{-1}\gamma K_{HM} \\ \gamma K_{MH} & \alpha^{-1}\gamma^2 K_{MM} \end{bmatrix} \tag{28}$$

and $\gamma = L/H$.

The horizontal force H_S and the moment M_S that the foundation exerts on the soil can also be obtained by consideration of the variation of the linear and angular momenta of the superstructure and foundation. For the lumped mass model of the superstructure shown in Fig. 13, it is found that

$$H_S = F_T + \omega^2 M_o \overline{U}_b + \omega^2 \{1\}^T [M] \{\overline{U}\} \tag{29}$$

$$M_S = HF_T + \omega^2 I_o \overline{\Phi}_b + \omega^2 I_{ob} \Phi_b + \omega^2 \{h\} [M] \{\overline{U}\} \tag{30}$$

where M_o corresponds to the mass of the foundation, I_o to the mass moment of inertia of the foundation with respect to a horizontal axis through the center of the basement slab, and I_{ob} to the sum of the moments of inertia of all floors with respect to horizontal axes through the centers of each floor. In Eq. (30) the contribution of the rotary inertia associated with deformation of the superstructure has been neglected.

Substitution from Eq. (16) into Eqs. (29) and (30), leads to

$$\begin{Bmatrix} H_S \\ M_S/H \end{Bmatrix} = \omega^2 M_b [\overline{M}] \begin{Bmatrix} U_b \\ H\Phi_b \end{Bmatrix} + \{\overline{F}\} F_T \tag{31}$$

where

$$[\overline{M}] = \begin{bmatrix} \left(1 + \dfrac{M_o}{M_b}\right) & \left(\dfrac{S_b}{HM_b}\right) \\ \left(\dfrac{S_b}{HM_b}\right) & \left(\dfrac{\alpha^{-1} I_o + I_{ob} + I_b}{H^2 M_b}\right) \end{bmatrix} + \sum_{r=1}^{N} \begin{bmatrix} \beta_r^2 & \beta_r \gamma_r \\ \beta_r \gamma_r & \gamma_r^2 \end{bmatrix} \frac{M_r}{M_b} Z_r \tag{32}$$

and

$$\{\overline{F}\} = \begin{Bmatrix} 1 \\ 1 \end{Bmatrix} + \sum_{r=1}^{N} \begin{Bmatrix} \beta_r \\ \gamma_r \end{Bmatrix} Z_r \quad . \tag{33}$$

In the above equations,

$$Z_r = \left((\omega_r/\omega)^2 - 1 + 2i\,\xi_r(\omega_r/\omega) \right)^{-1} \tag{34}$$

and

$$S_b = \{h\}^T [M] \{1\} \tag{35}$$

$$I_b = \{h\}^T [M] \{h\} \ . \tag{36}$$

Eliminating H_S and M_S from Eqs. (27) and (31), and solving for U_b and Φ_b results in

$$\left\{ \begin{array}{c} U_b \\ H\Phi_b \end{array} \right\} = \left(\frac{\omega}{\omega_1} \right)^2 \kappa \left([\overline{K}] - \left(\frac{\omega}{\omega_1} \right)^2 \kappa [\overline{M}] \right)^{-1} \{\overline{F}\} \left(\frac{F_T}{\omega^2 M_b} \right) \tag{37}$$

where κ is a dimensionless parameter defined by

$$\kappa = \frac{\omega_1^2 M_b}{GL} \ , \tag{38}$$

characterizing the relative stiffness of the structure as compared with that of the soil. Equation (37) provides the means to compute the translation and rotation of the foundation from knowledge of the properties of the superstructure, foundation and soil. Once the translation and rotation of the foundation have been obtained, other quantities of interest may be easily calculated. For instance, substitution from Eq. (37) into Eq. (27) leads to the following expressions for the force and moment that the foundation exerts on the soil

$$\left\{ \begin{array}{c} H_S/F_T \\ M_S/HF_T \end{array} \right\} = [\overline{K}] \left([\overline{K}] - \left(\frac{\omega}{\omega_1} \right)^2 \kappa [\overline{M}] \right)^{-1} \{\overline{F}\} \ . \tag{39}$$

The total displacement $\overline{U}_T$ at the top of the structure ($\overline{U}_T = \overline{U}_N$) may be obtained by substitution from Eq. (37) into Eq. (16), resulting in

$$\overline{U}_T/(F_T/\omega^2 M_b) = \left(\sum_{r=1}^{N} \frac{M_b}{M_r} Z_r \right) + \left(\frac{\omega}{\omega_1} \right)^2 \kappa \{\overline{F}\}^T \left([\overline{K}] - \left(\frac{\omega}{\omega_1} \right)^2 \kappa [\overline{M}] \right)^{-1} \{\overline{F}\} \tag{40}$$

The first term in the right-hand side of Eq. (40) represents the total displacement at the top of the structure if the soil were rigid ($\kappa = 0$); the second term corresponds to the motion at the top

associated with the flexibility of the soil. After discussing the foundation and soil models employed to evaluate the foundation impedance functions, Eqs. (37) and (40) will be used to calculate estimates of the response which may be compared with the experimental observations.

9. IMPEDANCE FUNCTIONS FOR THE FOUNDATION

In plan, the foundation of the Millikan Library building is rectangular with dimensions of 25.1 m × 23.3 m (82.5 × 76.5 ft) with additional areas of 9.9 × 1.7 m (32.5 × 5.5 ft) and 9.9 × 3.5 m (32.5 × 11.5 ft) at the east and west extremes, respectively. The radius of a circular foundation of equal area is 14.2 m (46.7 ft), while the radii for circular foundations with equal moments of inertia about E-W and N-S axes are 13.6 m (44.7 ft) and 15.2 m (49.7 ft), respectively. The embedment depth varies from about 4.0 m (13 ft) along the north and south ends to about 5.5 m (18 ft) on the central E-W foundation pad. For the purpose of calculating the impedance functions in the N-S direction, the foundation was modelled as a rigid cylinder with a base radius of 13.7 m (45 ft) embedded in the soil to a depth of 4.0 m (13 ft). For vibrations in the E-W direction, the foundation was modelled as a rigid cylinder with a radius of 13.7 m (45 ft) embedded to a depth of 5.5 m (18 ft). The embedment depths of the equivalent cylinders were selected to correspond to embedment depths of the active elements of the actual foundation for rocking vibrations in the N-S and E-W directions.

The soil properties at the site were investigated by Converse Foundation Engineers (1959) six years before construction of the library. A summary of test results has been presented by Jennings and Kuroiwa (1968). The soil consists of medium to dense sands with gravel. Firm soil was found at a depth of about 5.5 m (18 ft) below the ground level. The shear wave velocities in the upper layers at the Millikan Library and at the Athenaeum Building (located 370 m) from the Library) have been determined by Eguchi *et al.* (1976). The shear wave velocities at a boring next to the Arms Laboratory at a distance of 76 m from the library have been measured by Shannon and Wilson and Agbabian Associates (1976). The shear wave velocities at these three sites are listed in Table 5. For the purpose of the model studied here, the shear waves velocities below the depth of 9.75 m (32 ft) were averaged to obtain the velocity profile listed in the last column of Table 5. The velocity profile thus obtained is consistent with the soil mechanics information available. The soil model considered consists of nine viscoelastic layers resting on a uniform viscoelastic half-space. The unit weight of soil in all layers is taken to be 18.1×10^3 N/m^3

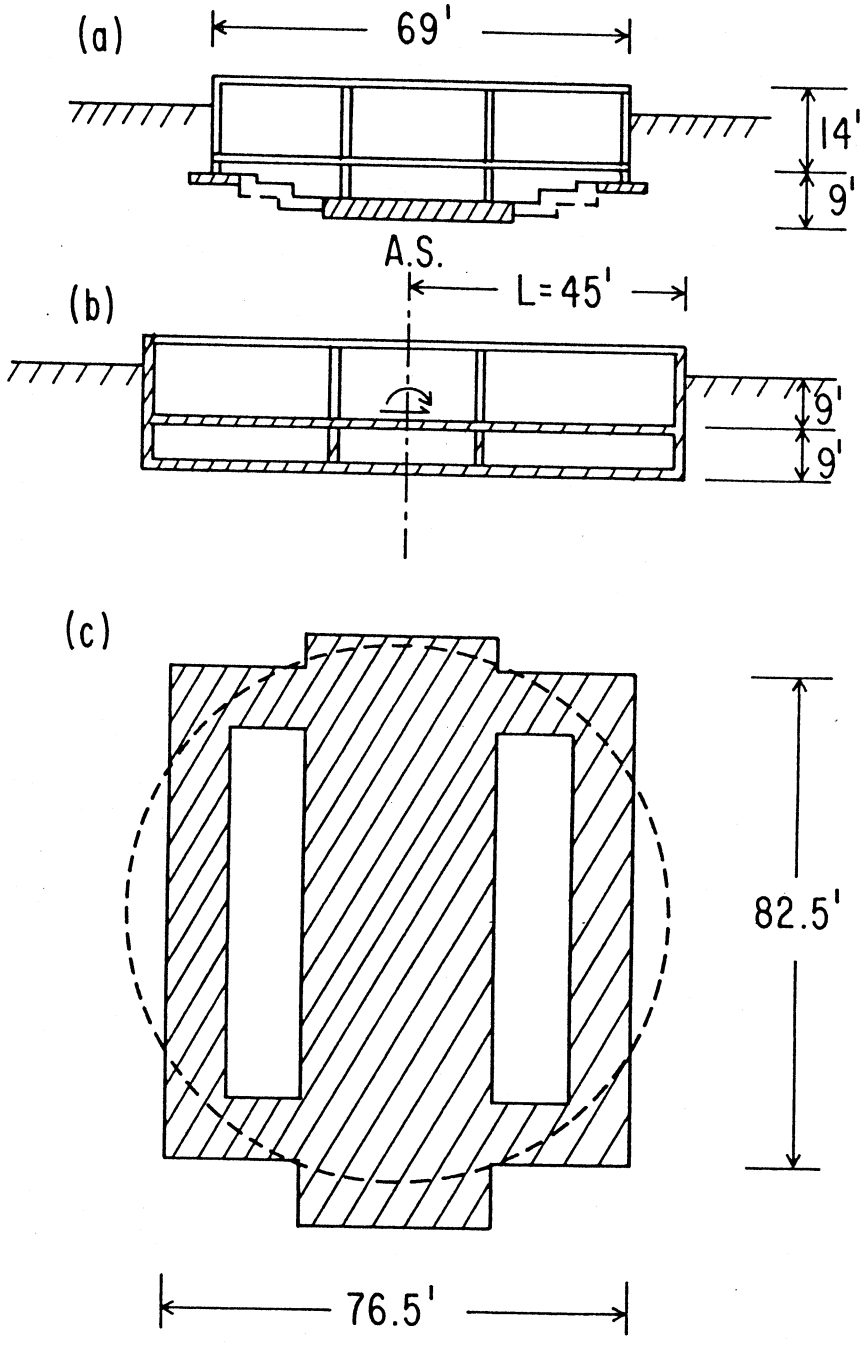

Figure 19. Foundation model

(a) N-S section of actual foundation,

(b) section of foundation model for E-W vibrations, and

(c) plan view of actual foundation and model.

TABLE 5. SHEAR WAVE VELOCITIES

Depth Range m (ft)	SHEAR WAVE VELOCITIES, m/sec (ft/sec)							
	Millikan Library[1]		Athenaeum Building[1]		Arms Laboratory[2]		Average Model	
0-1.83 (0- 6)	298.7	(980)	262.1	(860)	192.0	(630)	298.7	(980)
1.83-2.74 (6- 9)	298.7	(980)	262.1	(860)	338.3	(1110)	298.7	(980)
2.74-5.49 (9- 18)	298.7	(980)	365.8	(1200)	338.3	(1110)	298.7	(980)
5.49-7.01 (18- 23)	387.1	(1270)	420.6	(1380)	338.3	(1110)	387.1	(1270)
7.01-9.75 (23- 32)	387.1	(1270)	420.6	(1380)	487.7	(1600)	837.1	(1270)
9.75-13.41 (32- 44)			420.6	(1380)	487.7	(1600)	454.2	(1490)
13.41-20.12 (44- 66)					487.77	(1600)	487.7	(1600)
20.12-102.41 (66-336)					609.6	(2000)	609.6	(2000)
102.41-118.57 (336-389)					762.0	(2500)	762.0	(2500)
118.57- (389-)					944.8	(3100)	944.8	(3100)

(1) Eguchi *et al.* (1976).
(2) Shannon and Wilson, Inc. and Agbabian Associates (1976).

(115 lb/ft^3) and the P wave velocities were taken to be twice the corresponding shear wave velocities. It was assumed that the hysteretic damping ratios for P and S waves are equal $\xi_P = \xi_S$. Calculations were performed for a value of $\xi_S = 0.02$ for all layers.

The rocking, horizontal and coupling impedance functions for the foundation model were evaluated by use of an indirect boundary integral equation approach which involves the Green's functions for the layered viscoelastic soil model (Luco and Apsel, 1986). The calculated impedance functions were referred to the center of the basement slab located 4.3 m (14 ft) below the first floor slab as illustrated in Fig. 19. The horizontal impedance functions were multiplied by the factor (14.23/13.72) to account for the difference between the equivalent radius for a circular foundation of equal area (a_{eq} = 14.23 m) and the radius of the model (a = 13.72 m). Similarly, the rocking impedance functions for vibrations in the N-S and E-W directions were multiplied by the factors $(13.62/13.72)^3$ and $(15.15/13.72)^3$, respectively. The coupling impedance functions were left unmodified. The real parts of the corrected impedance functions are shown versus frequency in Figs. 20 and 21 (solid lines). The imaginary parts divided by the dimensionless frequency $a_o = \omega L/\beta$, where L = 13.7 m (45 ft) and β = 382 m/sec (1253 ft/sec) are a length and shear wave velocity of reference, are shown with segmented lines in the same figures. The impedance functions are normalized by the shear modulus of reference $G = 2.68 \times 10^8$ N/m^2 (38.9×10^3 psi) and the length of reference L.

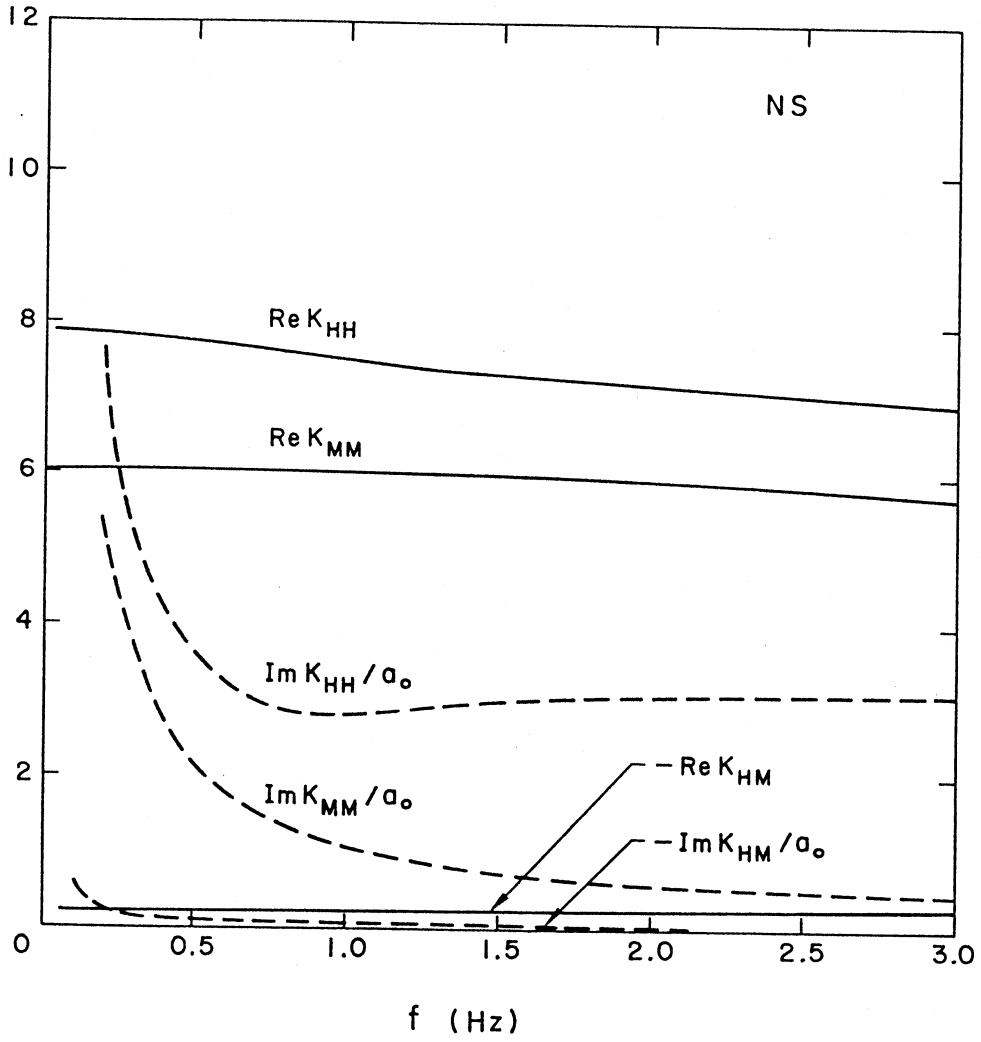

Figure 20. Foundation impedance functions for N-S vibrations.

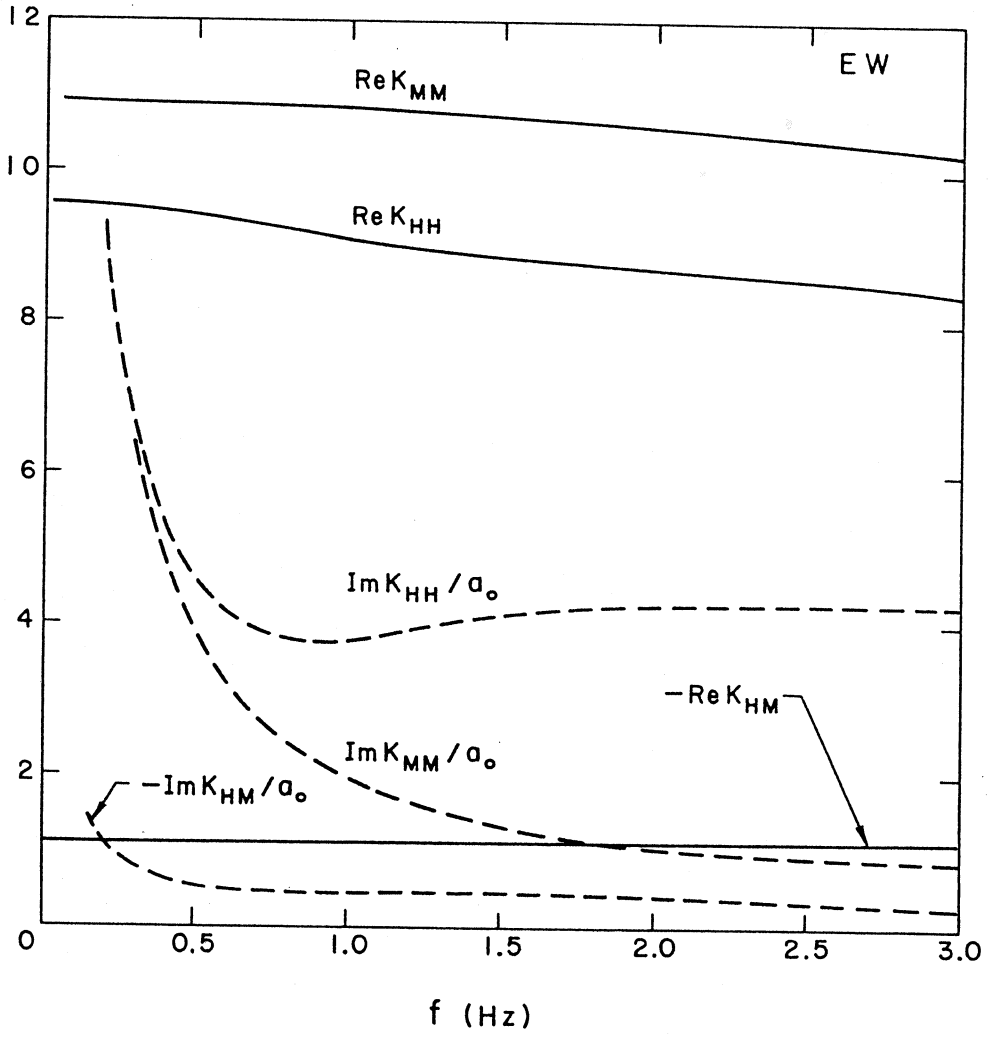

Figure 21. Foundation impedance functions for E-W vibrations.

10. COMPARISON OF EXPERIMENTAL AND THEORETICAL RESULTS

The structural, foundation and soil models described in the previous sections have been used to calculate the response of the Millikan Library Building during forced vibration tests. The model of the superstructure involves the parameters M_b, S_b, I_b, I_{ob} and H, and the modal quantities ω_r, ξ_r, M_r, β_r and γ_r. The first set of parameters was evaluated on the basis of the geometry of the structure and from the mass distribution reported by Jennings and Kuroiwa (1968). The quantities M_r/M_b, β_r and γ_r for the first two fixed-base modes, appearing in the last line of Table 4, were obtained from knowledge of the geometry and mass distribution of the superstructure and from the experimental mode shapes reported by Jennings and Kuroiwa (1968) and Foutch *et al.* (1975). The quantities ω_2 and ξ_2 were estimated from the results of forced vibration tests. The values used for the fundamental fixed-base frequencies (ω_1) and modal damping ratios (ξ_1) are estimates based on the results shown in Figs. 14 to 17 for two cases corresponding to the assumptions of "rigid" and "flexible" foundations, respectively. An exception, to be discussed later on, is the fixed-base damping ratio ξ_1 for E-W vibrations which is assigned a value of 1.5 percent for both the "rigid" and "flexible" foundation models (Table 6). No attempt was made to evaluate the fundamental fixed-base frequencies directly from the elastic properties of the structure. Such calculations have limited accuracy and would not permit us to discriminate whether the "rigid" or "flexible" foundation model is more appropriate.

The foundation model is characterized by the parameters M_o and I_o listed in Table 6 and by the normalized impedance functions shown in Figs. 20 and 21. The shear modulus of reference has been taken to be $G = 2.68 \times 10^8$ N/m^2 (38.9×10^3 psi) and the length of reference is $L = 13.72$ m (45 ft). The flexibility of the foundation is characterized by the parameter α defined by Eq. (5) ($\alpha = 1$ for the "rigid" foundation model). The values of α for the "flexible" foundation model were determined on the basis of the observed deformation of the basement slab (Table 6).

TABLE 6. CHARACTERISTICS OF THE STRUCTURAL AND FOUNDATION MODELS

	N-S		E-W	
	Rigid	Flexible	Rigid	Flexible
α	1.00	1.33	1.00	3.33
$\omega_1/2\pi$ (Hz)	2.16	2.30	1.26	1.38
ξ_1	0.012	0.012	0.015	0.015
$\omega_2/2\pi$ (Hz)	10.0	10.0	6.20	6.20
ξ_2	0.012	0.012	0.015	0.015
κ	0.533	0.605	0.181	0.218
S_b/HM_b	0.554		0.554	
I_b/H^2M_b	0.395		0.395	
I_{ob}/H^2M_b	0.027		0.030	
M_o/M_b	0.136		0.136	
I_o/H^2M_b	0.004		0.005	

The theoretical results for "flexible" and "rigid" foundation models and for vibrations in the N-S and E-W directions are compared with the experimental values in Table 7 and Figs. 22 to 25. Considering first the comparisons for N-S vibrations, it is observed that the theoretical calculations for both the "flexible" and "rigid" foundation models lead to a system frequency of 1.81 Hz which is only one percent larger than the observed system frequency of 1.79 Hz. The amplitudes of the total response at the top U_T, normalized rotation $H\Phi_b$ and normalized average rotation of the foundation $H\overline{\Phi}_b$ agree closely with the observed amplitudes at the system frequency (Table 7). The calculated translation of the base $\overline{U}_b$ at the system frequency, on the other hand, is 26 to 29 percent lower than the observed response. The comparisons of the frequency response curves for "flexible" and "rigid" foundation models shown in Figs. 22 and 23, respectively, also illustrate excellent agreement between theoretical and experimental values for U_T, $H\Phi_b$ and $H\overline{\Phi}_b$ and some discrepancy on the calculated value of the translation of the base $\overline{U}_b$. The quality of the comparison for the "flexible" and "rigid" foundation models is similar and, consequently, it is not possible to discriminate between the two models on the basis of these comparisons.

For E-W vibrations it is found that the calculated system frequency is 1.205 Hz which is only half-of-one-percent lower than the observed value of 1.21 Hz. At the system frequency, the calculated amplitudes of $\overline{U}_T$, $H\Phi_b$, $H\overline{\Phi}_b$ and U_b match the corresponding observed amplitudes with an error of less than 3 percent (Table 7). The comparisons of the frequency response curves presented in Figs. 24 and 25 show excellent agreement between calculated and observed responses for frequencies below 1.21 Hz. For higher frequencies, the theoretical results are lower than the observed values. This discrepancy, as explained in the following section, may be associated with the failure of the theoretical model to predict the large observed radiation damping for E-W horizontal vibrations. It has been indicated that the fixed-base modal damping value for E-W vibrations ξ_1 was taken to be 1.5 percent instead of the values of 0.8 (flexible foundation) and 1.2 (rigid foundation) percent which resulted from the identification shown in Fig. 17. This larger value of $\xi_1 = 0.015$ for the damping in the structure leads to the excellent agreement in response

TABLE 7. COMPARISON OF CALCULATED AND OBSERVED RESPONSE AT THE SYSTEM FREQUENCY

		N-S			E-W		
		Calculated		Observed	Calculated		Observed
		Rigid	Flexible		Rigid	Flexible	
$\tilde{f}_1$	(Hz)	1.810	1.810	1.79	1.205	1.205	1.21
$\lvert \overline{U}_T \rvert$	(10^{-4}m)	7.99	7.57	7.59	8.76	8.58	8.49
$\lvert H\Phi_b \rvert$	(10^{-4}m)	-	2.53	2.51	-	1.81	1.76
$\lvert H\overline{\Phi}_b \rvert$	(10^{-4}m)	1.99	1.90	1.94	0.54	0.54	0.53
$\lvert U_b \rvert$	(10^{-4}m)	0.218	0.225	0.306	0.103	0.102	0.100

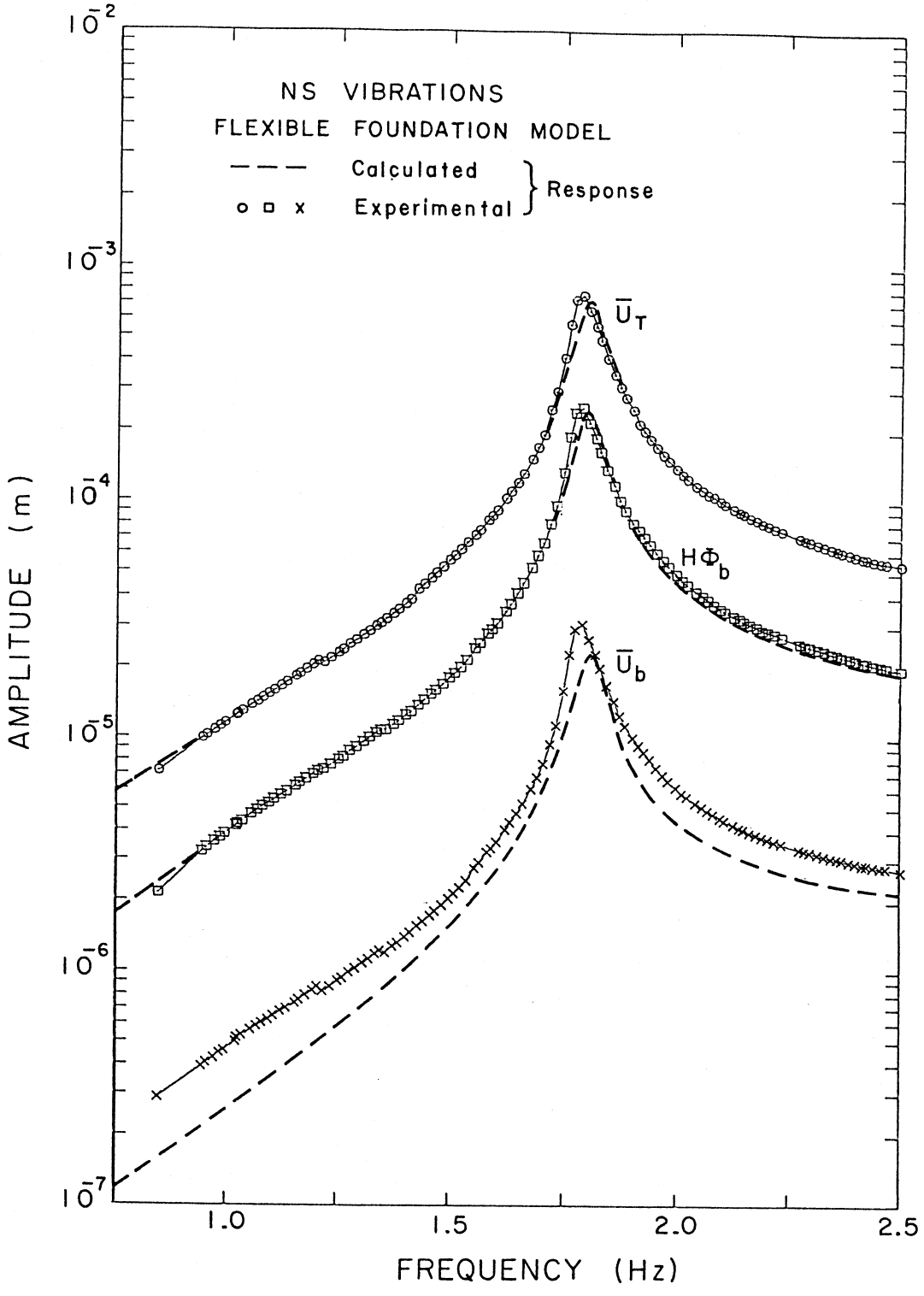

Figure 22. Comparison of the calculated and observed response in the N-S direction (flexible foundation).

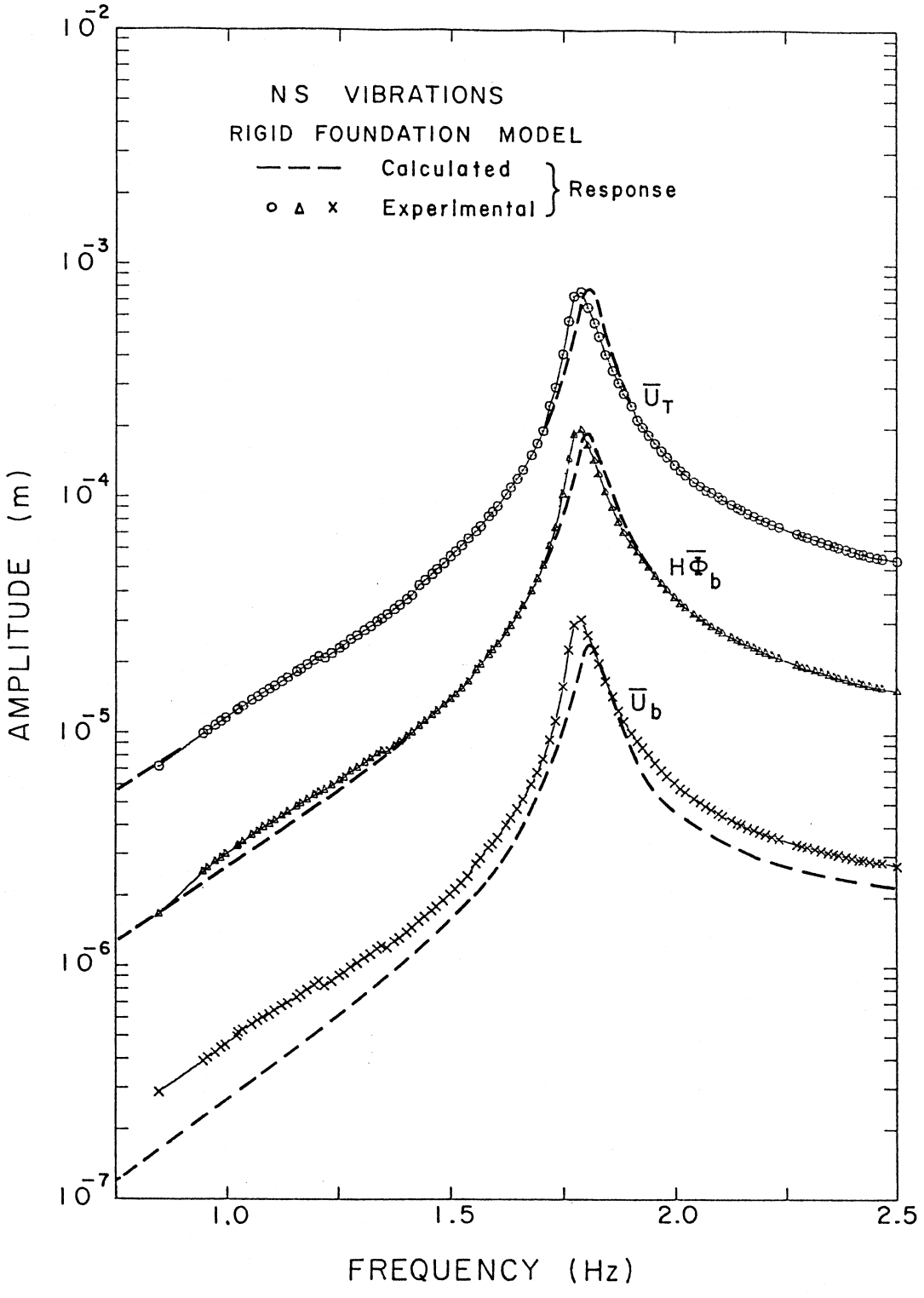

Figure 23. Comparison of the calculated and observed response in the N-S direction (rigid foundation).

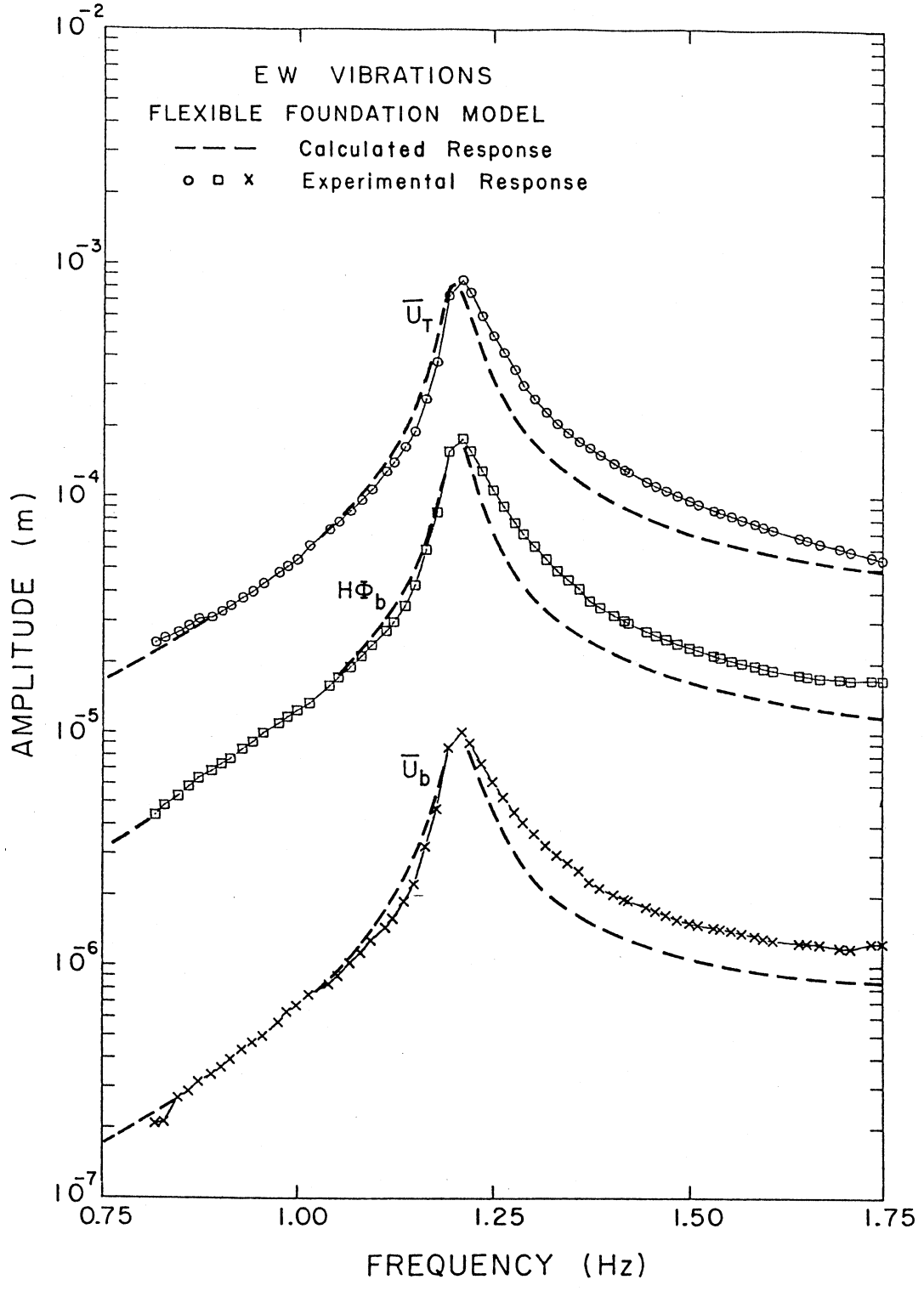

Figure 24. Comparison of the calculated and observed response in the E-W direction (flexible foundation).

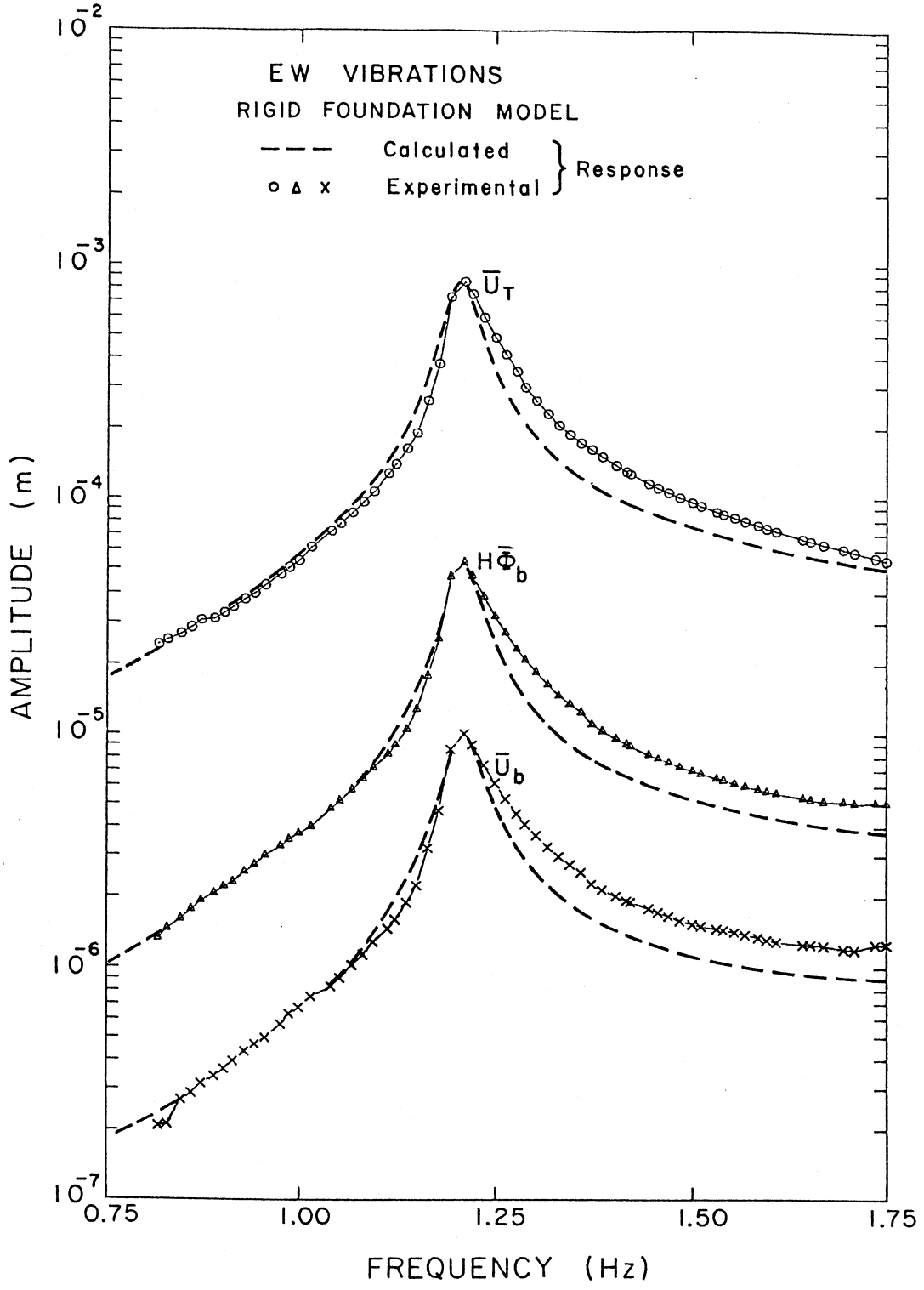

Figure 25. Comparison of the calculated and observed response in the E-W direction (rigid foundation).

at the system frequency but cannot compensate for the lack of radiation damping at frequencies higher than 1.21 Hz.

Given the lack of experimental accuracy in determining damping values (as a result of the experimental difficulty of accurately determining the phase of the response) the agreement between theoretical and observed results can be considered encouraging.

Finally, it is necessary to discuss the effects of the assumed value for the material damping in the soil ξ_S and its interdependence with the fixed-base damping value ξ_1 assumed for the superstructure. In Fig. 26, the calculated amplitude $| \overline{U}_T (\tilde{\omega}_1) |$ of the total response on the roof at the system frequency is shown versus the value of ξ_1 for soil material damping ratios ξ_S of 2 and 2.5 percent. Considering first the results for N-S vibrations, it is found that if ξ_S = 2 percent then for the calculations to match the observed response it is necessary that ξ_1 = 1.2 percent. If ξ_S = 2.5 percent then the required value for ξ_1 is 0.77 percent. For E-W vibrations, if ξ_S = 2 percent then ξ_1 must be 1.53 percent while if ξ_S = 2.5 percent then ξ_1 must be 1.33 percent. This example shows that different combinations of material damping in the soil and damping in the superstructure may lead to the same value of the response amplitude at resonance. The process of matching response amplitudes by itself is not sufficient to completely determine the damping in the superstructure.

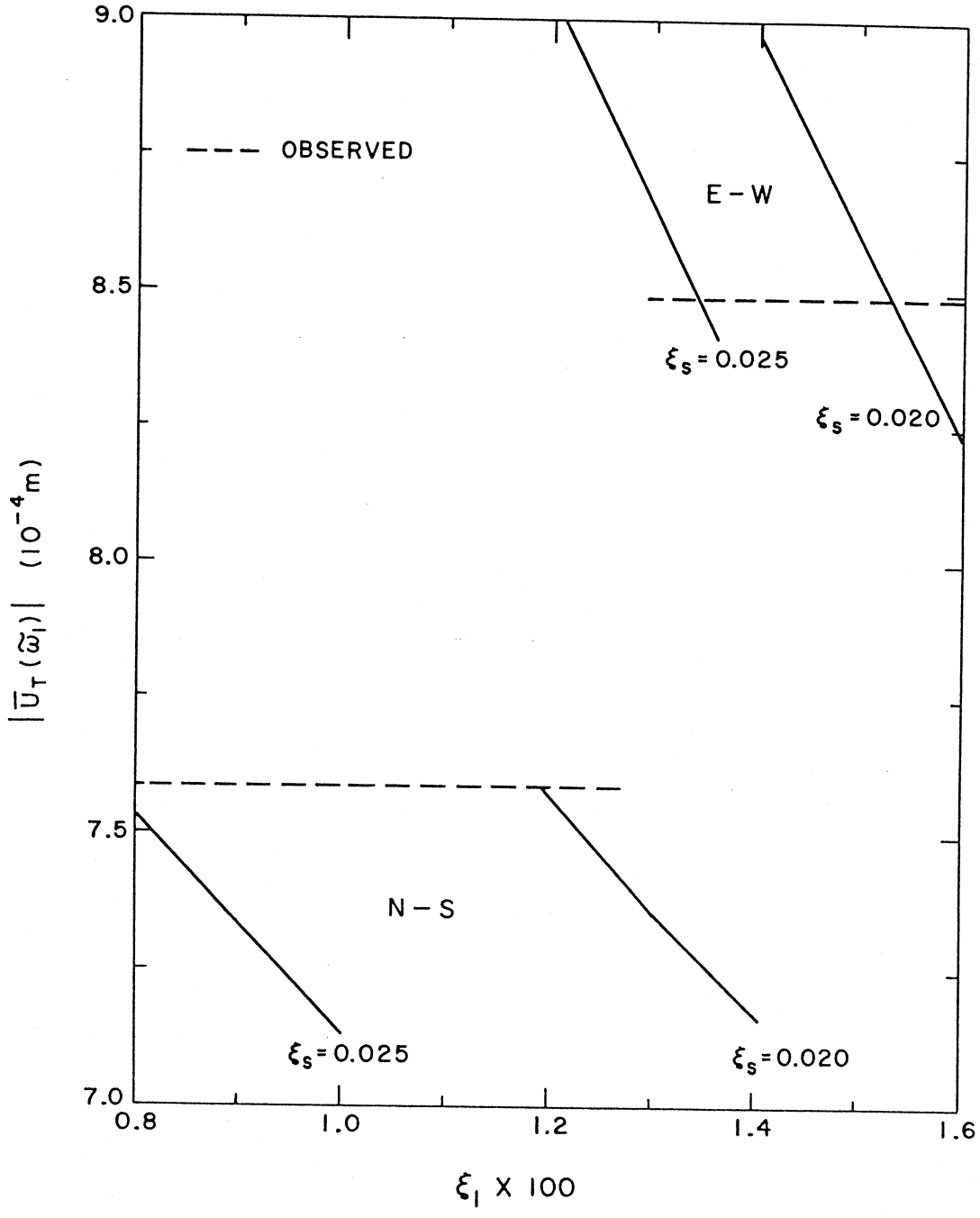

Figure 26. Effects of structural (ξ_1) and soil (ξ_S) damping on the calculated resonant response amplitude at the top of the building.

11. EXPERIMENTAL EVALUATION OF IMPEDANCE FUNCTIONS

The foundation impedance functions play an important role in soil-structure interaction studies. It is of interest to explore the possibility of determining these functions experimentally. The relations between the force and the moment that the foundation exerts on the soil and the translation and rotation of the foundation involve impedance functions as indicated by Eqs. (25) and (26) repeated here for convenience

$$H_S = GLK_{HH}\overline{U}_b + GL^2K_{HM}\overline{\Phi}_b \tag{41}$$

$$M_S = GL^2K_{MH}\overline{U}_b + GL^3K_{MM}\overline{\Phi}_b \quad . \tag{42}$$

The coupling impedance functions K_{HM} and K_{MH} are equal. By experiments of the type described herein, it is possible to determine the force and moment that the foundation exerts on the soil and the displacement and rotation of the foundation. Once these quantities have been obtained, the problem of determining the impedance functions reduces to solving the two linear equations (41) and (42) for the three unknowns K_{HH}, K_{MM} and $K_{HM} = K_{MH}$. It is apparent that it is not possible to obtain a unique solution.

Analytical evaluations of the impedance functions reveal that the normalized coupling terms $K_{HM} = K_{MH}$ are considerably smaller than the normalized diagonal terms K_{HH} and K_{MM}, which are numerically of the same order. It is possible, then, to define the following approximations to the horizontal and rocking impedances:

$$K'_{HH} = \frac{H_S}{GL\overline{U}_b} \tag{43}$$

$$K'_{MM} = \frac{M_S}{GL^3\overline{\Phi}_b} \quad . \tag{44}$$

From Eqs. (41)-(44) it is found that

$$K'_{HH} = K_{HH} + K_{HM}(L\overline{\Phi}_b/\overline{U}_b) \tag{45}$$

$$K'_{MM} = K_{MM} + K_{MH}(\overline{U}_b / L\overline{\Phi}_b) \tag{46}$$

which indicate that the error of the estimates depends on the ratio of the rocking of the foundation to the corresponding translation. It will be shown that for a superstructure of height H, the ratio $L\overline{\Phi}_b/\overline{U}_b$ is approximately proportional to the slenderness ratio H/L. For tall structures, K'_{MM} will provide an accurate approximation to K_{MM}, while K'_{HH} may not properly represent K_{HH}.

When the frequency of the excitation is in the neighborhood of fundamental fixed-base natural frequency, it is possible to obtain expressions for the force and moment that the foundation exerts on the soil from which the approximate impedance functions K'_{HH} and K'_{MM} can be readily computed. For $\omega < \omega_2$, the contributions of the second and higher modes to the base force and moment can be neglected. In this case Eqs. (31), (32) and (17) lead to

$$\frac{H_S}{\omega^2 M_b} = \frac{F_T}{\omega^2 M_b} + \left(1 + \frac{M_o}{M_b} - \beta_1 \frac{M_1}{M_b}\right)\overline{U}_b + \alpha\left(\frac{S_b}{HM_b} - \beta_1 \frac{M_1}{M_b}\right) H\overline{\Phi}_b + \beta_1 \frac{M_1}{M_b}\overline{U}_T$$

$$(\omega \ll \omega_2) \tag{47}$$

$$\frac{M_S}{\omega^2 M_b H} = \frac{F_T}{\omega^2 M_b} + \left(\frac{S_b}{HM_b} - \gamma_1 \frac{M_1}{M_b}\right)\overline{U}_b + \alpha\left(\frac{\alpha^{-1} I_o + I_{ob} + I_b}{H^2 M_b} - \gamma_1 \frac{M_1}{M_b}\right) H\overline{\Phi}_b + \gamma_1 \frac{M_1}{M_b}\overline{U}_T$$

$$(\omega \ll \omega_2)\ . \tag{48}$$

These expressions for H_S and M_S involve quantities that can be estimated (M_o, I_o, M_b, I_b, I_{ob}, M_1/M_b, β_1, γ, α) or experimentally determined ($\overline{U}_b$, $\overline{\Phi}_b$, $\overline{U}_T$).

The estimates of the approximate impedance functions K'_{MM} and K'_{HH} based on the experimental data and obtained by use of Eqs. (43), (44), (47) and (48) are shown versus frequency in Figs. 27, 28, 29 and 30. The rocking impedance functions for N-S and E-W vibrations are shown in Figs. 27 and 28 while the horizontal impedance functions for N-S and E-W vibrations are

shown in Figs. 29 and 30. In each figure the real part and the imaginary part divided by the dimensionless frequency $a_o = \omega L / \beta$ are shown for the "rigid" and "flexible" foundation models. Also shown in Figs. 27 through 30 are the theoretical estimates of K'_{MM} and K'_{HH} obtained by use of Eqs. (45) and (46) and based on the theoretical impedance functions shown in Figs. 20 and 21 and on the theoretical value of $(L\overline{\Phi}_b / \overline{U}_b)$ for the "flexible" foundation case.

A first feature of the comparison between experimental and theoretical impedance functions is the excellent agreement for the rocking stiffnesses (real part of the impedance functions) in both the N-S and E-W directions (Figs. 27 and 28). A reasonable agreement is also found for the imaginary parts of the rocking impedance functions in both directions. The comparison in Fig. 29 indicate that the theoretical horizontal stiffness in the N-S direction overestimates the corresponding experimental result by about 50%. This discrepancy is responsible for the differences shown in Figs. 22 and 23 between the observed and calculated N-S translation of the base. At the N-S resonant frequency (1.79 Hz) the theoretical and experimental imaginary parts of the N-S horizontal impedance functions are in excellent agreement but this agreement deteriorates at other frequencies.

Finally, the comparisons shown in Fig. 30 indicate that the theoretical horizontal stiffness in the E-W direction is only about 10 percent higher than the corresponding experimental value for $f = 1.21$ Hz. On the other hand, the theoretical values for the imaginary parts of the E-W horizontal impedance function are less than half of the experimental values. This discrepancy is responsible for the narrower theoretical frequency response curves for E-W vibrations shown in Figs. 24 and 25. The underestimation of the imaginary part of the horizontal impedance function in the E-W direction may have resulted from the presence of the foundation for a pond located to the east of the Library and to other details of the foundation not included in the theoretical model.

On the basis of the results presented in this section it can be concluded that estimates of the rocking and horizontal impedance functions can be obtained experimentally. Theoretical estimates of the impedance functions based on simplified models of the foundation match very closely

the experimental rocking impedances but deviate from the experimental horizontal impedance functions.

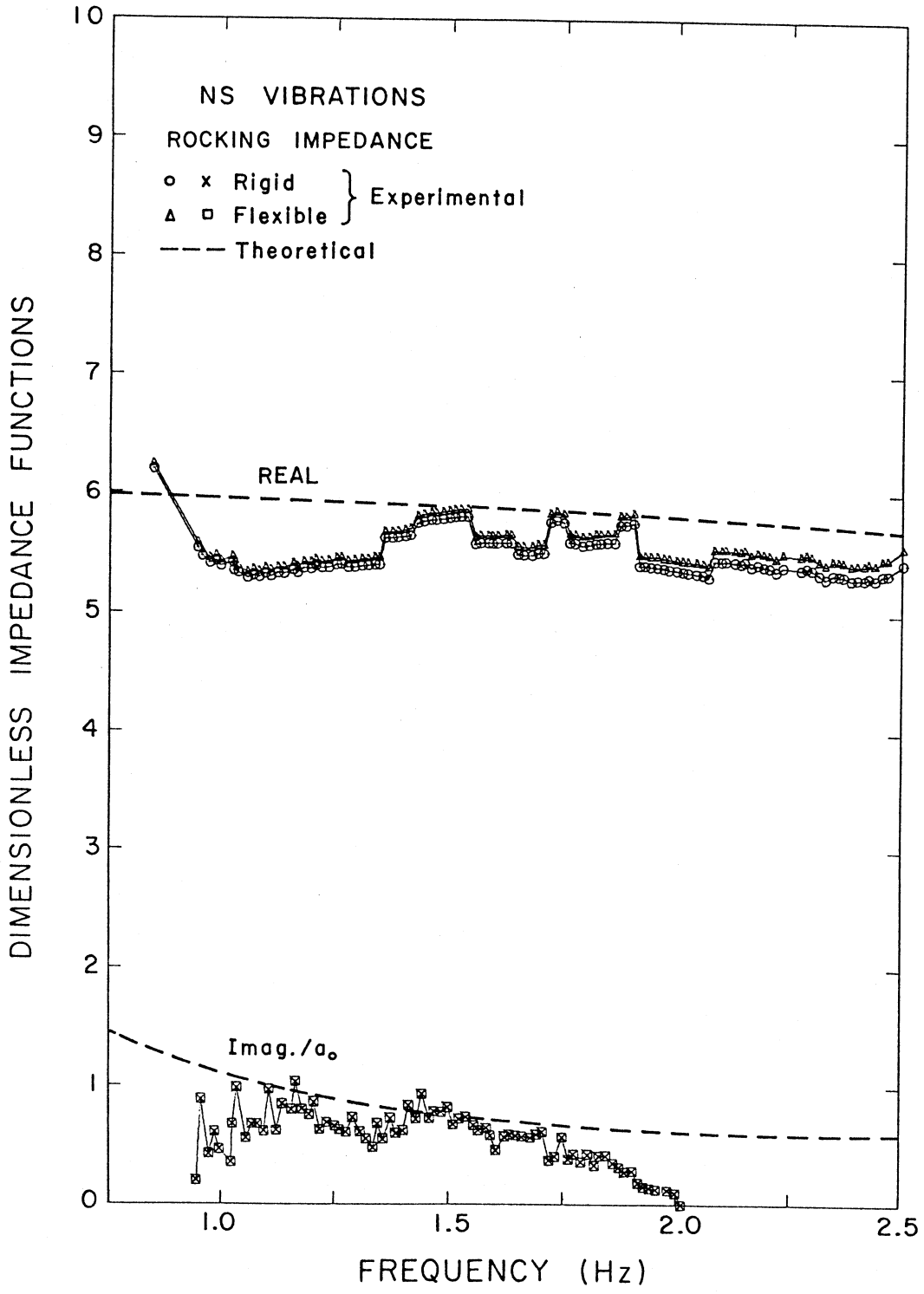

Figure 27. Comparison of calculated and observed rocking impedance functions: N-S vibrations.

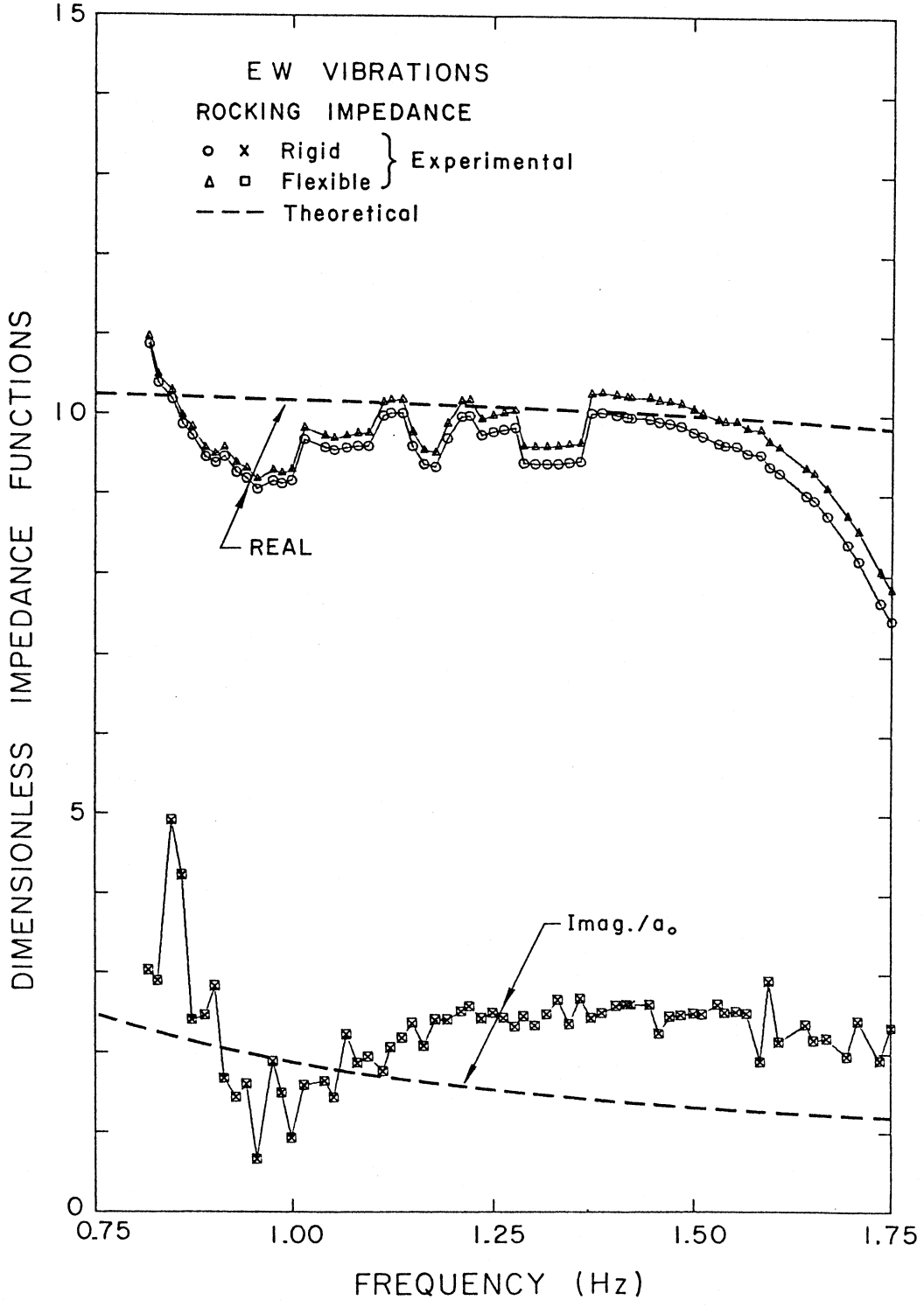

Figure 28. Comparison of calculated and observed rocking impedance functions: E-W vibrations.

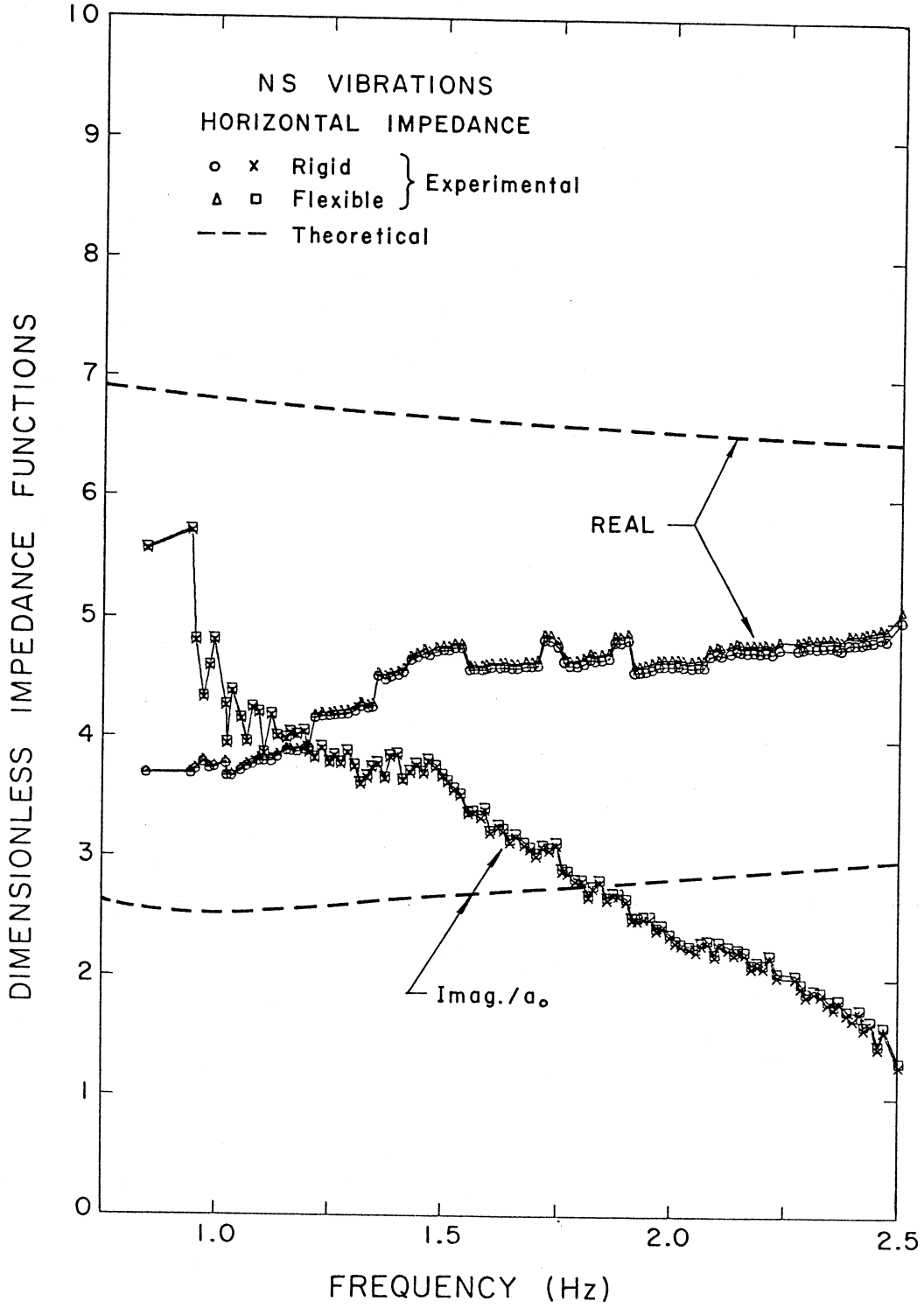

Figure 29. Comparison of calculated and observed horizontal impedance functions: N-S vibrations.

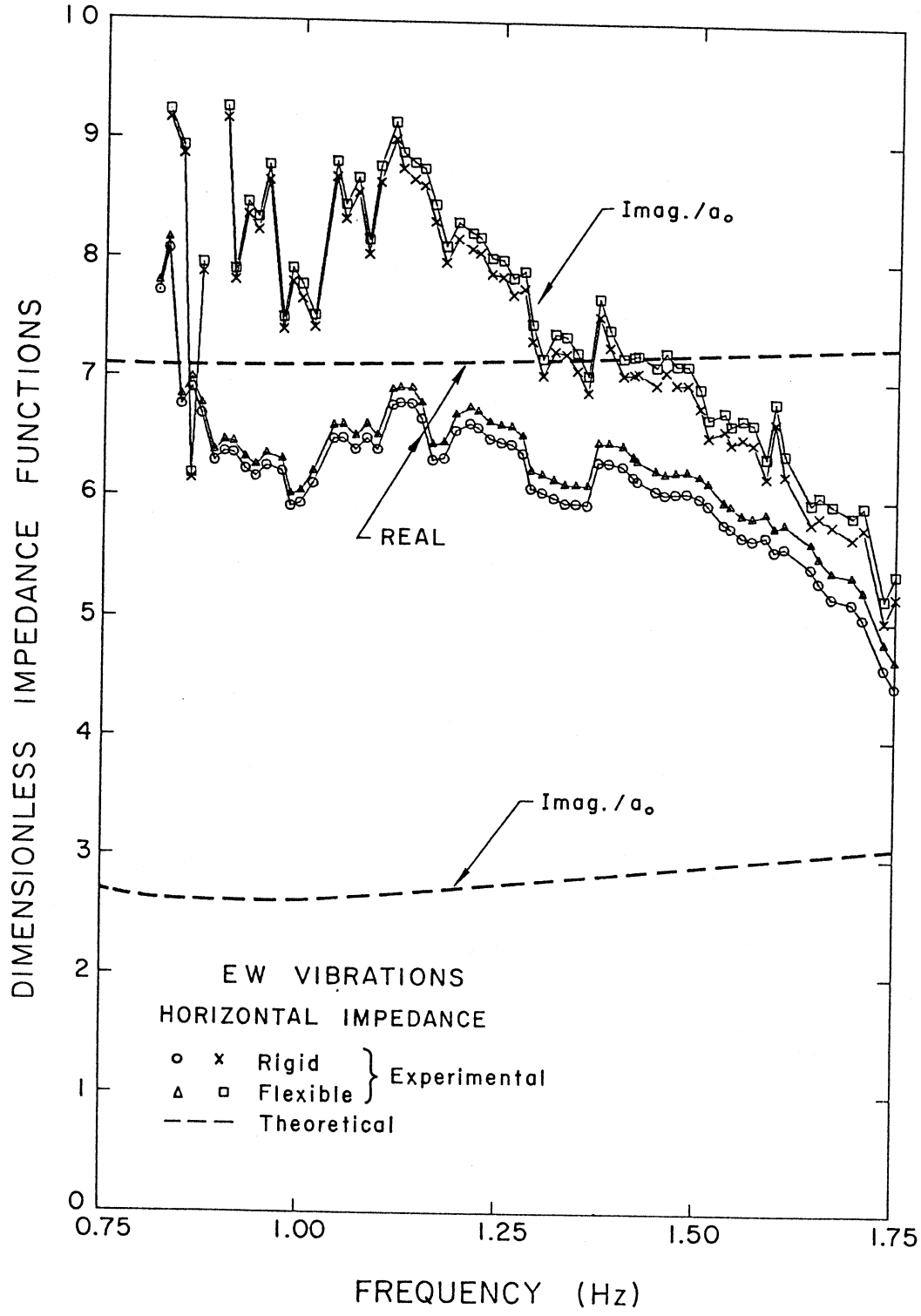

Figure 30. Comparison of calculated and observed horizontal impedance functions: E-W vibrations.

12. APPROXIMATE SOLUTION OF THE INTERACTION EQUATIONS

Preliminary analyses of the soil-structure interaction effects during forced vibration tests can be conducted on the basis of approximate solutions obtained by introducing some simplifying assumptions. These approximate solutions are also helpful in reaching a qualitative understanding of the interaction effects.

For forced vibrations in the neighborhood of the first fixed-base natural frequency, it is possible to neglect the contributions of the higher modes. In this case, the relative motion $\{U\}e^{i\omega t}$ and the total motion $\{\overline{U}\}e^{i\omega t}$ can be approximated by

$$\{U\} = \left\{\phi^{(1)}\right\} U_T \tag{49}$$

and

$$\{\overline{U}\} = \{1\}\, U_b + \{h\}\, \Phi_b + \left\{\phi^{(1)}\right\} U_T \tag{50}$$

where $U_T e^{i\omega t}$ represents the relative motion at the top of the structure ($U_T = U_N$), and $\left\{\phi^{(1)}\right\}$ denotes the fundamental fixed-base mode normalized to unity at the top of the structure ($\phi_N^{(1)} = 1$).

Substitution from Eqs. (49) and (50) into Eq. (8) and premultiplication by $\left\{\phi^{(1)}\right\}^T$ leads to

$$(-\omega^2 + 2i\omega\omega_1\xi_1 + \omega_1^2)\, U_T - \omega^2\beta_1 U_b - \omega^2\gamma_1 H\Phi_b = F_T/M_1 \tag{51}$$

in which the notation introduced in Eqs. (14) and (15) has been used.

In many cases, the mass of the foundation M_o and the moments of inertia I_o and I_{ob} are small compared with the total mass of the superstructure M_b and the moment of inertia I_b. In these cases, substitution from Eq. (50) into Eqs. (29) and (30) leads to

$$-\omega^2\beta_1 U_T - \omega^2\beta_1^2 U_b - \omega^2\beta_1\gamma_1 H\Phi_b + H_S/M_1 = F_T/M_1 \tag{52}$$

$$-\omega^2\gamma_1 U_T - \omega^2\beta_1\gamma_1 U_b - \omega^2\gamma_1^2 H\Phi_b + M_S/HM_1 = F_T/M_1 \tag{53}$$

in which terms involving M_o, I_o and I_{ob} have been neglected, and the approximations

$$M_b \sim \beta_1^2 M_1\,,\ S_b \sim \beta_1\gamma_1 M_1 H\,,\ I_b \sim \gamma_1^2 M_1 H^2 \tag{54}$$

have been introduced.

Next, the force-displacement relationships for the foundation given by Eqs. (25) and (26) are simplified by neglecting the coupling terms associated with $K_{HM} = K_{MH}$. The force-displacement relationships for the foundation reduce, then, to

$$H_S = GLK_{HH}\,U_b \tag{55}$$

and

$$M_S = GL^3 K_{MM}\,\alpha^{-1}\Phi_b \tag{56}$$

in which $U_b = \overline{U}_b$ and $\Phi_b = \alpha\overline{\Phi}_b$. The complex frequency-dependent impedance functions $K_{HH}(\omega)$ may be written in the form

$$K_{HH}(\omega) = k_{HH}(\omega) + i\left[2\xi_S k_{HH}(\omega) + \omega c_{HH}(\omega)\right] \tag{57}$$

$$K_{MM}(\omega) = k_{MM}(\omega) + i\left[2\xi_S k_{MM}(\omega) + \omega c_{MM}(\omega)\right] \tag{58}$$

where k_{HH} and k_{MM} are the translational and rocking stiffness coefficients, respectively, while c_{HH} and c_{MM} represent the translational and rocking radiation damping coefficients. The constant ξ_S represents the hysteretic damping ratio in the soil. In Eqs. (57) and (58), the imaginary parts of K_{HH} and K_{MM} have been decomposed into two parts: the first part is associated with material damping in the soil, while the second reflects the radiation of energy into the soil.

At this point, it is convenient to introduce the notation

$$\omega_H^2 = GLk_{HH}(\omega)/\beta_1^2 M_1 \tag{59}$$

$$\omega_R^2 = GL^3 k_{MM}(\omega)/\alpha\gamma_1^2 M_1 H^2 \tag{60}$$

$$\xi_{RH} = GLc_{HH}(\omega)/2\omega_H\beta_1^2 M_1 \tag{61}$$

$$\xi_{RR} = GL^3 c_{MM}(\omega)/2\omega_R\alpha\gamma_1^2 M_1 H^2 \ . \tag{62}$$

By use of Eqs. (55)-(62), it is found that Eqs. (51)-(53) reduce to

$$\left[D(\omega)\right]\left\{\begin{array}{c} U_T \\ \beta_1(\omega_H/\omega_1)U_b \\ \gamma_1(\omega_R/\omega_1)H\Phi_b \end{array}\right\} = \left\{\begin{array}{c} 1 \\ (\omega_1/\omega_H)/\beta_1 \\ (\omega_1/\omega_R)/\gamma_1 \end{array}\right\}\frac{F_T}{\omega_1^2 M_1} \tag{63}$$

where the matrix $D(\omega)$ is given by

$$\left[D(\omega)\right] = \left[\begin{array}{ccc} 1-(\omega/\omega_1)^2+2i(\omega/\omega_1)\xi_1 & -(\omega/\omega_1)(\omega/\omega_H) & -(\omega/\omega_1)(\omega/\omega_R) \\ -(\omega/\omega_1)(\omega/\omega_H) & 1-(\omega/\omega_H)^2+2i\left[\xi_S+(\omega/\omega_H)\xi_{RH}\right] & -(\omega/\omega_H)(\omega/\omega_R) \\ -(\omega/\omega_1)(\omega/\omega_R) & -(\omega/\omega_R)(\omega/\omega_H) & 1-(\omega/\omega_R)^2+2i\left[\xi_S+(\omega/\omega_R)\xi_{RR}\right] \end{array}\right] . \tag{64}$$

Solving Eq. (63) and recalling that the total displacement at the top of the structure $\overline{U}_T$ is given by $\overline{U}_T = U_T + U_b + H\Phi_b$, it is found that in the neighborhood of the resonant frequency of the complete system

$$\left\{\begin{array}{c} \overline{U}_T \\ U_T \\ U_b \\ H\Phi_b \end{array}\right\} \approx \frac{(\omega/\tilde{\omega}_1)^2}{1-(\omega/\tilde{\omega}_1)^2+2i\tilde{\xi}_1(\omega/\tilde{\omega}_1)}\left\{\begin{array}{c} 1 \\ (\tilde{\omega}_1/\omega_1)^2 \\ \beta_1^{-1}(\tilde{\omega}_1/\omega_H)^2 \\ \gamma_1^{-1}(\tilde{\omega}_1/\omega_R)^2 \end{array}\right\}\frac{F_T}{\omega^2 M_1} \tag{65}$$

where

$$\frac{1}{\tilde{\omega}_1^2} = \frac{1}{\omega_1^2} + \frac{1}{\omega_R^2} + \frac{1}{\omega_H^2} \tag{66}$$

and

$$\tilde{\xi}_1 = \left(\frac{\tilde{\omega}_1}{\omega_1}\right)^3 \xi_1 + \left[1-\left(\frac{\tilde{\omega}_1}{\omega_1}\right)^2\right]\xi_S + \left(\frac{\tilde{\omega}_1}{\omega_H}\right)^3 \xi_{RH} + \left(\frac{\tilde{\omega}_1}{\omega_R}\right)^3 \xi_{RR} \ . \tag{67}$$

In deriving Eq. (65), terms proportional to the damping coefficients ξ_1, ξ_{RH} and ξ_{RR} have been neglected from the numerator, while terms involving squares or products of the damping coefficients have been neglected from the denominator. For use of these approximate relations, the stiffness and radiation damping coefficients k_{HH}, k_{MM}, c_{HH} and c_{MM} entering into Eqs. (59)-(62) should be evaluated at the fundamental system frequency $\tilde{\omega}_1$. When the frequency is not known *a priori*, an iterative process starting with an estimate of $\tilde{\omega}_1$, may be required. Equation (65) is similar to the expression obtained by Bielak (1975) for the case of seismic excitation. Equations (66) and (67), except for notation, are equivalent to results previously obtained by Bielak.

Equation (65) indicates that, to a first approximation, the different response components are in phase with each other and reach peak amplitudes at the fundamental system frequency $\tilde{\omega}_1$. This is in agreement, for example, with the experimental observations presented in this report. Equation (65) also reveals that the total response at the top of the superstructure $\overline{U}_T$ may be obtained on the basis of an equivalent fixed-base system with fixed-base frequency and damping ratio equal to the system frequency $\tilde{\omega}_1$ and system damping ratio $\tilde{\xi}_1$, respectively. In addition, from Eq. (65) it is found that

$$U_T/\overline{U}_T = (\tilde{\omega}_1/\omega_1)^2, \quad U_b/\overline{U}_T = \beta_1^{-1}(\tilde{\omega}_1/\omega_H)^2, \quad H\Phi_b/\overline{U}_T = \gamma_1^{-1}(\tilde{\omega}_1/\omega_R)^2 \tag{68}$$

indicating that the ratios between the different response components are frequency independent in the neighborhood of the fundamental system frequency. This is also in agreement with the experimental results shown in Figs. 9 and 11. In particular, from Eqs. (65), (59), (60) and (5) it is found that the ratio

$$\frac{L\overline{\Phi}_b}{U_b} = \left(\frac{\gamma_1}{\beta_1}\right)\left(\frac{k_{HH}}{k_{MM}}\right)\left(\frac{H}{L}\right) \tag{69}$$

is proportional to the slenderness ratio H/L and is essentially independent of the relative stiffness of the superstructure to that of the soil. If the reference length L is taken equal to the radius of a

circular foundation of area equal to that of the actual foundation, then, for most foundations, $k_{HH}/k_{MM} \sim 1$. Also, for most structures, $\gamma_1/\beta_1 \sim 2/3$ indicating that $L\overline{\Phi}_b/U_b \sim (2/3)(H/L)$.

As discussed previously, the ratio $(\beta_1 U_b + \gamma_1 H\Phi_b)/(F_T/\omega^2 M_1)$ controls the relative contribution of the inertial forces induced by motion of the foundation to the deformation of the superstructure. From Eqs. (65) and (66), it may be shown that at the fundamental system frequency

$$\frac{\beta_1 U_b + \gamma_1 H\Phi_b}{F_T/\tilde{\omega}_1^2 M_1} \sim \frac{1 - \left(\frac{\tilde{\omega}_1}{\omega_1}\right)^2}{2i\tilde{\xi}_1}, \quad (\omega = \tilde{\omega}_1) \tag{70}$$

indicating that even if the system frequency is only slightly lower than the fixed-base frequency, the term $\beta_1 U_b + \gamma_1 H\Phi_b$ may have a larger amplitude than that of $F_T/\tilde{\omega}_1^2 M_1$, in which case the deformation of the superstructure will be dominated by the effects of the inertial forces induced by motion of the foundation.

The frequency ω_H defined by Eq. (59) corresponds approximately to the fundamental frequency of the system if the superstructure is assumed rigid and the foundation is prevented from rocking. Similarly, the frequency ω_R defined by Eq. (60) corresponds to the frequency of the system if the superstructure is assumed rigid and the foundation is only allowed to rock. The rocking frequency ω_R involves the constant α, and, consequently, is affected by the flexibility of the foundation (for a rigid foundation $\alpha = 1$). The frequency $(\omega_R^{-2} + \omega_H^{-2})^{-1/2}$ corresponds approximately to the frequency of the system if the superstructure is assumed rigid and the foundation is allowed to rock and translate. When the superstructure is flexible, the fundamental system frequency $\tilde{\omega}_1$ is given by Eq. (66). Although in most cases $\omega_1 < \omega_R < \omega_H$, for very rigid structures or soft soils it is possible to encounter cases in which ω_R is less than ω_1. Equation (66) indicates that the frequency shift due to soil-structure interaction depends essentially on the ratio ω_1/ω_R (for $\omega_1 = \omega_R$, the system frequency $\tilde{\omega}_1$ is approximately 30 percent lower than the fixed-base frequency ω_1).

Equation (67) reveals that the system damping ratio $\tilde{\xi}_1$ depends on the fixed-base structural damping ratio ξ_1, on the material damping on the soil ξ_S and on the radiation damping ratios

ξ_{RH} and ξ_{RR}. Depending on the relative stiffness of the structure to that of the soil, the system damping ratio may have values ranging from ξ_1 for very flexible structures ($\omega_1 \ll \omega_R < \omega_H$) to $\xi_S + (\omega_R/\omega_H)^3\xi_{RH} + \xi_{RR}$ for very soft soils ($\omega_R < \omega_H \ll \omega_1$). When the rigidity of the superstructure is high compared with that of the soil, the system damping ratio essentially measures the material and radiation damping in the soil. This is particularly important in interpreting the high values of the system damping observed under strong seismic excitation. In this case the high strains in the soil reduce the rigidity of the soil and increase the soil material damping.

The approximate relations described above have been used to calculate the response of the Millikan Library during forced vibration tests. The calculations are based on the structural properties listed in Tables 4 and 6 and on the impedance functions shown in Figs. 20 and 21. The results obtained are compared in Table 8 with the observed response. In the derivation of Eqs. (65)-(67) the effects of the coupling impedance functions have been neglected. The results calculated under this assumption are listed in Table 8 in the columns designated 1*st* iteration. After an estimate of $L\overline{\Phi}_b/\overline{U}_b$ has been obtained, it is possible to improve the accuracy of the approximation by substituting the impedance functions K_{HH} and K_{MM} (both real and imaginary parts) by the functions K'_{HH} and K'_{MM} defined by Eqs. (45) and (46). The results obtained after this substitution are listed in Table 8 under the columns designated 2*nd* iteration. The relative agreement between the calculated and observed response indicate that the approximations given by Eqs. (65)-(67) are sufficient for most practical applications.

One interesting aspect of the approximate calculations is that they provide a breakdown of the system damping into its components. For vibrations of the Millikan Library in the N-S direction Eq. (67) leads to

$$\tilde{\xi}_1 = 0.487\xi_1 + 0.381\xi_s + 0.0029 + 0.0003 \tag{71}$$

in which the last two terms correspond to the radiation damping in horizontal and rocking vibrations, respectively. For values of $\xi_1 = 0.012$ and $\xi_S = 0.02$, Eq. (71) leads to a system damping ratio of 0.0166. The contributions of the structural and material damping in the soil and of the

TABLE 8. COMPARISON OF OBSERVED AND CALCULATED RESPONSE (APPROXIMATE EQUATIONS)

	N-S			E-W		
	Calculated		Observed	Calculated		Observed
	1*st* iteration	2*nd* iteration		1*st* iteration	2*nd* iteration	
$f_H = \omega_H/2\pi$ Hz	9.50	9.02	-	10.57	9.20	-
$f_R = \omega_R/2\pi$ Hz	3.14	3.11	-	2.67	2.60	-
$\tilde{f}_1 = \tilde{\omega}_1/2\pi$ Hz	1.82	1.81	1.79	1.22	1.21	1.21
$U_T/\overline{U}_T$	0.626	0.619	0.631	0.779	0.766	0.781
$H\Phi_b/\overline{U}_T$	0.315	0.316	0.331	0.194	0.202	0.207
$U_b/\overline{U}_T$	0.026	0.028	0.040	0.009	0.012	0.012
$L\overline{\Phi}_b/\overline{U}_b$	2.91	2.65	1.97	1.97	1.59	1.68
$100\,\xi_{RH}$	34.5	35.8	-	20.5	16.7	-
$100\,\xi_{RR}$	0.18	0.15	-	-0.97	-1.03	-
$100\,\tilde{\xi}_1$	1.62	1.66	1.8	1.41	1.41	1.8
$\overline{U}_T(\tilde{\omega})$ m	8.58×10^{-4}	8.37×10^{-4}	7.59×10^{-4}	9.86×10^{-4}	9.86×10^{-4}	8.49×10^{-4}

radiation damping in the translation and rocking are, respectively: 0.0058, 0.0076, 0.0029 and 0.0003. In this case, 65 percent of the system damping stems from energy dissipation in the soil.

The approximate relations derived above can also be used to analyze the results of forced vibration tests. Assuming that U_b, $H\Phi_b$ and $\overline{U}_T$ and $\tilde{\omega}_1$ have been determined, Eqs. (66) and (68) may be used to obtain

$$\begin{Bmatrix} \omega_H \\ \omega_R \\ \omega_1 \end{Bmatrix} = \tilde{\omega}_1 \begin{Bmatrix} (\beta_1 U_b/\overline{U}_T)^{-1/2} \\ (\gamma_1 H\Phi_b/\overline{U}_T)^{-1/2} \\ (1 - \beta_1 U_b/\overline{U}_T - \gamma_1 H\Phi_b/\overline{U}_T)^{-1/2} \end{Bmatrix} . \tag{72}$$

Estimates of the horizontal and rocking stiffness can also be obtained by use of Eqs. (59), (60) and (72), leading to

$$k'_{HH} = \frac{\tilde{\omega}_1^2 \beta_1 M_1}{GL} \frac{\overline{U}_T}{U_b} \tag{73}$$

$$k'_{MM} = \alpha \frac{\tilde{\omega}_1^2 \gamma_1 M_1}{GL} \left(\frac{H}{L}\right)^2 \frac{\overline{U}_T}{H\Phi_b} . \tag{74}$$

An example of the use of these equations is provided in the following section.

13. EFFECTS OF THE SAN FERNANDO EARTHQUAKE ON THE MILLIKAN LIBRARY SYSTEM

It has been mentioned that forced vibration tests conducted by Jennings and Kuroiwa (1968) in 1966-67 seem to indicate a small contribution of the motion of the base to the total motion at the top of the structure in contrast to the results of the more recent tests conducted by Foutch *et al.* (1975) as well as of those described in this report. Foutch and Jennings (1978) argue that the modification of the soil-structure interaction effects is associated with degradation of the foundation system as a result of the San Fernando earthquake of 1971. In addition, the results of a number of forced and ambient vibration tests conducted before and after the San Fernando earthquake indicate a sharp reduction in the fundamental N-S and E-W system frequencies which occurred at the time of the earthquake (Udwadia and Trifunac, 1974). It is of interest to analyze these apparent changes in response and to establish if they are associated with degradation of the superstructure or of the foundation-soil system. This can be accomplished by use of the approximate relations derived in the previous section.

The pertinent results of the forced vibration tests reported by Jennings and Kuroiwa are compared in Table 9 with those obtained in the course of the present investigation. It may be observed that a significant reduction of the fundamental system frequencies has taken place in the nine years which separate both series of tests. In addition, the rocking of the foundation in the more recent tests is 24 and 14 times larger than the values reported by Jennings and Kuroiwa for vibrations in the N-S and E-W directions, respectively. The translation of the foundation in the more recent tests is 1.7 and 3.0 times larger for vibrations in the N-S and E-W directions, respectively. The rocking of the active elements of the foundation Φ_b listed in Table 9 has been obtained by multiplying the recorded average rotation of the foundation $\overline{\Phi}_b$ by the constant α also listed in Table 9, i.e. it has been assumed that the deformation pattern of the basement slab has not changed in the time comprised between the two series of tests.

TABLE 9. COMPARISON OF PRESENT AND INITIAL TEST RESULTS

	N-S		E-W	
	Present Experiment (1975)	Jennings and Kuroiwa (1968)	Present Experiment (1975)	Jennings and Kuroiwa (1968)
$\tilde{\omega}_1/2\pi$ Hz	1.79	1.92	1.21	1.48
$H\Phi_b/\overline{U}_T$	0.331	0.014	0.207	0.015
$U_b/\overline{U}_T$	0.040	0.024	0.012	0.004
α	1.3	1.3	3.33	3.33

By use of Eqs. (72)-(74) and of the data presented in Table 9, it is possible to obtain estimates of the frequencies ω_H, ω_R, of the fixed-base natural frequency of the superstructure ω_1, and of the horizontal and rocking stiffness coefficients for the foundation. The resulting estimates are presented in columns (1) and (2) of Table 10 corresponding, respectively, to the recent and the initial test data. The results presented in Table 10 indicate that the frequencies ω_H and ω_R would have experienced a significant reduction as a result of the San Fernando earthquake. Such reduction, if real, would reflect a drastic degradation of the stiffness of the foundation-soil system as revealed by the estimates of the rocking and horizontal stiffness coefficients k'_{MM} and k'_{HH}. The rocking stiffness coefficients k'_{MM} as calculated from the Jennings and Kuroiwa data for N-S and E-W vibrations would be 27 and 21 times larger, respectively, than the corresponding values calculated on the basis of the more recent test data. Similarly, the horizontal stiffness coefficients k'_{HH} computed on the basis of the pre-San Fernando earthquake data for N-S and E-W vibrations would be 2 and 4 times larger, respectively, than those values calculated from the more recent data. Comparison of the calculated fixed-base natural frequencies of the superstructure (ω_1) indicates that as a result of the San Fernando earthquake the N-S stiffness of the superstructure would have increased by 41 percent while the E-W stiffness of the superstructure would have suffered a reduction of 14 percent.

The hypothetical effects of the San Fernando earthquake just calculated do not seem plausible and indicate the possibility of an error in one of the two sets of data. In particular, the reduction of the foundation rocking stiffness by a factor of 27 and the 41 percent increase in the N-S structural stiffness seem unlikely. The radius of a circular foundation with N-S rocking stiffness equal to that of the foundation in the present condition is 13.6 m (44.7 ft). The radius of a circular foundation 27 times stiffer would be 3 larger and would correspond to 40.9 m (134.1 ft). Thus, the foundation before the San Fernando earthquake would have had an equivalent area 9 times larger than the area of the present foundation. Foutch and Jennings (1978) erroneously estimate the change in equivalent radius of the foundation to be 1.7 m (the correct change in radius required is 27.3 m) and argue that this change could be explained by cracking of the

TABLE 10. CHARACTERISTICS OF THE MILLIKAN LIBRARY BASED ON PRESENT AND INITIAL VIBRATION TESTS

	N-S		E-W	
	(1)	(2)	(1)	(2)
$f_H = \omega_H/2\pi$ Hz	7.51	10.40	9.27	19.64
$f_R = \omega_R/2\pi$ Hz	3.01	15.69	2.57	11.68
$f_1 = \omega_1/2\pi$ Hz	2.33	1.97	1.39	1.50
k'_{MM}	5.36	145.89	10.04	207.24
k'_{HH}	4.55	8.72	6.93	31.10

(1) Calculated by use of approximate relations and based on data obtained in 1975 (present experiment).

(2) Calculated by use of approximate relations and based on data obtained in 1966-67 by Jennings and Kuroiwa (1968).

foundation and by separation of small access structures initially connected to the first floor of the Library. It is difficult to justify a reduction of rocking stiffness by a factor of 27 on the basis of these small modifications.

The response of the Millikan Library in the present conditions as obtained in the tests performed in the course of this study is in agreement with the response obtained in an independent set of tests (Foutch *et al.*, 1975) and with the theoretical calculations described previously. Since the differences between the present tests and those of Jennings and Kuroiwa (1968) cannot be reconciled, it is highly likely that the results from the initial tests are subject to instrumental or data reduction errors. In these conditions, to study the effects of the San Fernando earthquake on the Millikan Library it will be necessary to rely only on the information describing the changes of the fundamental system frequencies.

During the period 1966-1975 the Millikan Library Building has been subjected to a number of forced and ambient vibration tests. The N-S and E-W fundamental system frequencies obtained in these tests are listed in Table 1 and their variation with time is illustrated in Fig. 31. In this figure the frequencies obtained by ambient, man-excited and shaker-excited vibration tests are designated by the letters A, M and S, respectively. In addition to the data from forced vibration tests, information on the change of the fundamental system frequencies during the 1970 Lytle Creek and the 1971 San Fernando earthquakes is also available (Udwadia and Trifunac, 1974). The range of variation of the fundamental system frequencies in these two earthquakes is illustrated in Fig. 31 by the segments of lines designated by E_1 and E_2.

Inspection of Fig. 31 indicates an apparent reduction in the system frequencies as a result of the San Fernando earthquake in which the base of the structure was subjected to peak acceleration of the order 0.2g. Considering the earliest and the latest shaker-excited tests as a reference, the system frequency in the N-S direction would have dropped from 1.92 Hz to 1.79 Hz, while the system frequency in the E-W direction would have dropped from 1.48 Hz to 1.21 Hz. The minimum values of the system frequencies during the strong motion part of the San Fernando

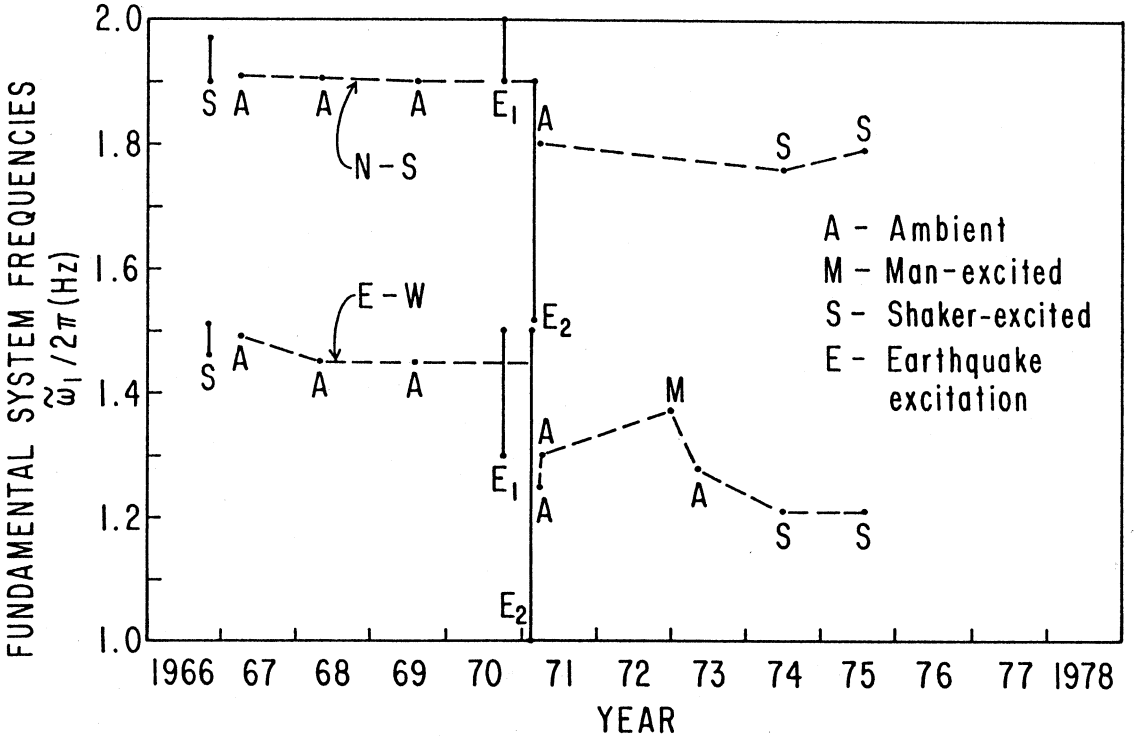

Figure 31. Variation of the observed system frequencies with time.

earthquake as calculated by Udwadia and Trifunac (1974) are approximately 1.5 and 1.0 Hz in the N-S and E-W directions, respectively.

To determine the possible modifications of the system which may have caused the observed changes in system frequencies it is convenient to refer to Eq. (66). This equation may be written in the form

$$\frac{1}{\tilde{\omega}_1^2} = \frac{1}{\overline{\omega}_1^2}\left(\frac{\overline{K}_1}{K_1}\right) + \frac{1}{\overline{\omega}_R^2}\left(\frac{\overline{K}_{MM}}{K_{MM}}\right) + \frac{1}{\overline{\omega}_H^2} \tag{75}$$

in which, $\tilde{\omega}_1$ corresponds to the fundamental system frequency when the modal stiffness of the superstructure is K_1 ($K_1 = \omega_1^2 M_1$) and the rocking stiffness of the foundation is K_{MM}. The reference values of the modal stiffness $\overline{K}_1$ and of the rocking stiffness $\overline{K}_{MM}$ correspond to those obtained in the present study and reflect the 1975 configuration of the system. The frequencies $\overline{\omega}_1$, $\overline{\omega}_R$ and $\overline{\omega}_H$ also correspond to the 1975 configuration of the system. (The values of these frequencies in Hz as calculated by use of the approximate equations are, respectively: 2.33, 3.01 and 7.51 for N-S vibrations, and 1.39, 2.57 and 9.27 for E-W vibrations). In writing Eq. (75) it has been assumed that the mass of the structure has not changed and that the small effects of variations of the horizontal stiffness of the foundation can be neglected.

For a given value of the system frequency $\tilde{\omega}_1$, Eq. (75) allows one to obtain all possible combinations of structural and foundation-soil stiffnesses consistent with that particular value of the system frequency. The combinations of values of $K_1/\overline{K}_1$ and $K_{MM}/\overline{K}_{MM}$ consistent with the system frequencies before, during and after the San Fernando earthquake are plotted in Figs. 32a and 32b corresponding to the N-S and E-W directions, respectively. The upper and middle curves in these Figs. correspond respectively to the system frequencies before and after the San Fernando earthquake. The bottom curves correspond to the system frequencies calculated at the time of the strongest shaking during the earthquake. The 1975 state of the system is represented by point A of coordinates (1,1). Since it is unlikely that before the San Fernando earthquake the structure or the foundation were more flexible than in 1975, the possible configurations of the system before the earthquake are restricted to lie on the solid line portion of the upper curves

shown in Figs. 32a and 32b. By the same type of argument it is possible to restrict the possible configurations consistent with the lower system frequencies to the solid line portion of the lower curves shown in these figures.

In trying to determine the path followed by the system during the San Fernando earthquake various alternatives are possible. One extreme interpretation is that the observed changes in the system frequencies are associated with degradation of the stiffness of the superstructure without any change in the stiffness of the foundation-soil system. In this case the path of the system would be described in Figs. 32a and 32b by $B'D'A$ and it would require permanent reductions (from B' to A) of structural stiffness of 22 and 43 percent in the N-S and E-W directions, respectively. This interpretation has been explored by Iemura and Jennings (1973) who found that a rigid-base nonstationary equivalent linear model and a nonstationary bilinear hysteretic model with degrading properties could represent the E-W response of the Millikan Library during the San Fernando earthquake.

On the other extreme, one may attempt to interpret the changes in system frequencies as resulting from degradation of the foundation-soil system without modification of the stiffness of the superstructure. In this case, the system in the N-S direction would have described the path $B''D''A$ shown in Fig. 32a which requires a permanent reduction (from B'' to A) of the N-S rocking stiffness of 37 percent. In the E-W direction it is not possible to explain the change in system frequencies solely on the basis of reduction of the rocking stiffness. Assuming that the foundation-soil system was initially rigid ($K_{MM} = \infty$) would require a permanent reduction in the E-W structural stiffness of the order of 14 percent. This extreme position of ascribing the frequency reduction to changes in the foundation-soil system has been adopted by Foutch and Jennings (1978) in their study of the N-S response of the Millikan Library.

By considering additional information it is possible to reduce the range of possibilities as to the system configuration prior to the San Fernando earthquake. Comparison of the torsional system frequencies obtained by ambient vibration tests conducted before and after the 1971 San Fernando earthquake indicates a 8.7 percent reduction of the fundamental torsional system frequency

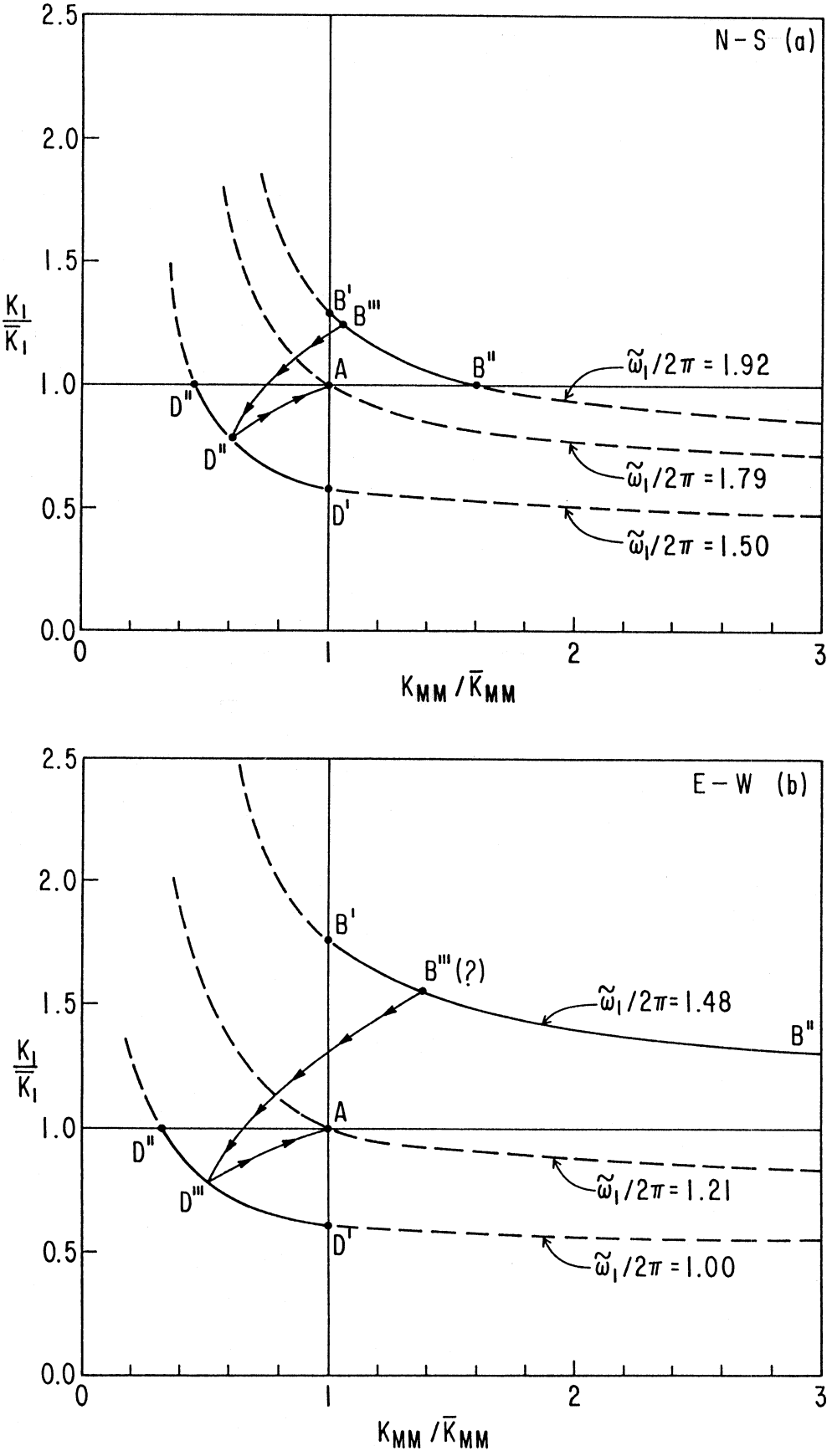

Figure 32. Structural and foundation stiffness before, during and after the San Fernando earthquake of 1971.

(Udwadia and Trifunac, 1974). There are indications that the torsional stiffness of the foundation did not suffer degradation during the earthquake (refer to Appendix B) and that the reduction of torsional system frequency was associated with a 17 percent reduction in torsional stiffness of the superstructure. Since most of the torsional stiffness of the superstructure is provided by the east and west shear walls, it seems that a 17 percent reduction of stiffness in these walls could explain the reduction in system frequencies in both N-S and torsional vibrations. A plausible initial configuration of the system in the N-S direction is shown as point B''' in Fig. 32a. In this case, as a result of the shaking, the N-S structural stiffness would have suffered a permanent reduction of the order of 17 percent while the N-S rocking stiffness of the foundation experienced no significant permanent degradation.

The initial configuration of the system in the E-W direction is more difficult to ascertain. The only information available is that small cracks have been observed in the interior plaster at the points of support of the precast window panels which constitute the north and south facades of the building (Iemura and Jennings, 1973). The results of tests described by Jennings and Kuroiwa (1968, Table 7) indicate that these panels which represent only 5 percent of the total mass contributed about 25 percent of the stiffness for small vibrations in the E-W direction. It is possible that the contribution of the window panels to the E-W stiffness has decreased significantly as a result of the shaking.

Hypothetical paths ($B''' D''' A$) describing the changes in structural and foundation stiffnesses during the San Fernando earthquake are shown in Fig. 32a and 32b. The actual path followed by the system was probably more complex as indicated by the temporal variation of the system frequencies determined by Udwadia and Trifunac (1974) and Iemura and Jennings (1973). The position of point D''' although hypothetical is consistent with the results of dynamic triaxial tests of the sands at the depth of the foundation which indicate that for shear strains of the order of 10^{-2} percent the shear modulus of the soil could be reduced by a factor of two, while for strains of the order of 10^{-1} percent the reduction would correspond to a factor of four (Shannon

and Wilson, Inc. and Agbabian Assoc., 1976). These reductions of the shear modulus would affect the rocking stiffness in the same proportion.

It should be mentioned that during the strong shaking portion of the San Fernando earthquake the ratio $\tilde{\omega}_1/\omega_1$ becomes lower than the value computed for the current configuration and consequently the soil-structure interaction effects during the earthquake were even more significant than those described for the present system characteristics. One particular effect of the increased interaction between the structure and the soil is that the weight given in Eq. (67) to the damping in the structure decreases while the weight given to the material damping in the soil increases. At the same time due to the seismic strains material damping in the soil increases significantly. The dynamic triaxial tests described above indicate values of the material damping in the soil of the order of 5 and 12 percent for shear strains of 10^{-2} and $10-1$ percent, respectively. As a result of these two factors the system damping increases significantly. It is apparent that the large values of system damping calculated on the basis of recorded seismic response of structures reflect to a high degree energy dissipation in the soil rather than in the structure.

The previous discussion illustrates the problems associated with attempting to determine loss of stiffness in the superstructure based only on knowledge of the changes in system frequencies. The present strong motion instrumentation of structures which only considers one instrument per level as well as most forced vibration tests which do not accurately measure the rocking response of the base do not provide sufficient information to decide whether a change of the system is mainly associated with modification of the structure or of the foundation-soil portion of system. Simple tests in which the amplitude of the rotation of the base at the resonant frequency of the system is recorded provide sufficient information to calculate via Eqs. (72)-(74) estimates of the fixed-base natural frequencies of the superstructure as well as the rocking and horizontal stiffness of the foundation. Tests of this type conducted immediately after completion of major structures and after large earthquakes could reveal with some degree of confidence where the changes in stiffness have taken place.

14. CONCLUSIONS

It has been shown that simple forced vibration tests in which the amplitude of the response at the top of the superstructure as well as the amplitudes of the translational and rotational components of the response at the base are recorded at the resonant frequency of the complete structure-soil system contain sufficient information to obtain estimates of the fixed-base fundamental frequencies of the superstructure and of the foundation stiffness coefficients (real parts of the foundation impedance functions). More detailed tests in which the phases of the response components with respect to the forcing function are also recorded give, in addition, information from which estimates of the fixed-base damping ratios of the superstructure as well as estimates of the foundation damping coefficients (associated with the imaginary parts of the foundation impedance functions) can be obtained. Analyses of the results of forced vibration tests of the nine-story reinforced concrete Millikan Library Building as well as theoretical considerations reveal that interpretations of forced vibration tests which do not include soil-structure interaction effects underestimate the fixed-base natural frequencies of the superstructure and overestimate the energy dissipation within the structure.

The theoretical and experimental results obtained indicate that the interaction between structures and the soil may have significant effects on the response during forced vibration tests. In addition to the frequency shifts and effects on the system damping already mentioned, the translation and rotation of the foundation associated with ground compliance lead to a rigid-body motion of the superstructure that may account for a significant portion of the total response. In the case of the Millikan Library Building, the rigid-body motion by itself accounts for more than 30 percent of the total N-S roof response. Perhaps even more important is the finding that the inertial forces associated with the rigid-body motion account for a major portion of the deformation of the superstructure at the resonant system frequency. This effect occurs even when the rigid-body motion is small compared with the total response. For torsional vibrations of the Millikan Library the rigid-body twist amounts to only 2.5 percent of the total twist at the roof. In this case, however, the amplitude of the torsional deformation at the top due to the inertial

torque associated with the rigid-body twist is 1.8 times larger than the amplitude of the deformation caused directly by the external torque applied by the vibration generator. It can be concluded that under very general conditions, the soil-structure interaction effects dominate the response at the resonant system frequency during forced vibration tests.

The agreement obtained in comparisons of experimental and calculated responses reveals that it is possible to predict accurately the effects of soil-structure interaction during forced vibration tests. The agreement obtained validates the soil-structure model considered and, in particular, gives confidence on the use of analytical methods to calculate the impedance functions for rigid foundations embedded in the soil. The importance of the effects of the flexibility of the foundation for E-W vibrations of the Millikan Library emphasizes the need for the development of analytical methods to obtain the dynamic response of flexible foundations.

After detailed study, it has been found that the discrepancy between the earlier results of Jennings and Kuroiwa (1968) based on forced vibration tests conducted in 1966-67 and the experimental results obtained by Foutch *et al.* (1975), as well as those described in this report, cannot be attributed to degradation of the foundation system resulting from the 1971 San Fernando earthquake as argued by Foutch and Jennings (1978). The results of Jennings and Kuroiwa would indicate that for N-S vibrations of the Millikan Library the rigid-body motion amounted to 3 percent of the total response at the roof while the more recent tests indicate a contribution higher than 30 percent. Such change would require a reduction of the rocking stiffness of the foundation by a factor of 27 which cannot be reconciled with minor modification of the foundation as a result of the San Fernando earthquake.

Analysis of the data available indicates that the torsional and N-S stiffnesses of the superstructure may have suffered permanent reductions of the order of 17 percent as result of the shaking induced by the San Fernando earthquake of 1971. The corresponding permanent loss of structural stiffness in the E-W direction lies between 14 and 43 percent. It appears that the N-S rocking stiffness as well as the torsional stiffness of the foundation suffered no permanent alteration as result of the earthquake shaking. The observed permanent reductions in torsional and N-S

system frequencies are probably associated with stiffness degradation in the superstructure. The permanent reduction in E-W system frequency may have resulted from loss of stiffness in both the structure and the foundation.

From the experimental point of view, it was found that reliable estimates of the damping ratio of the superstructure and of the foundation damping coefficients (associated with the imaginary part of the impedance functions) can only be obtained if the phase of the different response components with respect to the forcing function is recorded with high accuracy. Further studies on the nature of structural damping will require improved instrumentation and more complete calibration techniques.

ACKNOWLEDGMENTS

The experimental work described herein was planned by M. D. Trifunac and J. E. Luco in 1974 and it was conducted by M. D. Trifunac in 1975. The analysis of the data has been performed by H. L. Wong and J. E. Luco on an intermittent basis between 1975 and 1985. Support for the initial stage of this project from the U.S. Geological Survey and the Earthquake Research Affiliates Program at the California Institute of Technology is gratefully acknowledged.

REFERENCES

Apsel, R. J. and J. E. Luco (1986). "Impedance Functions for Foundations Embedded in a Layered Medium: An Integral Equation Approach," *Int. J. of Earthquake Engineering and Structural Dynamics* (in press).

Bielak, J. (1975). *Modal Analysis for Building-Soil Interaction*, Report E17, Instituto de Ingeniería, Universidad Nacional Autónoma de Mexico (July).

Blandford, R. B., V. R. McLamore and J. Aunon (1968). *Analysis of the Millikan Library from Ambient Vibrations*, Report No. 616-0268-2107, Earth Teledyne Co.

Converse Foundation Engineers (1959). *Foundation Investigation, Proposed Library Building, California Institute of Technology*, Project No. 59-110-A.

Crouse, C. B. (1973). *Engineering Studies of the San Fernando Earthquake*, EERL 73-04, Earthquake Research Laboratory, California Institute of Technology, Pasadena, California.

Eguchi, R. T., K. W. Campbell, C. M. Duke, A. W. Chow and J. Paternina (1976). *Shear Velocities and Near Surface Geologies at Accelerograph Sites that Recorded the San Fernando Earthquake*, Report UCLA-ENG-7653, School of Engineering and Applied Science, University of California, Los Angeles, California.

Foutch, D. A., J. E. Luco, M. D. Trifunac and F. E. Udwadia (1975). "Full Scale, Three-Dimensional Tests of Structural Deformation during Forced Excitation of a Nine-Story Reinforced Concrete Building," *Proceedings, U.S. National Conference on Earthquake Engineering*, Ann Arbor, Michigan, pp. 206-215.

Foutch, D. A. (1976). *A Study of the Vibrational Characteristics of Two Multistory Buildings*, EERL 76-03, Earthquake Engineering Research Laboratory, California Institute of Technology, Pasadena, California.

Foutch, D. A. and P. C. Jennings (1978). "A Study of the Apparent Change in the Foundation Response of a Nine-Story Reinforced Concrete Building," *Bulletin Seismological Society of America*, Vol. 68, No. 1, pp. 219-229.

Iemura, H. and P. C. Jennings (1973). *Hysteretic Response of a Nine-Story Reinforced Concrete Building during the San Fernando Earthquake*, EERL 73-07, Earthquake Engineering Research Laboratory, California Institute of Technology, Pasadena, California.

Jennings, P. C. and J. H. Kuroiwa (1968). "Vibration and Soil-Structure Interaction Tests of a Nine-Story Reinforced Concrete Building," *Bulletin Seismological Society of America*, Vol. 58, No. 3, pp. 891-916.

Jennings, P. C. (1970). "Distant Motion from a Building Vibration Test," *Bulletin Seismological Society of America*, Vol. 60, No. 6, pp. 2037-2043.

Keightley, W. O., G. W. Housner and D. E. Hudson (1961). *Vibration Test of the Encino Dam Intake Tower*, Earthquake Engineering Research Laboratory, California Institute of Technology, Pasadena, California.

Kuroiwa, J. H. (1967). *Vibration Test of a Multistory Building*, Earthquake Engineering Research Laboratory, California Institute of Technology, Pasadena, California.

Luco, J. E., M. D. Trifunac and F. E. Udwadia (1975). "An Experimental Study of Ground Deformations Caused by Soil-Structure Interaction," *Proceedings, U.S. National Conference on Earthquake Engineering*, Ann Arbor, Michigan

McLamore, V. R. (1972). *Post-Earthquake Vibration Measurements, Millikan Library* (unpublished report).

Shannon and Wilson, Inc. and Agbabian Associates (1976). *Geotechnical and Strong Motion Earthquake Data from U.S. Accelerograph Stations*, Vol. 1, CIT, Santa Barbara, Taft, Hollister, California, SW-AA.

Trifunac, M. D. (1972). "Comparison between Ambient and Forced Vibration Experiments," *Int. J. Earthquake Engineering and Structural Dynamics*, Vol. 1, pp. 133-150.

Udwadia, F. E. and M. D. Trifunac (1973). "Ambient Vibration Tests of Full-Scale Structures," *Proceedings, Fifth World Conference on Earthquake Engineering*, Rome.

Udwadia, F. E. and M. D. Trifunac (1974). "Time and Amplitude Dependent Response of Structures," *Int. J. Earthquake Engineering and Structural Dynamics*, Vol. 2, pp. 359-378.

Udwadia, F. E. and P. Z. Marmarelis (1976). "The Identification of Building Structural Systems: I. The Linear Case," *Bulletin Seismological Society of America*, Vol. 66, No. 1, pp. 125-151.

Wong, H. L. (1975). *Dynamic Soil-Structure Interaction*, EERL 75-01, Earthquake Engineering Research Laboratory, California Institute of Technology, Pasadena, California.

Wong, H. L., J. E. Luco and M. D. Trifunac (1977). "Contact Stresses and Ground Motion Generated by Soil-Structure Interaction," *Int. J. Earthquake Engineering and Structural Dynamics*, Vol. 5, pp. 67-79.

APPENDIX A

DESCRIPTION OF APPARATUS AND EXPERIMENTAL PROCEDURES

The forced vibration tests of the Robert Millikan Library were carried out in the summer of 1975 at night to avoid disturbances to building occupants and to minimize any interference with the measuring equipment. The force vibration generator and the recording equipment were placed on the roof. Seismometers in the basement of the library were connected by cables via the stairwell located in the western shear wall of the building (Figure 8).

The forced vibration generator was anchored to the roof slab. Its vertical axis was located approximately six feet south of the southern side of the core wall and east of the north-south axis of the building (21'6" east of the southwest corner of the core wall (Figure 8)). This generator operates in the frequency range up to $\sim$ 10 cps and is capable of producing a sinusoidally varying force with maximum amplitude of 5000 lbs. At any given frequency the amplitude of the force the generator applies to the building is a function of the number of layers of weights in its baskets. During the experiments discussed here the baskets were fully loaded (Figures A.1 and A.2). The corresponding force can be described by $F = 23.3\ \omega^2$ lb.

Vibrations in the library were monitored by four SS-1 Ranger Seismometers. These transducers have the moving coil in the magnetic field and produce an output voltage which is proportional to the velocity of the coil-mass relative to the fixed instrument housing. The natural period of these transducers is approximately equal to one second. The typical coil resistance is equal to several $\kappa\Omega$.

The voltage from the Ranger Seismometers was amplified by an Earth Sciences SC-1 signal conditioner and then recorded on Ampex SP-300, seven channel, tape recorder in FM mode. The signals were also recorded by Mark 220 Brush recorders to provide immediate indication of recorded amplitudes (Figure A.3).

The phase of the force generated by the shaker corresponds to the angles of individual baskets relative to the direction of maximum force. Zero or 180 ° phase corresponds to one of the

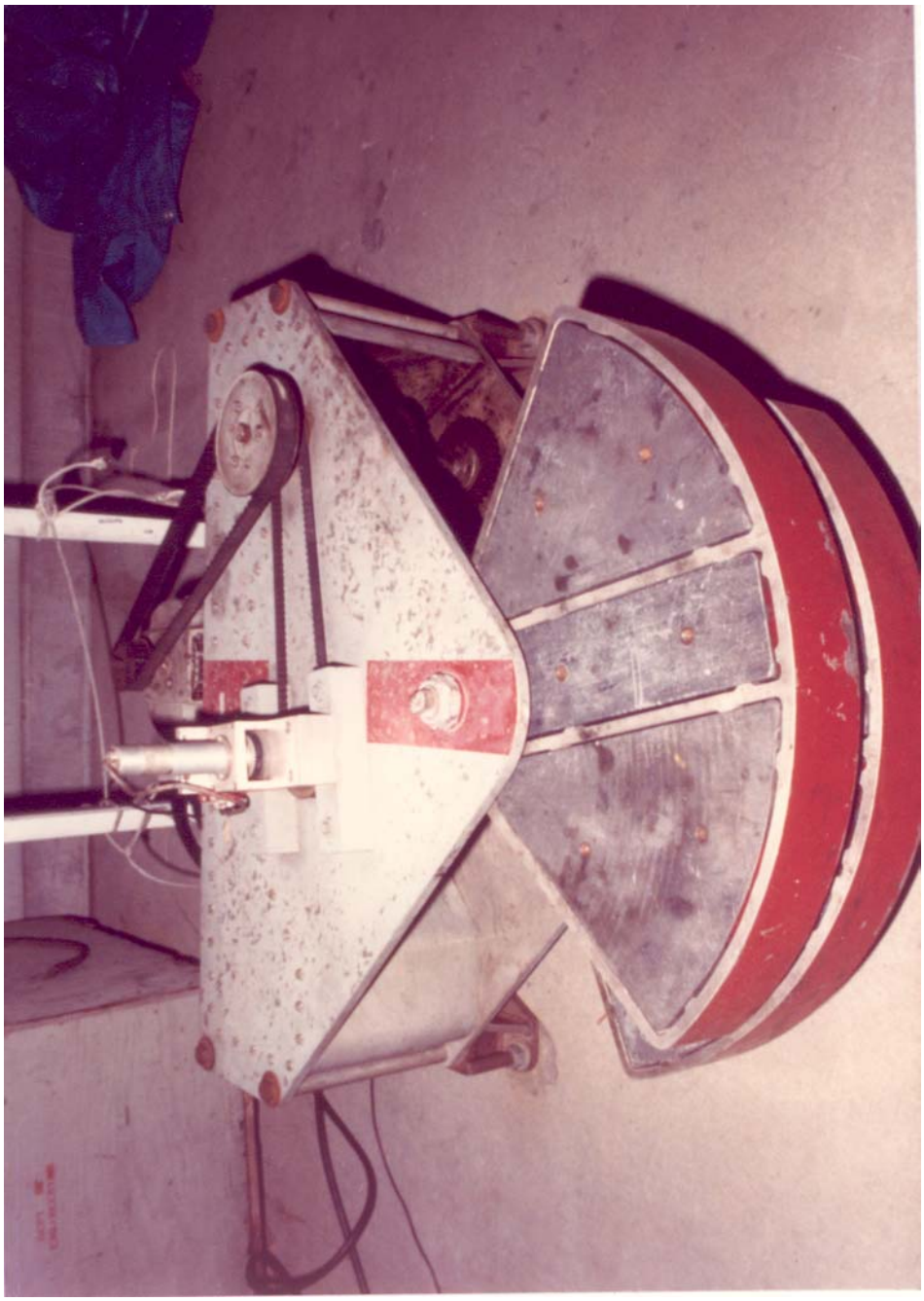

Figure A.1 Forced vibration generator (full baskets) during preparation for the north-south experiment in the nearly zero phase configuration.

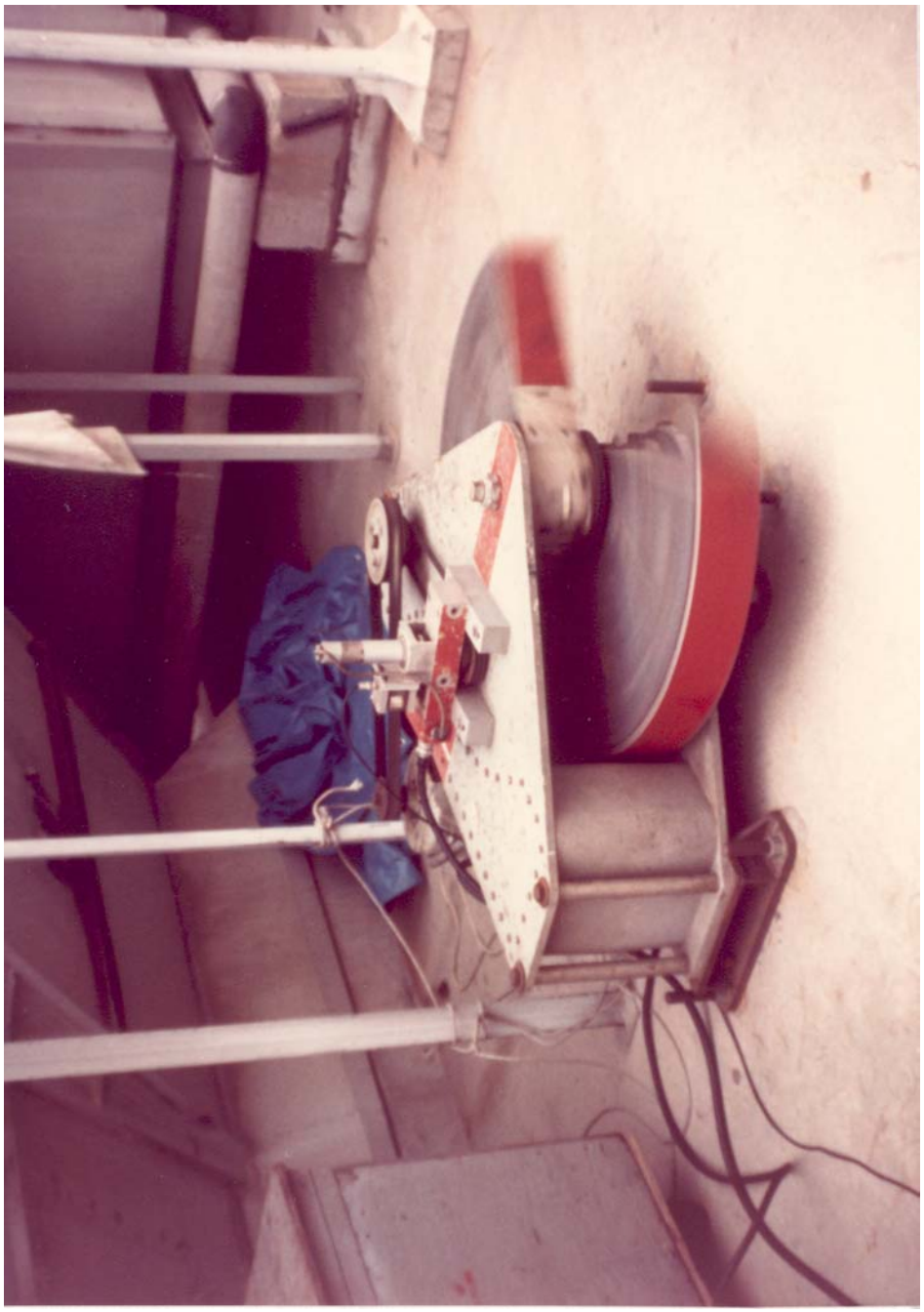

Figure A.2 Forced vibration generator during north-south excitation illustrating nearly 90° phase positions of the two baskets.

Figure A.3 Recording equipment. Signal conditioner (bottom, left), tape recorder (bottom, center), two brush recorders (top, center), and phase monitoring device (top, right).

baskets being above the other. Figure A.1 shows the baskets off the maximum force position (zero phase) by about 10°. Figure A.2 shows the baskets at about 90° angle which in this example corresponds to the zero north-south excitation force. During the north-south excitation of the library the basket positions corresponding to the maximum force in the south direction were selected to represent the zero phase configuration (Figures 8 and A.1). During east-west excitation of the library the zero phase angle was assigned to the maximum shaker force in the west direction (Figure 8).

In the experiment described here the assumption was made that the foundation slab deformation patterns do not change much for frequencies in the neighborhood of the fundamental system frequencies. On the basis of this assumption the translation and rotation of the basement slab were described by monitoring the motion at three points and by use of the deformation patterns shown in Figs. 6 and 7. The location of the Ranger Seismometers (No. 1 recording horizontal vibrations of the basement, Nos. 2 and 3 recording vertical motions in the basement of the library and No. 4 recording horizontal motion of the roof) for north-south and east-west vibrations are shown in Fig. 8.

During the north-south and east-west experiments the recorded motions were sampled at 138 and 122 frequencies, respectively, between ~.7 Hz and 2.5 Hz. At the end of both experiments, all four seismometers were placed on the roof slab and recorded the same north-south or east-west motions. This calibration run was designed to provide a check on all four recording amplitudes as those are operated on by the complete chain of signal processing (signal amplification, attenuation, integration, tape recording, tape playback into analog to digital converter and digital processing) and analysis.

Analog signals recorded in the field were played back through the Ampex SP-300 tape recorder and converted to digital data. For each frequency during north-south and east-west experiments, 30 seconds of selected analog recordings were used to generate digital data. The digitization rate was 100 pts/second. The high rate was chosen to permit accurate relative phase

determination among four recorded displacement functions and the forcing function and to enable digital low-pass filtering of signals in later processing.

To describe the seismometer and signal conditioner corrections it is convenient to define:

$f(t) = F(\omega)e^{i\omega t}$ = forcing function as a function of frequency

$y_j(t) = Y_j(\omega)e^{i\omega t}$ = displacement at location j $(j = 1, 2, 3, 4)$

$v_j(t) = V_j(\omega)e^{i\omega t}$ = voltage output of the jth seismometer

$A_j(t) = S_j(\omega)e^{i\omega t}$ = signal output of the jth channel of the signal conditioner.

The amplitude D_j and phase with respect to the forcing function ξ_j of the displacement at the jth location can be obtained from

$$Y_j(\omega) = D_j\, e^{-i\xi_j} = \frac{S_j(\omega)}{H_{2j}(\omega)\, H_{1j}(\omega)} \tag{A1}$$

where $S_j(\omega) = A_j e^{-i\eta_j}$ (A_j amplitude and η_j phase with respect to the forcing function) is the recorded output of the jth channel of the signal conditioner and $H_{1j}(\omega)$ and $H_{2j}(\omega)$ are the seismometer and signal conditioner transfer functions, respectively.

The seismometer transfer function (displacement to voltage output) is given by

$$H_{1j}(\omega) = \frac{i\omega \left(\frac{\omega}{\omega_{nj}}\right)^2 G_j}{\left[1 - \left(\frac{\omega}{\omega_{nj}}\right)^2\right] + 2ih_j\left(\frac{\omega}{\omega_{nj}}\right)} \cdot \left(\frac{R_{xj}}{R_{xj} + R_{cj}}\right) \tag{A2}$$

where

$$h_j = \varsigma_j + \frac{G_j^2}{2\omega_{nj} m_j (R_{xj} + R_{cj})} \tag{A3}$$

where h_j is the total damping of the jth transducer, and ω_{nj}, G_j, R_{cj}, R_{xj}, m_j are the natural frequency, the generator constant, the core resistance, the external resistance and the mass of the jth transducer, respectively.

The transfer function for the signal conditioner (seismometer voltage output to signal conditioner output) is written in the form

$$H_{2j}(\omega) = 350000\ e^{-0.115 dB_j}\ e^{-i\phi_j(\omega)} \tag{A4}$$

where dB_j is the dB setting and $\phi_j(\omega)$ is an empirically determined phase shift introduced by the jth channel of the signal conditioner. The functions $\phi_j(\omega)$ $(j = 1, 2, 3, 4)$ are shown in Fig. A4.

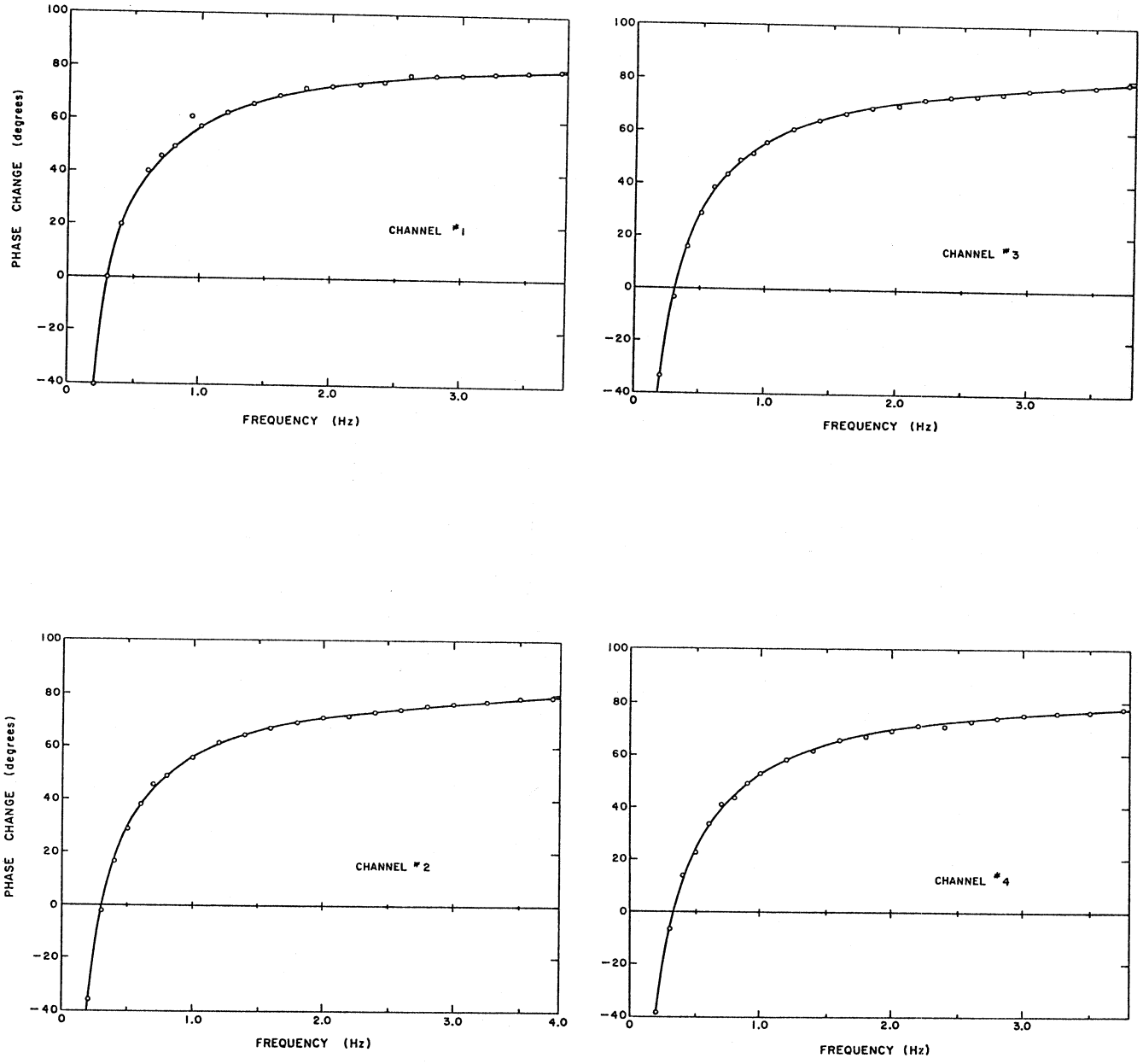

Figure A.4 Empirically determined phase shifts for the four channels of the signal conditioner.

APPENDIX B

EFFECTS OF SOIL-STRUCTURE INTERACTION ON THE TORSIONAL RESPONSE

To study the effects that the twist of the base may have on the torsional response of a symmetric structure, it is convenient to represent the superstructure by a lumped mass model. The excitation is represented by the torque $M_T e^{i\omega t}$ that the harmonic vibration generator applies on the *jth* level. The total harmonic twist at the *jth* level may be written in the form

$$\overline{\Phi}_j e^{i\omega t} = (\Phi_b + \Phi_j) e^{i\omega t} \tag{B.1}$$

where Φ_b denotes the twist of the base and Φ_j is the twist at the *jth* level associated with deformation of the superstructure. Using the fixed-base torsional modes of the superstructure, it can be shown that

$$\overline{\Phi}_j = \Phi_b + \sum_{r=1}^{N} \frac{(\omega/\omega_r)^2}{1 - (\omega/\omega_r)^2 + 2i\xi_r(\omega/\omega_r)} \left(\frac{M_T}{\omega^2 I_r} \phi_l^{(r)} + \beta_r \Phi_b \right) \Phi_j^{(r)} \tag{B.2}$$

where $\phi_j^{(r)}$ represents the amplitude of the *rth* fixed-base torsional mode of the superstructure ($\phi_N^{(r)} = 1$), while ω_r and ξ_r correspond to the *rth* fixed-base torsional natural frequency and damping ratio, respectively. The modal quantities I_r and β_r are defined by

$$I_r = \sum_{j=1}^{N} I_{zj} \left[\phi_j^{(r)} \right]^2 \tag{B.3}$$

and

$$\beta_r = \frac{1}{I_r} \sum_{j=1}^{N} I_{zj} \phi_j^{(r)} \tag{B.4}$$

in which I_{zj} represents the moment of inertia of the *jth* lumped mass about the vertical axis of symmetry.

By simultaneous measurement of the total twist at the top of the superstructure and at the base, it is possible to determine ω_1 and ξ_1 in the same manner utilized to find the translational fixed-base fundamental frequency and damping ratio.

The torque $T_S e^{i\omega t}$ that the foundation exerts on the soil can be expressed in the form

$$T_S = M_T + \omega^2 I_{zo} \Phi_b + \omega^2 \sum_{j=1}^{N} I_{zj} \overline{\Phi}_j \tag{B.5}$$

where I_{zo} corresponds to the moment of inertia of the foundation about the vertical axis of symmetry. Substitution from Eq. (B.2) into Eq. (B.5) leads to

$$T_S = M_T \left[1 + \sum_{r=1}^{N} \phi^{(r)} \beta_r Z_r \right] + \omega^2 I_{zb} \Phi_b \left[1 + \frac{I_{zo}}{I_{zb}} + \sum_{r=1}^{N} \beta_r^2 Z_r \frac{I_r}{I_{zb}} \right] \tag{B.6}$$

where $I_{zb} = \sum_{j=1}^{N} I_{zj}$ and Z_r is defined by Eq. (34).

The torque T_S can also be written in the form

$$T_S = GL^3 K_{TT} \Phi_b \tag{B.7}$$

where K_{TT} is the normalized torsional impedance function for the foundation, G is a shear modulus of reference and L is a characteristic length of the foundation. Eliminating T_S from Eqs. (B.6) and (B.7) leads to

$$\Phi_b = \left(\frac{\omega}{\omega_1} \right)^2 \kappa \left[K_{TT} - \frac{\omega}{\omega_1}^2 \kappa \left(1 + \frac{I_{zo}}{I_{zb}} + \sum_{1}^{N} \beta_r^2 Z_r \frac{I_r}{I_{zb}} \right) \right]^{-1} \left(1 + \sum_{1}^{N} \phi^{(r)} \beta_r Z_r \right) \frac{M_T}{\omega^2 I_{zb}} \tag{B.8}$$

where

$$\kappa = \frac{\omega_1^2 I_{zb}}{GL^3} \quad . \tag{B.9}$$

Equation (B.8) provides the means to calculate the base twist from which other quantities of interest may be easily obtained. Substitution from Eq. (B.8) into Eq. (B.2) leads to the following expression for the total twist $\overline{\Phi}_T = \overline{\Phi}_N$ at the top of the superstructure

$$\overline{\Phi}_T / (M_T / \omega^2 I_{zb}) = \left(\sum_{r=1}^{N} \frac{I_{zb}}{I_r} \phi_l^{(r)} Z_r \right) +$$

$$\left(\frac{\omega}{\omega_1} \right)^2 \kappa \left[K_{TT} - \left(\frac{\omega}{\omega_1} \right)^2 \kappa \left(1 + \frac{I_{zo}}{I_{zb}} + \sum_{1}^{N} \beta_r^2 Z_r \frac{I_r}{I_{zb}} \right) \right]^{-1} \left(1 + \sum_{1}^{N} \beta_r Z_r \right) \left(1 + \sum_{1}^{N} \phi^{(r)} \beta_r Z_r \right) \tag{B.10}$$

For frequencies in the vicinity of the fundamental fixed-base frequency of the superstructure, it is possible to obtain an approximate expression for the normalized torsional impedance function which involves quantities that can be measured or estimated. From Eqs. (B.2), (B.5) and (B.7) it is found that

$$K_{TT} \approx \frac{\omega^2 I_{zb}}{GL^3}\left[\frac{M_T}{\omega^2 I_{zb}\Phi_b} + \left(1 + \frac{I_{zo}}{I_{zb}} - \beta_1 \frac{I_1}{I_{zb}}\right) + \beta_1 \frac{I_1}{I_{zb}} \frac{\overline{\Phi}_T}{\Phi_b}\right] \quad (\omega \ll \omega_2) \tag{B.11}$$

This expression can be used to determine experimentally the torsional impedance function.

Approximate solutions of the interaction equations for the case of torsional excitation can be obtained by the procedure described in the text. The resulting expressions are

$$\begin{Bmatrix} \overline{\Phi}_T \\ \Phi_T \\ \Phi_b \end{Bmatrix} \approx \frac{(\omega/\tilde{\omega}_1)^2}{1 - (\omega/\tilde{\omega}_1)^2 + 2i\tilde{\xi}_1(\omega/\tilde{\omega}_1)} \begin{Bmatrix} 1 \\ (\tilde{\omega}_1/\omega_1)^2 \\ \beta_1^{-1}(\tilde{\omega}_1/\omega_T)^2 \end{Bmatrix} \frac{M_T}{\omega^2 I_1}\phi_l^{(1)} \tag{B.12}$$

in which

$$\frac{1}{\tilde{\omega}_1^2} = \frac{1}{\omega_1^2} + \frac{1}{\omega_T^2} \tag{B.13}$$

$$\tilde{\xi}_1 = \left(\frac{\tilde{\omega}_1}{\omega_1}\right)^3 \xi_1 + \left[1 - \left(\frac{\tilde{\omega}_1}{\omega_1}\right)^2\right] \xi_S + \left(\frac{\tilde{\omega}_1}{\omega_T}\right)^3 \xi_{RT} \ . \tag{B.14}$$

The frequency ω_T and the torsional radiation damping ξ_{RT} are defined by

$$\omega_T^2 = GL^3 k_{TT}(\tilde{\omega}_1)/\beta_1^2 I_1 \tag{B.15}$$

$$\xi_{RT} = \frac{\omega_T}{2} \cdot \frac{c_{TT}(\tilde{\omega}_1)}{k_{TT}(\tilde{\omega}_1)} \tag{B.16}$$

where

$$K_{TT}(\omega) = k_{TT}(\omega) + i\left[2\xi_S k_{TT}(\omega) + \omega c_{TT}(\omega)\right] \ . \tag{B.17}$$

The approximate expressions given by Eq. (B.12) can be used to estimate the effects of soil-structure interaction during torsional forced vibration tests. They can also be used to determine some characteristics of the superstructure and of the foundation from test results. From Eqs. (B.12), (B.13) and (B.15) it is found

$$\omega_1 = \tilde{\omega}_1 \left[1 - \beta_1 (\Phi_b / \overline{\Phi}_T) \right]^{-1/2} \tag{B.18}$$

$$\omega_T = \tilde{\omega}_1 (\beta_1 \Phi_b / \overline{\Phi}_T)^{-1/2} \tag{B.19}$$

$$k_{TT}(\tilde{\omega}_1) = \tilde{\omega}_1^2 \frac{\beta_1 I_1}{GL^3} \frac{\overline{\Phi}_T}{\Phi_b} \tag{B.20}$$

from which the fixed-base fundamental torsional frequency of the superstructure ω_1, the torsional frequency of the system assuming the superstructure rigid ω_T, and the torsional stiffness coefficient of the foundation k_{TT}, can be obtained from knowledge of $\tilde{\omega}_1$, $\Phi_b/\overline{\Phi}_T$, β_1, I_1 and GL^3.

The above equations can be used to analyze the torsional test results reported by Jennings and Kuroiwa (1968) for the Millikan Library. In these tests the Millikan Library building was excited in torsion by a vibration generator located on the ninth floor at a distance of 10.79 m (35.41 ft) from the axis of symmetry of the structure. Some of the results obtained by Jennings and Kuroiwa are summarized in Table B.1 for different values of the exciting torque M_T. In Test 9a, the fundamental torsional system frequency was 2.89 Hz and the twist of the base was 2.45 percent of the total twist at the roof. Based on the torsional mode shape reported by Jennings and Kuroiwa, it can be found that $\beta_1 = 1.4$ and $I_1/I_{zb} = 0.34$. The radius of gyration of the superstructure with respect to the vertical axis of symmetry is estimated to be $r = 10.36$ m (34 ft) leading to a moment of inertia for the superstructure of $gI_{zb} = 1.12 \times 10^{10}$ N-m^2 (2.7×10^{10} l b-ft^2).

Based on Eqs. (B.18)-(B.20) and on the test data, it is possible to obtain the estimates of ω_1, ω_T and k_{TT} listed in Table B.1. For test 9a the estimate of the fundamental fixed-base torsional frequency is 2.94 Hz while the corresponding system frequency is 2.89 Hz. In this case the effects of soil-structure interaction have lead to a system frequency only 1.7 percent lower than

the fixed-base frequency. Although the frequency shift is small and the rigid-body twist associated with ground compliance amounts to only 2.5 percent of the total twist at the roof, the effects of the inertial forces associated with rotation of the base are still significant. At the system frequency (2.89 Hz for test 9a) the quantity $| \beta_1 \Phi_b |$ which controls the contribution of the base rotation to the deformation of the superstructure (Eq. B.2) is 1.76 times larger than the term $| (M_T/\omega^2 I_1)\, \phi_l^{(1)} |$ which determines the deformation of the superstructure associated with the applied moment in absence of soil compliance ($\phi_l^{(1)} = 0.907$, $| \Phi_b | = 6.59 \times 10^7$ rad. for test 9a). In this case, the deformation of the superstructure associated with the inertial forces induced by rotation of the base represents the larger contribution to the total deformation.

The estimates obtained for the normalized ($G = 2.68 \times 10^8 \mathrm{N/m^2}$ (38.9×10^3 psi), $L = 13.72$ m (45 ft)) torsional stiffness coefficients k_{TT} which range from 9.91 to 10.51 are close to what would be expected on the basis of the foundation and soil models shown in Fig. 19 and listed in Table 5. These results indicate that the torsional stiffness of the foundation was not drastically affected by the San Fernando earthquake of 1971.

Comparison of the torsional system frequencies obtained by ambient vibration tests conducted before and after the 1971 San Fernando earthquake indicates a 8.7 percent reduction of the fundamental torsional system frequency (Udwadia and Trifunac, 1974). Since the torsional stiffness of the foundation seems to have remained unchanged, it appears that the torsional stiffness of the superstructure may have suffered a reduction of the order of 17 percent. Since the east and west shear walls provide most of the torsional stiffness of the superstructure, this suggests that the shear walls would have suffered a stiffness reduction of approximately 17 percent as a result of the San Fernando earthquake.

The torsional system damping $\tilde{\xi}_1$ obtained in forced vibration tests has a value of 1 percent which is significantly lower than the system damping values obtained for N-S and E-W vibrations (Jennings an Kuroiwa, 1968). This difference can be explained by use of Eq. (B.14). For torsional vibrations the system frequency is close to the fixed-base torsional frequency and the radiation damping is small. In this case Eq. (B.14) leads to

TABLE B.1 CHARACTERISTICS OF THE TORSIONAL RESPONSE

Test Data (Jennings and Kuroiwa, 1968)				Calculated Values		
Test	$M_T/\omega^2 I_1$	$\tilde{\omega}_1/2\pi$ Hz	$\Phi_b/\overline{\Phi}_T$	$\omega_1/2\pi$ Hz	$\omega_T/2\pi$ Hz	k_{TT}
9a	5.78×10^{-7}	2.890	0.0245	2.94	15.61	10.51
9b	10.64×10^{-7}	2.865	0.0255	2.92	15.16	9.93
9c	13.59×10^{-7}	2.857	0.0254	2.91	15.15	9.91

$$\tilde{\xi}_1 = 0.95\xi_1 + 0.034\xi_S + 0.0003 \tag{B.21}$$

indicating a small contribution of damping in the soil to the system damping. Assuming values of $\xi_1 = 0.012$ and $\xi_S = 0.02$, Eq. (B.21) leads to a value for $\tilde{\xi}_1$ of 1.2 percent. Thus the value of the torsional damping in the superstructure is consistent with the calculated value for damping in the shear walls under N-S excitation.

Finally, comparison of the frequencies determined from tests 9a and 9c indicates that the increase in level of the excitation has caused a reduction in the system frequency of 1.14 percent. This reduction in system frequency is associated with a 2.2 percent reduction in the stiffness of the superstructure and a 5.8 percent reduction in the stiffness of the foundation. In this case, both the superstructure and the foundation-soil system experienced a degradation of stiffness as a result of the higher strains. It is suggestive that the effects on the foundation and soil were higher than those on the superstructure. The recording of the base motion during forced vibration tests at different force levels may permit to analyze the sources of the apparent stiffness degradation of the complete system.